Aus dem Institut für Anatomie und Zellbiologie des Fachbereichs Medizin der
Philipps-Universität Marburg
Geschäftsführender Direktor: Prof. Dr. med. E. Weihe

in Zusammenarbeit mit dem Department for
Cardiovascular Medicine der University of Oxford, UK
Direktor: Prof. H. Watkins, M.D., Ph.D.

Investigation of the Phosphorylation of the C-terminal domains of the cardiac Myosin Binding Protein C by the 5'-AMP-activated Protein Kinase

Inaugural-Dissertation zur Erlangung des Doktorgrades der gesamten Humanmedizin dem Fachbereich Medizin der Philipps-Universität Marburg vorgelegt von

Bernhard Willibald Renz
aus Kronach
Marburg, 2009

Angenommen vom Fachbereich Medizin der Philipps-Universität Marburg
am: 24. September 2009

Gedruckt mit Genehmigung des Fachbereichs.

Dekan: Prof. Dr. med. M. Rothmund
Referent: Prof. Dr. med. G. Aumüller
1. Korreferent: Prof. Dr. med. H. Rupp
2. Korreferent: Prof. Dr. med. D. Oliver

Meinen Eltern und Grosseltern in grosser Dankbarkeit

Summary of Results

Investigation of the Phosphorylation of the C-terminal domains of the cardiac Myosin Binding Protein C by the 5'-AMP-activated Protein Kinase

Inaugural-Dissertation zur Erlangung des Doktorgrades der gesamten Humanmedizin aus dem Fachbereich Medizin der Philipps-Universität Marburg vorgelegt von

Bernhard Willibald Renz
aus Kronach
Marburg, 2009

The existence of MyBP-C in striated muscle has been known for over 35 years and about 150 mutations in the gene encoding cMyBP-C have been found to be a common cause of hypertrophic cardiomyopathy. Despite this, the structure and function of MyBP-C remains less well understood than most other sarcomeric proteins, with roles in both regulation of contraction and thick filament formation/stability being proposed. In addition to the well known interactions of MyBP-C with other proteins of the sarcomeric apparatus (LMM, titin, actin) and with PKA, CaMKK and PKC at the N-terminal end of the protein, the aim of this study was to investigate interactions of MyBP-C's C-terminus with the 5'-AMP-activated protein kinase. This enzyme came in the focus of research during the last decade as it appears to function in a plethora of cell processes. Further, it has been elucidated that mutations in *PRKAG2*, encoding for the γ2 subunit of AMPK, causes left ventricular hypertrophy associated with conduction system diseases (e.g. Wolf-Parkinson-White syndrome). Important questions that have to be answered for a better understanding of this issue are, beside others, the identification of the full repertoire of cardiac protein targets.

My project aimed at identifying the site or sites of AMPK phosphorylation within the C-terminal three domains of cMyBP-C as suggested by earlier yeast-two-hybrid-screen data and biochemical work. The latter hinted that the C8 domain was most likely the target, and it is this fragment that my work began with. Having optimised the expression and purification of recombinant wild type MyBP-C C8 domain and a

number of mutated C8 domains as discussed in Chapter 3, it was possible to disprove the hypothesis of phosphorylatable residues being in this domain. In contrast, it was revealed that a phosphorylatable serine moiety was present in the N-terminal leader of the recombinant protein, encoded by the vector pET-28a. This serine lies in the thrombin recognition sequence itself and its phosphorylation inhibits cleavage. However, it was shown *in vitro* that a phosphorylatable serine residue is located in the C10 domain of the protein and this further confirms the association of the C8-C10 fragment of MyBP-C with AMPK, first observed in the yeast two-hybrid assay. The hypotheses that arise from these results will be discussed in this chapter. Additionally, I showed that the N-terminal domains of cMyBP-C (C0-C2), which contain the well characterized PKA and CaMII sites, are not a good substrate for AMPK *in vitro*.

Zusammenfassung

Investigation of the Phosphorylation of the C-terminal domains of the cardiac Myosin Binding Protein C by the 5'-AMP-activated Protein Kinase

Inaugural-Dissertation zur Erlangung des Doktorgrades der gesamten Humanmedizin aus dem Fachbereich Medizin der Philipps-Universität Marburg vorgelegt von

Bernhard Willibald Renz
aus Kronach
Marburg, 2009

Seit mehr als 35 Jahren kennt man das Myosin-Bindungs-Protein-C (MyBP-C). In dieser Zeit wurden in dem Gen, welches für die kardiale Isoform dieses Proteins kodiert (*MYBPC3*) mehr als 150 Mutationen gefunden, die zur hypertrophischen Kardiomyopathie (HCM) führen. Damit sind Mutationen in diesem Gen für mehr als ein Drittel aller HCM-Fälle verantwortlich.

Es werden für dieses Protein sowohl eine Rolle in der Regulation der Kontraktion, als auch strukturstabilisierende Aufgaben in der Filamentformation postuliert. Trotz all dieser Tatsachen ist die Funktion des MyBP-C, im Vergleich zu den meisten anderen Proteinen des sarkomerischen Apparates, nicht ausreichend verstanden.

Zusätzlich zu den direkten Interaktionen zwischen MyBP-C und den sarkomerischen Proteinen Titin, der leichten Meromyosinkette und Aktin, sind Interaktionen mit der cAMP-abhängigen Protein Kinase (PKA), der Ca^{2+}/Calmodulin-abhängigen Protein Kinase II (CaMKII) und der Protein Kinase C (PKC) am N-terminalen Ende des Proteins bekannt.

Die Absicht dieser Abeit war es, die C-terminalen Interaktionen des Proteins mit der AMP-aktivierten Proteinkinase (AMPK) zu untersuchen. Dieses Enzym wurde in den letzten 10 Jahren Gegenstand umfassender Forschungen. Es werden der Kinase die Beteiligung an zahlreichen regulierenden Prozessen in der Zelle zugeschrieben. Ausserdem wurden Mutationen im *PRKAG2*-Gen, welches für die γ2-Untereinheit der Kinase kodiert, gefunden. Diese zur Hypertrophie des linken Ventrikels führenden Mutationen sind zudem noch mit Reizleitungsabnormalien (z.B.: Wolf-Parkinson-

White-Syndrom) vergesellschaftet. Die wichtigen Fragestellungen, die es in diesem Zusammenhang, neben anderen, für ein umfassenderes Verständnis zu beantworten gilt, betreffen die Identifikation weiterer kardialer Proteine, die mit dieser Kinase in Interaktion treten.

Durch meine Arbeit sollten die Aminosäure oder die Aminosäuren des C-terminalen Endes des kardialen Myosin-Bindungs-Protein-C (cMyBP-C) identifiziert werden, die von der AMPK *in vitro* phosphoryliert werden können. Eine Interaktion zwischen dem C-terminalen Ende (C8-C10) und der Kinase wurde von Professor David Carling und seinen Mitarbeitern am Imperial College in London mittels Yeast-two-hybrid-assay und weiteren biochemischen Untersuchungen postuliert. Die letzt genannten machten die C8-Domäne des cMyBP-C zum wahrscheinlichsten Ziel der Kinase. Aus diesem Grund habe ich bei meinen Arbeiten mit der Untersuchung dieser Domäne begonnen. Nach Optimierung sowohl der Expressions- und Purifikationsmethoden zur Herstellung der rekombinanten Wildtyp Domäne, als auch einer Reihe mutierter C8-Domänen, war es möglich die Hypothese zu widerlegen, dass sich in der C8-Domäne des cMyBP-C eine durch die AMPK phosphorylierbare Aminosäure befindet. Es zeigte sich vielmehr, dass sich in der N-terminalen leader Sequenz des rekombinanten Proteins ein phosphorylierbarer Serinrest befindet, der von dem Vektor pET-28a kodiert wird. Dieses Serin liegt in der Thrombinerkennungssquenz und seine Phosphorylierung verhindert die Abspaltung dieser Sequenz.

Des Weiteren wurde *in vitro* gezeigt, dass ein von der AMPK phosphorylierbares Serin in der C10-Domäne lokalisiert ist, und dies bestätigt die ursprünglich angenommene Interaktion des C-terminalen Fragmentes (C8-C10) mit der Kinase.

Zusätzlich konnte gezeigt werden, dass die N-terminalen Domänen des Proteins (C0-C2), die die gut charakterisierten Phosphorylierungsstellen der PKA and CaMII enthalten, *in vitro* kein Substrat für die AMPK sind.

Die C-terminale Phosphorylierungsstelle des cMyBP-C könnte zum einen die Formation des Proteins um das Myosinfilament beeinflussen, andererseits wäre auch denkbar, dass durch eine Mutation im *PRKAG2* Gen und der daraus resultierenden Änderung des Phosphorylierungsstatusses des MyBP-C, die postulierte Funktion in der Regulation des kardialen Querbrücken-Zyklusses beeinträchtigt wird.

Table of Contents

Index of Tables and Figures

List of Abbreviations

Acetyl-CoA	Acetyl-coenzyme A carboxylase
ADP	Adenosine diphosphate
Akt	Protein kinase B
a-MHC	a-myosin heavy chain
AMP	Adenosine monophosphate
AMPK	AMP-activated protein kinase
AMPKK	AMP-activated protein kinase kinase
APS	Ammonium persulfate
ARVC	Arrhythmogenic right ventricular cardiomyopathy
ARVD	Arrhythmogenic right ventricular dysplasia
ATP	Adenosine triphosphate
AV	Atrioventricular
BCA	Bicinchoninic acid
BSA	Bovine serum albumin
CaMKK	Ca_{2+}/calmodulin-dependent protein kinase kinase
CBS	Cystathionine b-synthase
cMyBP-C	cardiac Myosin-binding-protein-C
CPT1	Carnitin palmitoyl transferase 1
DCM	Dilated cardiomyopathy
DLU	Digital light units
DMSO	Dimethyl sulphoxide
DNA	Deoxyribonucleic acid
dNTP	Desoxynucleoside triphosphate,
DTT	Dithiothreitol
E.coli	Escherichia coli
EDTA	Ethylenediaminetetracetic acid
FPLC	Fast Protein Liquid Chromatography
GS	Glycogen synthase
HCM	Hypertrophic cardiomyopathy
HMG-CoA reductase	3-hydroxy-3-methylglutaryl-coenzyme A reductase
HRP	Horseradish peroxidase
IPTG	Isopropyl-1-thio-b-D-galactopyranoside
LB	Luria-Bertani
LKB1	Serine threonine kinase 11 (STK11)
LMM	Light meromyosin portion of the myosin rod
MLP	cardiac muscle LIM protein
MOPS	3-morpholinopropanesulphonic acid
MyBP-C	Myosin-binding-protein-C
NCC	Non-compaction cardiomyopathy
Ni^{2+}-NTA	Nickel nitrilotriacetic acid
PCR	Polymerase chain reaction
pI	Isoelectric point
PFK	Phosphofructokinase
PKA	cAMP-dependent protein kinase
PKB	Protein kinase B
PKC	Protein kinase C
PMSF	Phenylmethylsulphonylfluoride
PVDF	Polyvinylidene difluoride

SDS	Sodium dodecyl sulphate
SDS-PAGE	Sodium dodecyl sulphate polyacrylamide gel
TAE	Tris-acetate/EDTA buffer
TAME	N-a-tosyl-L-arginine methyl ester
TBE	Tris-borate/EDTA buffer
TCA	Trichloroacetic acid
TEMED	N,N,N',N'-tetramethylethylenediamine
TLCK	N-tosyl-L-lysine chloromethyl ketone
Tn	Troponin
TnC	Troponin C
TnI	Troponin I
TnT	Troponin T
UV	Ultraviolett
VLCAD	Very long chain acid dehydrogenase
WPW	Wolff-Parkinson-White syndrom

1 Chapter Introduction

1.1 Cardiovascular Disease

1.1.1 General

Heart failure is a world-wide public health problem. Usually, it is the common end-stage of most primary cardiovascular diseases, comprising coronary artery disease, hypertension, cardiomyopathy, myocarditis, diabetes, valvular disease and congenital heart malformations. Heart failure is a complex pathophysiological condition occurring as the myocardial performance being unable to adequately supply blood to other organs.

It is one of the most common diseases in internal medicine with estimated more than 10 million affected people in Europe and 1.5 million in Germany. Furthermore, there are another 10 million suffering from a cardiac insuffiency without symptoms. Prevalence and incidence are age-related. In the population of people between 45 and 55 years of age less than 1% are suffering from heart failure. In the class of 65 and 75 2- 5% are affected already, whereas in the group of people older than 80 years of age heart failure is present in almost 10% (Herold, 2005).

In Germany in a gender relation of 1.5 : 1, men are more affected than women with the same years of age. Particularly the proportion of diastolic heart failure increases in older women and accounts for more than 40% in contrast to 30% in men.

In the United States it accounts for about 40% of all postnatal deaths, totalling more than 750.000 individuals annually and nearly twice the number of deaths caused by all forms of cancer combined (Robbins & Cotran, 2006).

Although the proteins that are addressed in this study deal with a hereditary form of cardiomyopathy, it is important to keep in mind that ischemic heart disease is responsible for 80% to 90% of cardiovascular deaths in the developed world. Additionally, it is the predominant cause of disability and death in the industrialized nations.

The annual burden of heart failure in Germany is estimated to be about 3.000 million € (knhi.de/Kompetenznetz/Veranstaltungen/Symposien/2006-Essen/KNHISym2006 Essen-13.pdf). That is more than 50 % of the yearly cost of the entire health system.

Most treatments slow down the process of progression but cannot abolish it. As a result an increasing proportion of the population is living with heart disease and is at risk of heart failure.

Five categories of diseases account for almost all cardiac mortality:

- Congenital heart disease
- Ischemic heart disease
- Hypertensive heart disease (systemic and pulmonary)
- Valvular heart disease
- Nonischemic (primary) myocardial disease

The failing human heart is distinguishable from the normal heart in structure as well as in its function. The exquisitely designed muscle of the heart serves in physiologic conditions as a pressure-and-suction-pump integrating two independent vascular systems, the pulmonary and the systemic circulation. Subsequently to the initiation of cardiovascular disease, the heart most often remodels along one of two pathways, hypertrophy or dilation (Seidman & Seidman, 2001). The process of remodelling may be a compensatory mechanism to adjust the function of the organ in the disease state. In response to systemic hypertension, aortic valve disease or congenital malformations, the heart develops hypertrophy, which is defined as an increase in the muscle mass in order to maintain the blood supply under these conditions. Myocardial hypertrophy as a compensatory mechanism takes place through increase of cardiac muscle cell mass not through increase of cell number (hyperplasia). Hypertrophy often occurs with a rise in cardiac fibrosis. Consequently there is an increase in the extracellular matrix and an increase in the interstitial fibrosis of the affected heart. This may impair the elasticity of the myocardium and therefore ventricular relaxation. The increased stiffness of the cardiac wall can alter the function of the organ in a broader sense. Due to impaired relaxation, blood emptying from the atrium is not complete, which causes stretching of the atrial walls and secondary a dilation of these thin walled chambers. Unsurprisingly, atrial dilation is a commonly seen feature of the hypertrophied heart.

The remodelling mechanism occurring in response to diminished contractile function produces a dilated ventricular chamber, which results from myocyte death (apoptosis). Dilation is always associated with mild increase in myocyte hypertrophy as well as increase in interstitial fibrosis. The extension of the intraventricular volume reflecting

predominantly a physiological adjustment mechanism, stretches the myocytes and improves the pressure-volume relationship within the heart as well as it augments the cardiac output (Frank-Starling-mechanism).

One has to keep in mind that compensatory remodelling mechanisms of the heart initially are beneficial to the cardiac function, although they eventually become maladaptive.

Ultimately, the cardiac remodelling may cause a failing heart. Hypertrophy as well as dilation of the heart increase the stiffness of the myocardium triggering an impeded ventricular relaxation, which worsens the coronary artery blood flow, because private blood supply of the heart tissue occurs predominantly during the diastole (cardiac relaxation). Furthermore, it will cause an increasing energy demand.

Unlike the gross anatomical and pathohistological findings in remodelled hearts, the cellular, molecular and triggering mechanisms are largely unknown (Seidman & Seidman, 2001).

1.2 Primary Cardiomyopathies

The term cardiomyopathy (literally, heart muscle disease) is used for describing heart diseases resulting primarily from the myocardium (Richardson *et al.*, 1996). In many cases cardiomyopathies are idiopathic.

In contrast to the situation described above, there has been significant progress in understanding the pathomechanism of primary cardiomyopathies. These diseases cause also cardiac remodelling, but in absence of other underlying cardiovascular pathologies.

A major advance in our understanding in myocardial diseases, previously considered as idiopathic, has been the identification of specific genetic mutations in structural or contractile proteins, but also in proteins involved in the cardiac energy metabolism of the cardiomyocyte, which are responsible for myocardial dysfunction in many patients.

The clinical approach is largely determined by one of the following clinical, functional and pathological patterns:

- Hypertrophic cardiomyopathy (HCM)
- Dilated cardiomyopathy (DCM)
- Restrictive cardiomyopathy
- Arrhythmogenic right ventricular dysplasia (ARVD, also known as arrhythmogenic right ventricular cardiomyopathy or ARVC)
- Non-compaction cardiomyopathy (NCC)

DCM is the most common disease among these five categories, followed by HCM and the others.

The gene *MYBPC3* encoding for the Myosin binding protein-C is causing about 30-35% of all HCM cases (Watkins *et al.*, 1995) meaning it is one of the most common affected sarcomeric genes. But as discussed further down in this study, HCM reveals to be a much more complex disease, most likely also emerging from mutations concerning the energy metabolism of the cell, e.g. mutations in the *PRKAG2*-Gene, which encodes for the AMP-activated proteinkinase.

1.3 Hypertrophic cardiomyopathy

1.3.1 Disease Phenotype

The British pathologist Donald Teare presented the first description of hypertrophic cardiomyopathy in detail in 1958 (Teare, 1958). According to the current available textbooks it is inherited in a mendelian autosomal dominant pattern caused by mutations in any of 9 sarcomeric genes. Epidemiological studies have pointed out a prevalence of phenotypically expressed HCM of one in 500, and therefore, the most common genetic cardiovascular disorder (Maron *et al.*, 1995).

It is characterised at the gross anatomical and clinical level by hypertrophy of the left ventricular myocardium in the absence of any other diagnosed etiology.

The overall clinical phenotype of patients suffering from HCM is broad, ranging from a complete lack of cardiovascular symptoms to exertional dyspnea, angina pectoris and cardiac death often due to arrhythmias. However, the most devastating component is the sudden cardiac death (SCD), often in the absence of precedent

symptoms (Spirito *et al.*, 1997). It is the most common cause of SCD death in young athletics.

The mechanism of heart failure is an impairment of compliance, which causes a diastolic dysfunction.

1.4 Molecular Genetics of Hypertrophic Cardiomyopathy

1.4.1 HCM- a Sarcomeric Disease?

HCM has become to be considered as a "disease of the cardiac sarcomere" (Richard *et al.*, 2003). Until today, 9 gene loci encoding for proteins of the sarcomeric apparatus, with more than 400 mainly missense mutations have been identified predominantly by positional cloning. Despite this knowledge, in only about 60% of patients suffering from HCM a sarcomeric gene mutation is detected. This raised the hypothesis that some mutations may have been missed by the indirect sequencing techniques used, but such a significant proportion suggests also other causative genes leading to HCM remain to be identified (Ashrafian *et al.*, 2003; Ashrafian & Watkins, 2007).

Studying the genetic findings led to the proposal that incorporation of mutant sarcomeric proteins is not capable to permit normal myocyte contractility, triggering compensatory mechanisms that cause muscular hypertrophy (Lankford *et al.*, 1995; Watkins *et al.*, 1996; Marian, 2000). However, *in vitro* protein assays revealed divergent results: the majority of known mutations in sarcomeric proteins enhance contractility (Redwood *et al.*, 1999). Therefore, the compensatory theory was consequently refuted.

More recently, in patients with a hypertrophied myocardium a couple of genetic missense mutations were detected, encoding for proteins linked to the energy metabolism in the cell (e.g. *PRAKG2*, *CSRP3*) (Blair *et al.*, 2001; Geier *et al.*, 2003).

Chromosomal Locus	*Gene*	*Protein*	*Inheritance*
1q32	TNNT2	Cardiac troponin T	AD
2q31	TTN	Titin	AD
3p21	MYL3	Ventricular essential myosin light chain	AD & AR(?)
7q36	PRKAG2	AMPK-γ2 subunit	AD
11p11	MYBPC3	Cardiac myosin-binding protein C	AD
11p15	CSRP3	Cardiac muscle LIM protein	AD
12q23–q24	MYL2	Ventricular regulatory myosin light chain	AD
14q12	MYH7	β-myosin heavy chain	AD
15q14	ACTC	α-cardiac actin	AD
15q22	TPM1	α-tropomyosin	AD
19q13	TNNI3	Cardiac troponin I	AD
Xq24	LAMP2	Lysosome-associated membrane protein	X-linked

Table 1-1: *HCM and phenotypically similar syndromes: Genes, chromosomal loci, gene product and mode of inheritance; AD, autosomal dominant; AR, autosomal recessive; AMPK, AMP-activated protein kinase; (Ashrafian & Watkins, 2007)*

Further, it is well known that diseases causing defects in cardiac energy metabolism, such as Friedreich's ataxia and Senger's syndrome exhibit HCM-like phenotypes. These data arose the widely accepted theory that HCM is a disease of energy deficiency (Ashrafian *et al.*, 2003; Ashrafian & Watkins, 2007). Mutations in sarcomeric proteins are a potent source of energy deficiency subsequently to inefficient ATP usage (Sweeney *et al.*, 1998; Ashrafian *et al.*, 2003).

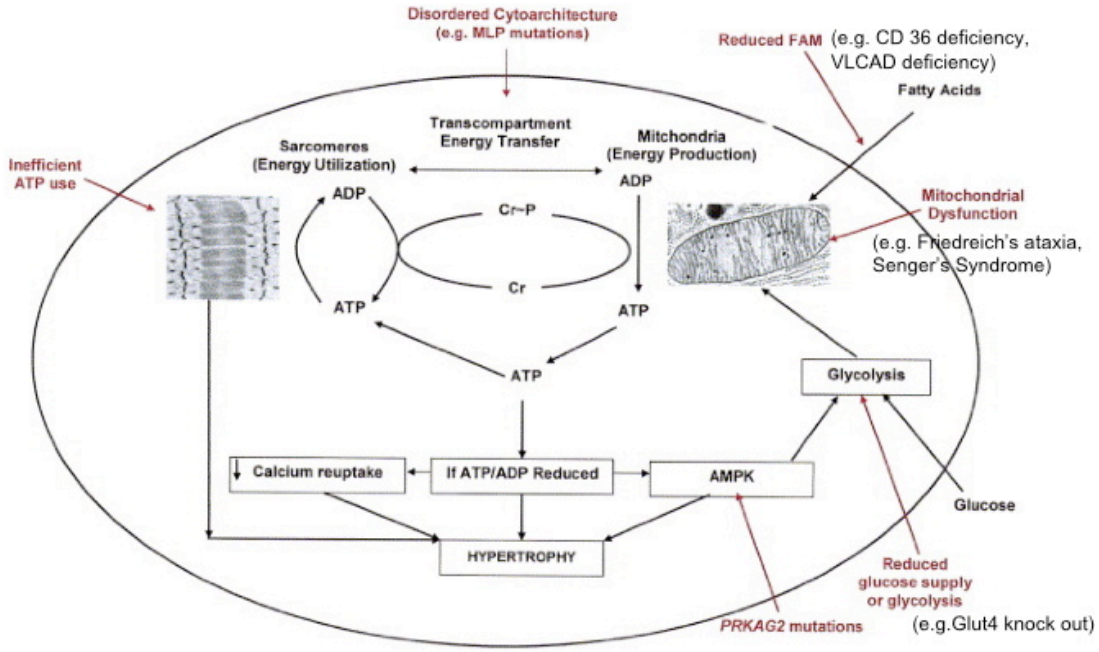

Figure 1–1*: As indicated in red, the phenotype of hypertrophic cardiomyopathy (HCM) can arise from: 1) excessive energy use (e.g., by aberrant sarcomeres); 2) inadequate energy production (e.g., from poorly functioning mitochondria), inadequate metabolic substrates, or a failure to transfer energy across cellular compartments owing to cytoarchitectural defects as exemplified by muscle LIM protein*

(MLP) mutations; or 3) aberrant signaling of energy deficiency (e.g., with AMP-activated protein kinase [AMPK] mutations). The final common path for these diverse defects is energy deficiency and ensuing hypertrophy. ADP, adenosine diphosphate; AMP, adenosine monophosphate; ATP, adenosine triphospate; Cr, creatine; FAM, fatty acid metabolism; VLCAD, Very long chain fatty acid dehydrogenase. Modified from Ashrafian & Watkins, 2007.

Taken together, HCM has revealed to be more complex than anticipated and the mutual feature of left ventricular hypertrophy of the mentioned genetic disorders seems to emerge from energy deficiency, caused by ineffective use (e.g. sarcomeric protein mutations), inadequate production (e.g. Friedreich's ataxia) or inappropriate response of energy generating pathways (e.g. *PRKAG2* mutations).

1.5 The Myosin Binding Protein C

The myosin binding protein-C (MyBP-C) is a thick filament-associated protein, which is localized to the crossbridge containing C-zones of the sarcomere. 35 years after its discovery, the precise function remains still obscure. Via interaction at its C-terminus with the light meromyosin proportion of myosin and the giant protein titin, MyBP-C contributes to the structure of the sarcomeric apparatus. On the other hand, the N-terminal region seems to play a regulatory role for the actomyosin ATPase, and therefore for the rate of crossbridge cycling. Additionally, evidence has recently emerged that alteration of the phosphorylation status of the MyBP-C may contribute to cardiac ischemia-reperfusion injury (Sadayappan *et al.*, 2006; Yuan *et al.*, 2006).
The C-terminal domains of MyBP-C are the subject of this study. Hence, the properties and functions of this protein will be described in detail.

1.5.1 Characterisation of MyBP-C

1.5.1.1 Initial Isolation as a Novel Myosin-Binding Protein

Early X-ray diffraction and electron microscopy studies on vertebrate skeletal muscle revealed the presence of meridional reflections solely located in the A-band. In 1971, Offer and co-workers were interested in these reflections, which were unlikely thought to originate from myosin itself, due to their specific localisation. Separation of myosin preparations by SDS-polyacrylamide electrophoresis consistently revealed a series of unidentified thick filament associated proteins (Starr & Offer, 1971). Further fractionation of these led to the identification of MyBP-C (originally termed

C-protein from impurifying band C) as a myosin associated protein (Offer *et al.*, 1973). It occurs as a single polypeptide with a molecular weight of 135± 15 kDa.

1.5.1.2 Localisation to the A-Band of the Sarcomere

Determination of the localisation of the MyBP-C took place via antibody staining of skeletal muscle fibers (Pepe & Drucker, 1975; Craig & Offer, 1976). On each filament in the C-zone of the A-band, 11 stripes appear, irrespective of the filament lengths (Craig & Offer, 1976), 7-9 of which are thought being caused by the MyBP-C; the precise number seems to be dependent on muscle type and has not been reported for cardiac muscle. Each stripe is 43 ± 0.2nm apart (see also refs. Rome *et al.*, 1973; Bennett *et al.*, 1986). Due to the fact that myosin cross-bridges have a periodicity of 42.9 nm (Huxley & Brown, 1967), it is possible that the spacing of both proteins is in register, but alternative studies by Squire and co-workers (Squire *et al.*, 1982) proposed that there are in fact two slightly different axial repeats in the C-zone: 42.9 nm repeats assigned to myosin cross-bridges, and 43.4 nm repeats which may correspond to MyBP-C. The fact that MyBP-C can be labeled with antibody indicates that it lies on the surface of the myosin filaments, and transverse sections of stained muscle also suggest that it wraps around the circumference of the thick filament (Craig & Offer, 1976).

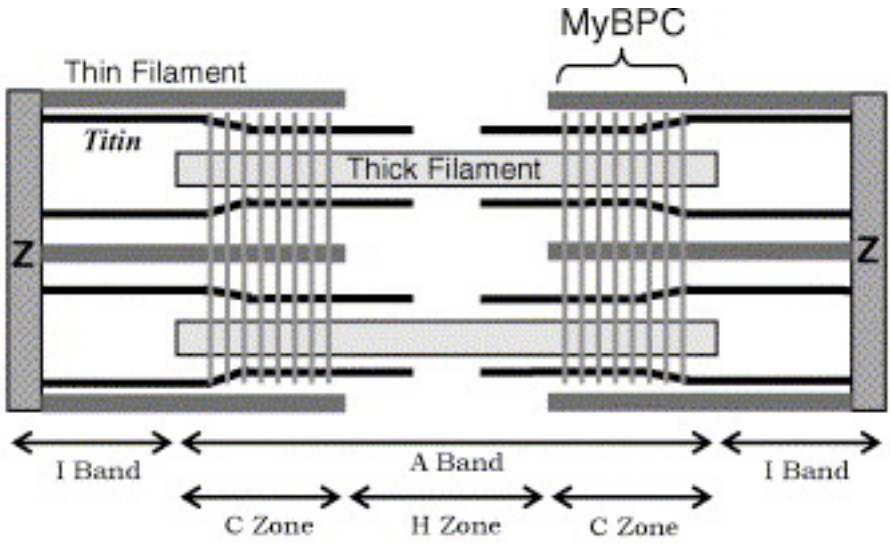

***Figure 1–2**: Location of MyBP-C in the sarcomere. It is seen as 7-9 transverse stripes 43nm apart in the C- zone. (Oakley* et al.*, 2007)*

1.5.1.3 Early Structural Characterisation of MyBP- C

The purified skeletal C-protein occurs as a single polypeptide chain primarily as β-sheet with a very low α-helical fraction, as its high proline content suggests (Offer *et al.*, 1973; Furst *et al.*, 1992). At low (physiological) ionic strength, the sedimentation

coefficient indicates a dimerisation of the protein (Offer *et al.*, 1973). This has been supported by further work carried out by Hartzell & Sale, 1985. The full length of the extended bovine skeletal isoform is about 50nm (Furst *et al.*, 1992). In contrast, investigations on cardiac and skeletal chicken MyBP-C has been delineated that a large proportion of the molecules occurs in a V-shape with one arm consistently longer than the other. The vertex of the V- shape seems to have a globular form (Hartzell & Sale, 1985; Swan & Fischman, 1986).

1.5.1.4 Isoforms of MyBP C and other Myosin Binding Proteins

MyBP-C is present not only in cardiac muscle, but also in fast skeletal and slow skeletal (originally described as MyBP-X) muscle. The genes encoding for the human fast *(MYBPC2)* and slow skeletal (*MYBPC1*) isoform are on chromosomes 19q13.33 and 12q23.3, respectively (Weber *et al.*, 1993) and the gene for the cardiac isoform (*MYBPC3*) is found on chromosome 11p11.2 (Gautel *et al.*, 1995). These data demonstrate that the isoforms are not products of alternative splicing. In 1980, Jeacocke and England identified the cardiac isoform via phosphorylation studies of heart muscle extract (Jeacocke & England, 1980). Immunohistochemistry studies revealed that the fast and the skeletal isoform can be seen together in some muscle types (Reinach *et al.*, 1983; Dhoot *et al.*, 1985), and one year later they were seen even to coexist within the same sarcomere (Reinach *et al.*, 1983). Yet in early studies, was reported the cardiac isoform being larger than the skeletal ones (Yamamoto & Moos, 1983).

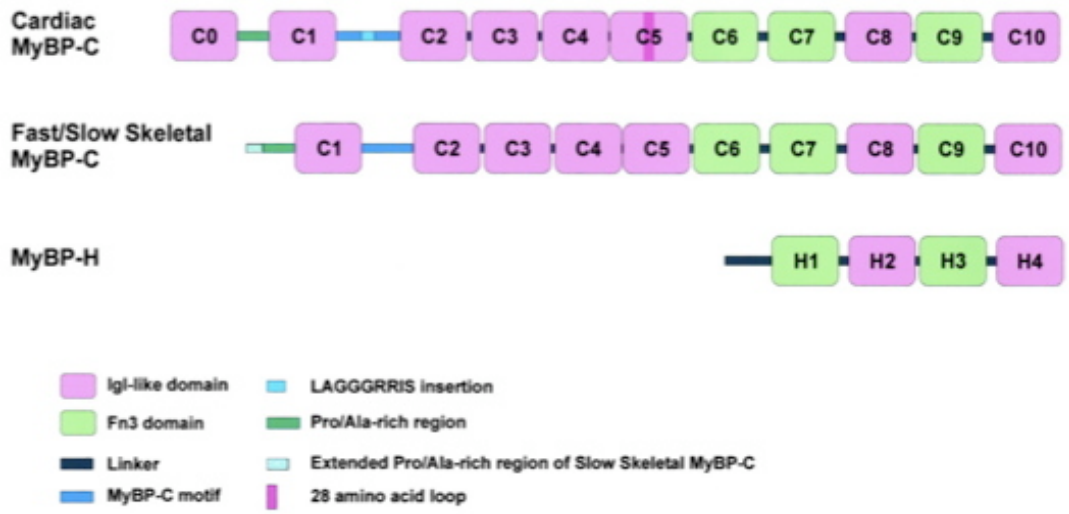

***Figure 1–3**: Sequence structure of MyBP-C isoforms. (Flashman* et al.*, 2004)*

Furthermore, Starr and Offer detected a related protein, MyBP- H (Starr & Offer, 1971) consisting of 4 domains that has a 50% identity to the four C terminal domains of MyBP-C (Vaughan *et al.*, 1993a; Vaughan *et al.*, 1993b). It has been localized to the third stripe of the 11 seen in the C-zone (Bennett *et al.*, 1986; Starr *et al.*, 1985).

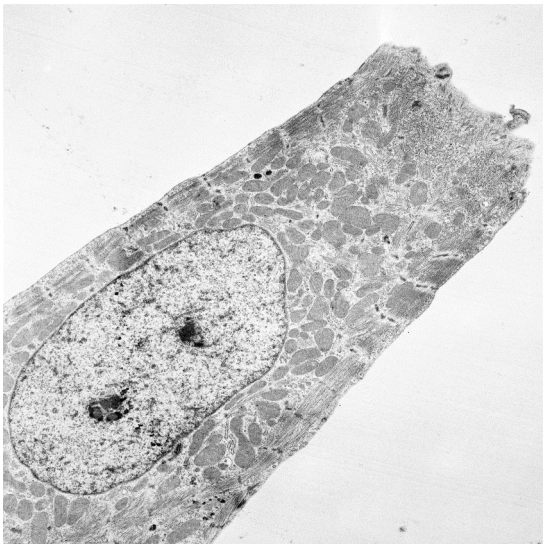

***Figure 1–4**: EM photograph of isolated chicken heart muscle cell (own micrograph; magnification x2500)*

1.5.1.5 MyBP-C Expression Patterns

In the mammalian heart, MyBP-C is expressed along with myosin and titin at an early stage (gestation day 8 for mice and week 11 for the human foetus). At no point is either of the skeletal isoforms expressed in the heart. In the skeletal muscle development, the skeletal MyBP-C isoforms are seen later, after myosin and titin expression. Gautel *et al.* have also reported an embryonic isoform (Gautel *et al.*, 1998), which is believed to be the cardiac isoform at least in chicken and axolotl (Ambystoma mexicanum) (Bahler *et al.*, 1985; Kawashima *et al.*, 1986; Ward *et al.*, 1996), unlike in mice, where the cardiac isoform is not transcribed at all during skeletal muscle development (Kurasawa *et al.*, 1999).

1.5.1.6 Structure of MyBP- C

All three isoforms share a common structure of 10 globular domains numbered C1-C10, 7 of which are IgI-like domains with the remaining three being Fn3 domains. Domains C1 and C2 are separated by a conserved linker, called MyBP-C motif (Gautel *et al.*, 1995) consisting of approximately 100 amino acids. The N-terminus of C1 is extended by a short proline/alanine-rich sequence.

There are three specific characteristics occurring just in the cardiac isoform: an additional N-terminal Ig-I like domain termed C0 (Carrier *et al.*, 1997), a nine amino

acid insertion (LAGGGRRIS) within the MyBP-C motif (Gautel *et al.*, 1995) and a 28-amino acid insertion within the C5 domain (Gautel *et al.*, 1995).

Additionally, there are three phosphorylation sites within the MyBP-C motif (A, B and C), one of which being on the LAGGGRRIS insertion (B). These cardiac specific features are conserved across species and have been shown in the sequence of mouse and chicken cardiac MyBP-C (Carrier *et al.*, 1997).

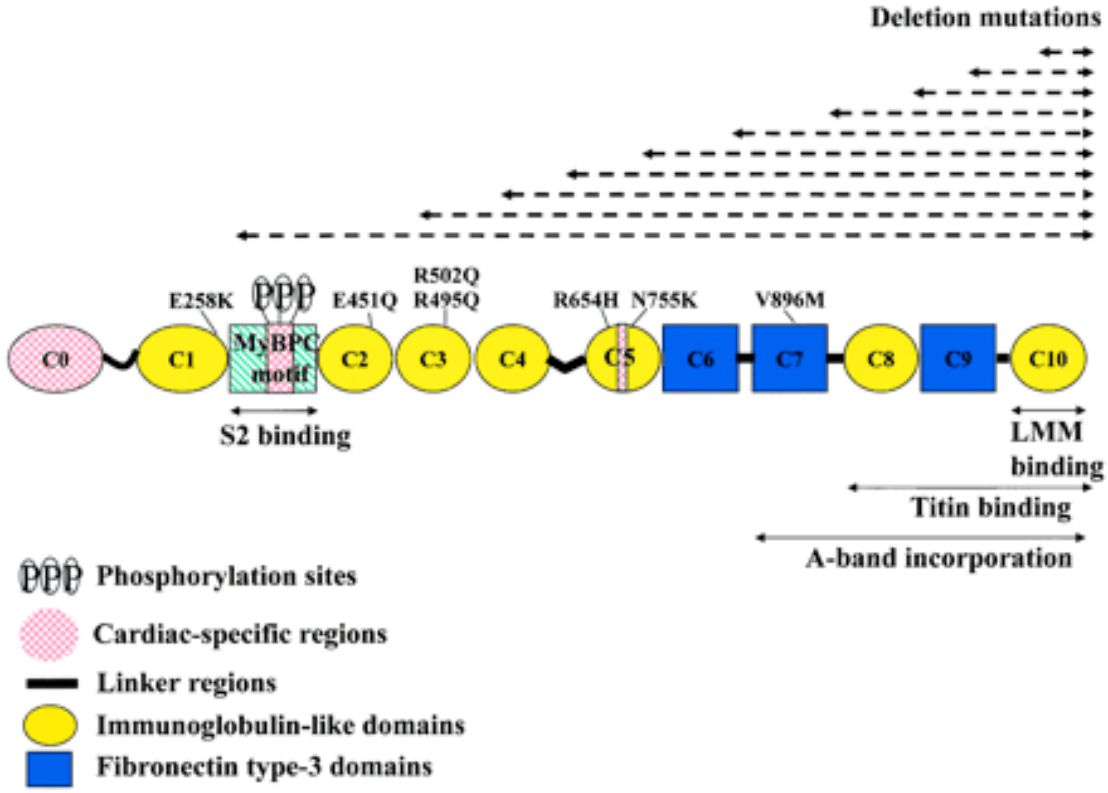

***Figure 1–5**: Structure of cMyBP-C; (Moolman-Smook* et al.*, 2002)*

1.5.2 Biological Function

1.5.2.1 Sarcomere Assembly and Stability

1.5.2.1.1 Binding to the Light Meromyosin Portion of the Myosin Rod

Studies performed by Okagaki *et al.* (Okagaki *et al.*, 1993) confirmed the expectation that MyBP-C binds to the light meromyosin (LMM) portion of the myosin rod, forming the backbone of the thick filament.

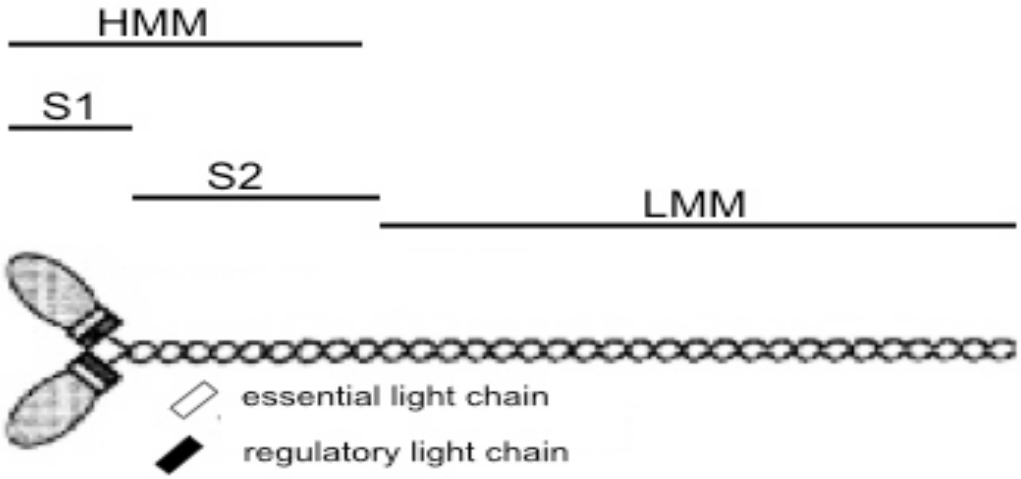

***Figure 1–6**: Structural elements of the myosin molecule; (Gruen & Gautel, 1999)*

The domain involved in this interaction could be narrowed to the C-terminal domain C10 of MyBP-C (Okagaki *et al.*, 1993; Alyonycheva *et al.*, 1997) for all isoforms and the homologous H4 domain of MyBP-H. By using a range of N-terminally truncated LMM fragments, Flashman *et al*. have shown the cMyBP-C site on LMM lying between the residues 1554 and 1581 *in vitro* (Flashman *et al.*, 2007).

1.5.2.1.2 Binding to Titin

Another interaction of the C-terminal region of MyBP-C occurs with the giant protein titin (Furst *et al.*, 1992; Labeit *et al.*, 1992; Koretz *et al.*, 1993; Soteriou A, 1993). Titin lies most likely as three pairs along the length of the filament (Squire *et al.*, 1998; Liversage *et al.*, 2001). Furthermore, C9 or C10 of MyBP-C has been shown being the binding domain, due to the fact that C8-C10 fragment binds to titin, whereas C5-C10 does not (Freiburg & Gautel, 1996).

The precise localisation of the MyBP-C is thought being defined by its interaction with titin. This hypothesis is supported by the facts that the 11 super-repeats only occur in the C-zone and each 11-domain repeat has a periodicity of 43 nm like the MyBP-C rich stripes (Flashman *et al.*, 2004). It is important to keep in mind that MyBP-C does not appear in stripes 1 and 2, therefore it seems reasonable to assume that additional factors must be present to direct MyBP-C in its particular position.

Interactions of MyBP-C with LMM and titin are considered to stabilise the sarcomeric structure at least *in vitro*. This suggestion emerged from studies carried out by Moos *et al.*, 1975 as in the presence of MyBP-C recombinant myosin filaments displayed an increased length, improved structure and compactness of the bulk (Flashman *et al.*, 2004). Furthermore, a disordered sarcomeric structure has been shown, if binding

sites of the MyBP-C and/or titin are missing (Winegrad, 1999). Therefore, MyBP-C might act as a molecular regulator for length of the thick filament due to assembly of the sarcomere.

Two different MyBP-C knock out mouse models have been established (Harris *et al.*, 2002; Carrier *et al.*, 2004). Surprisingly, both models were viable, suggesting that MyBP-C acts in a modulatory way rather than in an essential one. As one would expect, these models exhibited severe cardiac hypertrophy, myocyte disarray and increased amounts of interstitial fibrosis.

In summary, the *in vitro* and *in vivo* data suggest that beside the MyBP-C other factors must be responsible for correct sarcomeric assembly.

1.5.2.2 Contribution of the Regulation of Contraction

As mentioned above, the second role of the MyBP-C is characterized by its contribution to the regulation of muscle contraction, which is exerted by N-terminal binding to the subfragment-2 (S2) of myosin.

Gruen & Gautel, 1999 have shown this interaction is mediated by C1-C2, the N-terminal fragment that can incorporate in the A-band of the sarcomere without disrupting myofibrillar integrity. This interaction occurs in a phosphorylated state of the protein and is abolished following dephosphorylation (Gruen *et al.*, 1999; Flashman *et al.*, 2004).

In the cardiac isoform, three phosphorylation sites Ser273, Ser282 and Ser302 (A-C), have been reported. The order in which these sites are phosphorylated seems to be hierarchical, and it has been shown that kinases can modify these residues *in vitro*. Like the other two sarcomeric proteins, phospholamban and troponin I, cMyBP-C can be phosphorylated in response to β-adrenergic stimulation via cAMP-dependent protein kinase (PKA) (Jeacocke & England, 1980; Hartzell & Titus, 1982; Lim & Walsh, 1986; Garvey *et al.*, 1988; Venema & Kuo, 1993). *In vitro* studies also revealed a phosphorylation of all three sites by the tightly associated calcium/calmodulin-dependent kinase II (CaMII) (Hartzell & Sale, 1985; Schlender & Bean, 1991). A further kinase, the calcium/phospholipid dependent kinase (PKC), seems to phosphorylate only site A and C (Mohamed *et al.*, 1998; Winegrad, 1999; Flashman *et al.*, 2004; Sadayappan *et al.*, 2005). McClellan *et al.*, 2001 suggested phosphorylation of site B by PKA or CaMII lying on the cardiac specific LAGGGRRIS insertion as indispensable, before sites A and C could become

sterically available for phosphorylation by PKA. These results raised the presumption that site B may play an important role in modulation of the phosphorylation level of cMyBP-C. In response to cholinergic stimulation, cMyBP-C is dephosphorylated by phosphatase 1 or 2A (Schlender *et al.*, 1987).

Regarding the aims of this study is also worthwhile to mention that in the chicken sequence of cMyBP-C Ser1169, located closed to the C-terminus, could phosphotrylated by PKC (Mohamed *et al.*, 1998).

The precise role of cMyBP-C is still under investigation; a current model is shown in **Figure 1–7**.

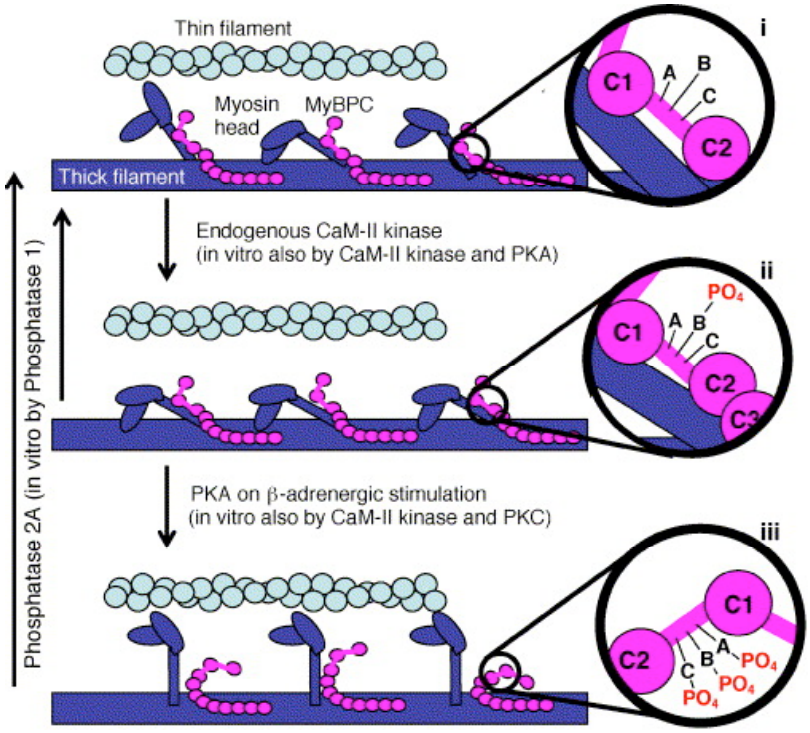

Figure 1–7: *Cardiac MyBP-C phosphorylation. (i) When dephosphorylated MyBP-C binds to myosin-S2 via some part of the C1–C2 region, Myosin heads appear disordered. (ii) The endogenous CaM-II-like kinase adds the first phosphate to site B (this serine can also be phosphorylated in vitro by PKA). Myosin heads appear to be lying on the backbone. It is unclear whether C1–C2 is still binding. (iii) The second and third phosphates are added to site A and site C by PKA, or in vitro by PKC or CaM-II kinase. C1–C2 no longer binds to myosin-S2 and the myosin heads appear ordered and extended. There is also a decrease in ATPase activity and an increase in Fmax and Ca^{2+} sensitivity. MyBPC is dephosphorylated by phosphatase 2A in vivo and phosphatase 2A or phosphatase 1 in vitro.(Oakley* et al.*, 2007)*

Upon MyBP-C phosphorylation, an alteration in thick filament structure seems to occur. Levine *et al*. described an increased optical diffraction and filament thickness after phosphorylation of MyBP-C by PKA (Levine *et al.*, 2001).

Following phosphorylation of all three sites, myosin heads appear extended from the myosin rod (Weisberg & Winegrad, 1996). Furthermore, there was an increase in

order of the myosin heads and they took up a position that was more favourable for actin binding analogous to the pre-force generation "weak-binding" state of crossbridge cycle (Levine *et al.*, 2001). Additionally, McClellan and co-workers also found a positive correlation of force and Ca^{2+}-sensitivity with MyBP-C phosphorylation (McClellan *et al.*, 2001). An increase in the phosphorylation level revealed an increase in time to half-relaxation, maximum Ca^{2+}-activated force and also in Ca^{2+}-sensitivity leading to stimulation of contraction at a lower Ca^{2+} level (McClellan *et al.*, 2001). When the three phosphorylatable serine residues were replaced by nonphosphorylatable alanines in a transgenic mouse model, a depressed cardiac contractility was also observed (Sadayappan *et al.*, 2005). These data raised the view that phosphorylation of MyBP-C abolish the interaction of C1-C2 with the S2 fragment of the myosin molecule.

Furthermore, a report by Herron *et al.*, 2006 is notable. They presented for the first time data, showing that N-terminal fragments (C0C1 and C0C2) of cMyBP-C could affect force production and crossbridge activity in skinned myocyte fibers from rodent and human ventricles in a previously unknown way. These results indicate that cMyBP-C could switch on crossbridge cycling in the virtually absence of Ca^{2+}. In previous studies, as N-terminal fragments of cMyBP-C either containing C0 (Kulikovskaya *et al.*, 2003) or C1C2 (Wolff *et al.*, 1995) were used, this phenomenon was not seen.

Taken together, MyBP-C contributes to myosin thick filament structure, but the importance of this issue is not well understood. However, the abolished interaction of MyBP-C and subfragment 2 increases the actomyosin ATPase activity (Flashman *et al.*, 2004) and MyBP-C acts, therefore, with other proteins as a regulator of contraction.

1.5.2.3 Models of the Arrangement of cMyBP-C on the Thick Filament

Early publications about MyBP-C suggested a multimerization of this protein (Offer *et al.*, 1973; Hartzell & Sale, 1985), and subsequently several models of MyBP-C's arrangement in the sarcomere have been proposed. In 1999, Winegrad suggested a model, whereby three MyBP-C molecules form a collar around the myosin rod, with the three C-terminal domains of one molecule binding to the three N-terminal domains of the next one (Winegrad, 1999). Based on the observation of an increase in thick filament diameter on cMyBP-C phosphorylation of this group (Weisberg &

Winegrad, 1998; Winegrad, 1999; Levine *et al.*, 2001), it has also been speculated that the postulated interaction between C1-C2 and C8-C9 would be disrupted on phosphorylation of the MyBP-C motif. Thus, the interacting domains would shift, and binding would instead occur between domains C0 and C10, resulting in an expansion of the collar sufficient to still encircle the myosin filament. Another model for the binding of MyBP-C to the thick filament incorporating a potential interaction of MyBP-C to the thin filament has been hypothesized recently (Squire *et al.*, 2003). In this model, the C-terminal domains of MyBP-C lie along the thick filament, and the N-terminal region is extending perpendicularly in the interfilamental space toward the actin filament. This arrangement respects the fact that C8-C10 is involved in titin binding (Freiburg & Gautel, 1996).

Based on work carried out in the laboratory of Prof. H. Watkins, pointing an interaction of C5:C8 and C7:C10 (Moolman-Smook *et al.*, 2002), Flashman *et al.* proposed a trimeric collar model, which is the most favoured one in the literature today (Flashman *et al.*, 2004). More recently new support regarding this model arose from yeast-two-hybrid- and *in vitro* binding-assays (Flashman *et al.*, 2008). In this model intermolecular interactions between staggered parallel cMyBP-C molecules encircle the thick filament. The C-terminal domains C5-C10 are believed to form the collar, whereas the N-terminal C0-C4 veer toward the interfilamental space, thereby interacting with subfragment S2 of the myosin molecule and very likely with the actin filament. This hypothesis is based on data suggesting an interaction between MyBP-C and actin via its proline/alanine rich region that is located at the N-terminus between C0 and C1 (Kulikovskaya *et al.*, 2003; Squire *et al.*, 2003).

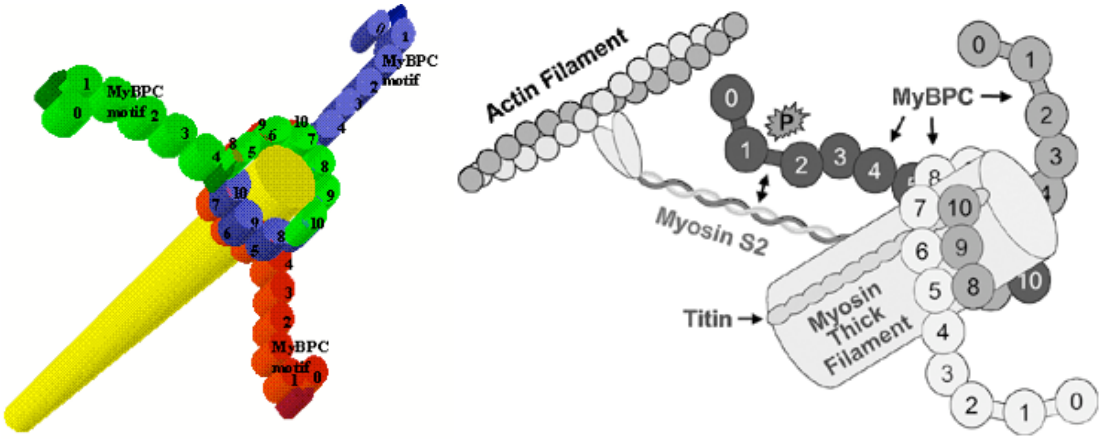

Figure 1–8: *(A) Proposed trimeric collar of MyBP-C molecules around the myosin backbone. Domains C5-C10 of each molecule overlap in staggered parallel arrangement, stabilized by interactions between domains C5-C8 and C7-C10. (B) Arrangement of MyBP-C in the structure of sarcomeric apparatus. (Moolman-Smook* et al.*, 2002)*

This model is consistent with early characterisation of MyBP-C (Moos *et al.*, 1975; Hartzell & Sale, 1985). The collar would have the circumference of the length of nine domains. Assuming that domains C5-C10 are equivalent to the long arm of a V-shaped structure seen by Hartzell & Sale, 1985, which is reported to be about 26 nm, and that these would account for about two thirds of the thick filament circumference, the collar dimensions would fit with the calculated backbone diameter of about 13-15 nm (Squire *et al.*, 1998; Flashman *et al.*, 2004). Furthermore, it seems very likely that the collar represents the ring of mass, seen by Eakins *et al.* at every third crown of the myosin head (Eakins *et al.*, 2002; Squire *et al.*, 2005).

1.5.3 Medical Implications

1.5.3.1 Hypertrophic Cardiomyopathy

As described earlier in this chapter familial hypertrophic cardiomyopathy (FHCM) is an autosomal dominant inherited disease that affects people with mutations in genes encoding for proteins in the contractile apparatus.

Mutations in *MYBPC3*, encoding for the cardiac myosin binding protein-C, is responsible for more than one third of all cases. Since the report of the first mutation in this gene in 1995 (Watkins *et al.*, 1995) until today nearly 150 mutations have been discovered (Richard 2006)(see also http://genetics.med.harvard.edu/%7eseidman/cg3/muts/MYBPC3_mutations_TOC.html for a full list). Approximately two thirds of them cause generation of truncated protein products either by mutation of a splice donor or acceptor site leading to irregular splicing or deletion mutations that cause a shift in the reading frame leading to translation of a nonsense protein or giving a premature stop codon. Furthermore, a few single-base mutations resulting directly in a premature stop codon have also been published. It is worthy of mention that for the remaining missense mutations, particular hot spots have not been reported. Due to the fact that patients with mutations in *MYBPC3* usually have a mild phenotype with a delayed onset of symptoms and a good prognosis (Arad *et al.*, 2002b), it is hypothesized that mutations in *MYBPC3* are the most common cause of HCM and the prevalence is underestimated (Richard *et al.*, 2003).

1.5.3.2 Ischemia-Reperfusion Injury

Recent reports have suggested that changes in MyBP-C phosphorylation are linked to cardiac ischemia reperfusion injury.

As mentioned above, Sadayappan *et al.* have shown a significant decrease of MyBP-C phosphorylation during the development of heart failure or pathologic hypertrophy (Sadayappan *et al.*, 2005). These findings are consistent with results obtained by Decker *et al.*, 2005, showing decreased phosphorylation of MyBP-C and accelerated degradation of the protein during low-flow ischemia.

Sadayappan's group generated a transgenic mouse model, which had phosphorylation sites A-C mutated to alanine residues. These animals revealed depressed contractility, altered sarcomeric structure and upregulation of mRNA-transcripts associated with hypertrophic response.

Taken together, these data suggest an essential role of MyBP-C phosphorylation for normal heart function.

One year after Sadayappan's report, a model has been constructed where the known three phosphorylation sites were mutated to aspartic acid, mimicking constitutive phosphorylation of cMyBP-C. Changes in sarcomeric ultrastructure, characterized by increased distances of thick filaments, as well as yeast two-hybrid- and cosedimentations-assays confirmed the presumption that charged residues in these positions sufficiently prevent interactions between MyBP-C and the myosin heavy chain. Furthermore, their data indicate a role of cMyBP-C in protection of the myocardium from ischemic injury (Sadayappan *et al.*, 2006).

In 2006, evidence was raised for novel phosphorylation sites that were detected in experiments during myocardial stunning, a period following episodes of ischemia and reperfusion (Yuan *et al.*, 2006). The finding of previously unknown phosphorylation sites demonstrates once more the essential role of MyBP-C phosphorylation associated with various stages of heart pathology.

1.6 The 5'-AMP- Activated Protein Kinase in the Heart

1.6.1 Characterization of the AMPK

The AMP-activated protein kinase (AMPK) is the central component of a highly conserved serine/threonine protein kinase cascade that exists in most mammalian tissues including heart muscle. This cascade plays a key role in the regulation of ATP levels in all tissues. The kinase, often referred to as a "fuel gauge" of cell energetic status, monitors the AMP/ATP ratio, making critical and continuous adjustments to

the relative balance of ATP-consuming and generating metabolic processes. Once activated, AMPK switches-on ATP-generating pathways, such as fatty acid oxidation and glycolysis, and switches–off many nonessential ATP-consuming anabolic pathways, such as fatty acid and protein synthesis, thus restores the energetic balance (Hardie & Carling, 1997; Hardie & Hawley, 2001; Hardie *et al.*, 2006).

Further, recent data have demonstrated that AMPK is also involved in the regulation of energy balance at the whole-body level (Kahn *et al.*, 2005; Towler & Hardie, 2007).

For a long time, the roles of AMPK were underestimated, but the past decade has revealed an exponential increase in interest in the function of this protein during health and disease. Nevertheless, the AMPK is far away from being completely understood.

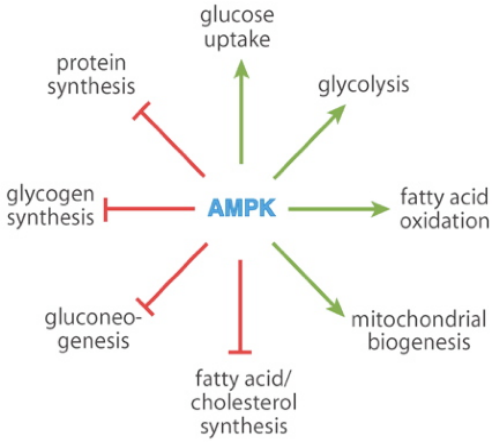

***Figure 1–9**: Key processes of energy metabolism regulated by AMPK. (Hardie* et al.*, 2006)*

1.6.1.1 The Structure of the Mammalian AMPK

AMPK is a heterotrimeric enzyme complex, consisting of one catalytic subunit (α) and two regulatory subunits (β and γ). Two isoforms of α and β subunit and three isoforms of the γ subunit are encoded in the mammalian genome (α1, α2, β1, β2, γ1, γ2, γ3) (Hardie & Carling, 1997; Hardie & Hawley, 2001), each being encoded by a different gene (*PRKAA1, PRKAA2, PRKAB1, PRKAB2, PRKAG1, PRKAG2, PRKAG3*). In humans, there have been two different γ2 mRNA transcripts reported, resulting from alternative promoters within *PRKAG2*. One encodes a 569 amino acid protein (here termed AMPK γ2 long) (Cheung *et al.*, 2000) and the other a shorter 328 amino acid protein, lacking the N-terminal extension (here termed AMPK γ2 short) (Lang *et al.*, 2000). Therefore, 16 heterotrimeric complex combinations are possible.

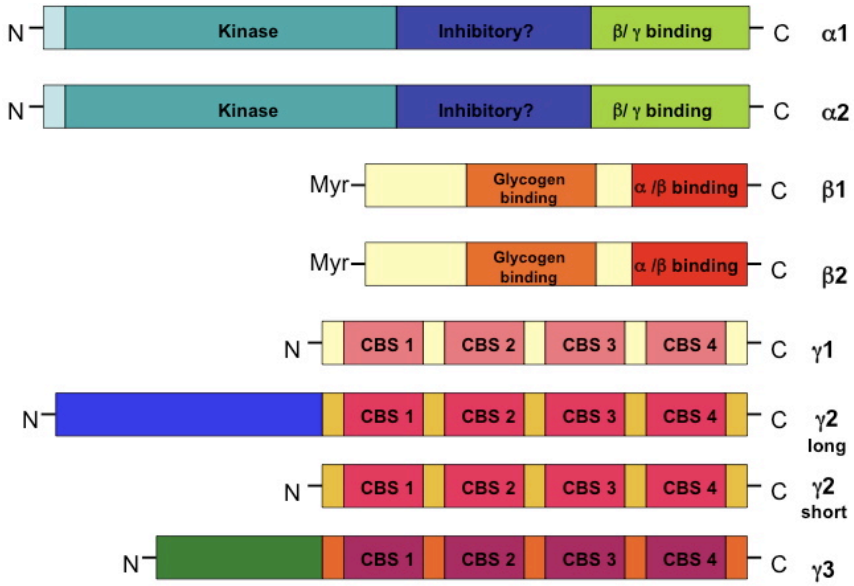

Figure 1–10: *Schematic representation of the structure of the known subunit isoforms of AMPK; Myr, myristoylation; CBS, cystathione β-synthase domain*

α1, β1 and γ1 are expressed in virtually every tissue and are described as housekeeping genes, therefore, they account for the majority of AMPK activity in the cell (Cheung *et al.*, 2000). In humans α2 and β2 are strongly expressed in skeletal and heart muscle and are thought to account for particular AMPK functions. The γ2 subunit has the highest sensitivity to AMP and is significantly expressed in several tissues including heart muscle. It is less abundant in skeletal muscle, where γ3 is expressed. In heart muscle predominantly appears a complex, consisting of α 2, β 2 and γ2 subunits (Arad *et al.*, 2007).

Each α subunit contains a phosphorylation site (Thr172) that plays a critical role in regulating AMPK activity. The β subunit has not only structural maintaining properties, but also myristoylation, phosphorylation and glycogen binding sites (Warden *et al.*, 2001; Hudson *et al.*, 2003; Polekhina *et al.*, 2003). One γ subunit is built out of four CBS motifs, named after cystathione β-synthase, which is found in a wide variety of proteins. A pair of CBS sequences forms a nucleotide-binding module called the Bateman domain. These modules can bind adenosyl compounds. Each γ subunit contains two of these nucleotide-binding-pockets, which are capable of a cooperative binding of two molecules either AMP or ATP, thereby regulating the interaction between γ and α subunits (Bateman, 1997; Hudson *et al.*, 2003; Kemp, 2004). At high levels of ATP, as occurs at rest, the enzyme is inhibited due to binding of ATP to the γ subunit (Frederich & Balschi, 2002). In contrast, AMP binding to the

γ subunit, activates the enzyme by three different mechanisms: allosteric activation, conformational changes that enables phosphorylation of Thr172 by upstream kinases (AMPKK) and the prevention of dephosphorylation of the α subunit (*Hardie*, 2003).

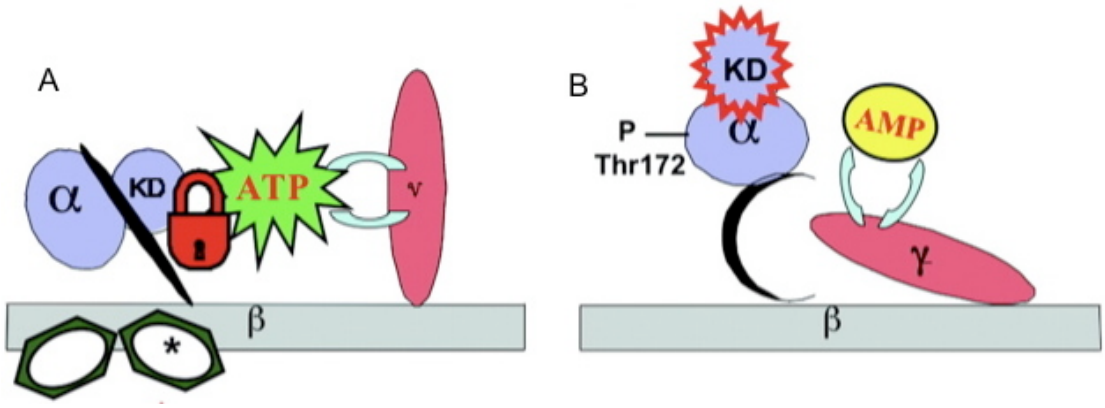

***Figure 1–11**: (A) under resting conditions, the enzyme is inhibited by ATP and possibly glycogen*. (B) During energetic stress, the γ subunit binds AMP causing a conformational change thereby allowing phosphorylation of the α subunit at Thr172 by upstream kinase, leading to activation of the enzyme. KD indicates the kinase domain of the enzyme complex. (Arad* et al.*, 2007)*

1.6.2 Biological Functions

1.6.2.1 AMPK in Cardiac Metabolism

As mentioned above, AMPK is thought to act as a regulator of the energy status of the cell metabolism (**Figure 1–12**). Nevertheless, the precise role played by AMPK in the cardiac metabolism is not well understood.

Questions that have to be answered in this context affect (i) particular functions of specific isoforms, (ii) identification of downstream targets and (iii) definition of activating stimuli as are known of AMP/ATP ratio.

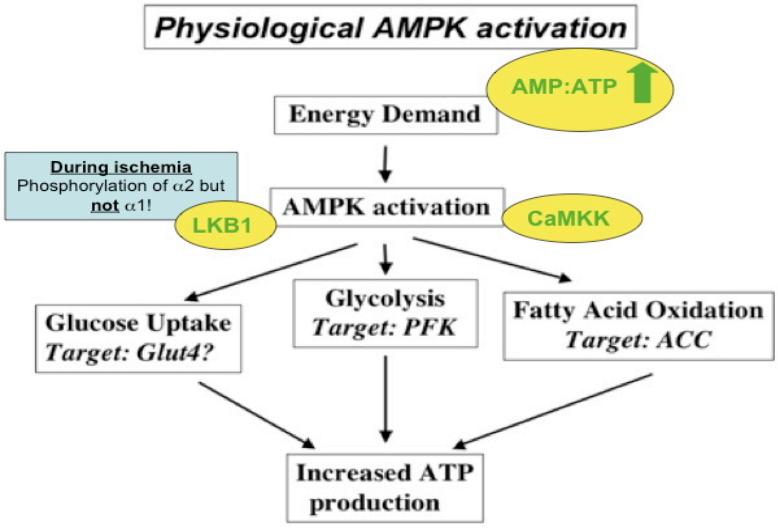

***Figure 1–12**: AMPK increases ATP production in response to increased energy demand via several mechanisms. CaMKK, calmodulin-dependent protein kinase kinase; Glut4, glucose 4 transporter; PFK, phosphofructokinase; ACC, acetyl-CoA carboxylase. Modified from Arad* et al.*, 2007*

Until today, two upstream kinases have been yet identified. LKB1, a kinase that appears to play a role in several cell processes including AMPK activation and the calcium/calmodulin-dependent kinase kinase (CaMKK) (Hawley *et al.*, 2003; Hawley *et al.*, 2005) that is activated in endothelial cells by nucleotides released from damaged tissue. Further, activation of AMPK via CaMKK occurs independently of AMP/ATP ratio (da Silva *et al.*, 2006).

1.6.2.2 AMPK in Cardiac Fatty Acid Metabolism

AMPK impairs fatty acid metabolism by regulating fatty acid uptake as well as oxidative phosphorylation (Dyck & Lopaschuk, 2006). Enhancing of the oxidative phosphorylation is mediated by inhibition via phosphorylation of the actetyl-CoA carboxylase. Subsequently, the concentration of malonyl-CoA decreases and disinhibition of carnitin palmitoyl transferase (CPT1) occurs. CPT1 is the key enzyme of oxidative phosphorylation and is located at the outer membrane of the mitochondria. Disinhibition of CPT1 means cardiac mitochondria are provided with the preferred substrate for energy production: alcyl carnitine.

Further, AMPK affects fatty acid metabolism by an increase of fatty acid uptake to cardiomyocytes by stimulation of protein expression and plasmalemma content of fatty acid transporter (FAT/CD36) and membrane-associated binding protein (FABPm) (Chabowski *et al.*, 2006). However, the exact mechanisms of stimulation are not yet known.

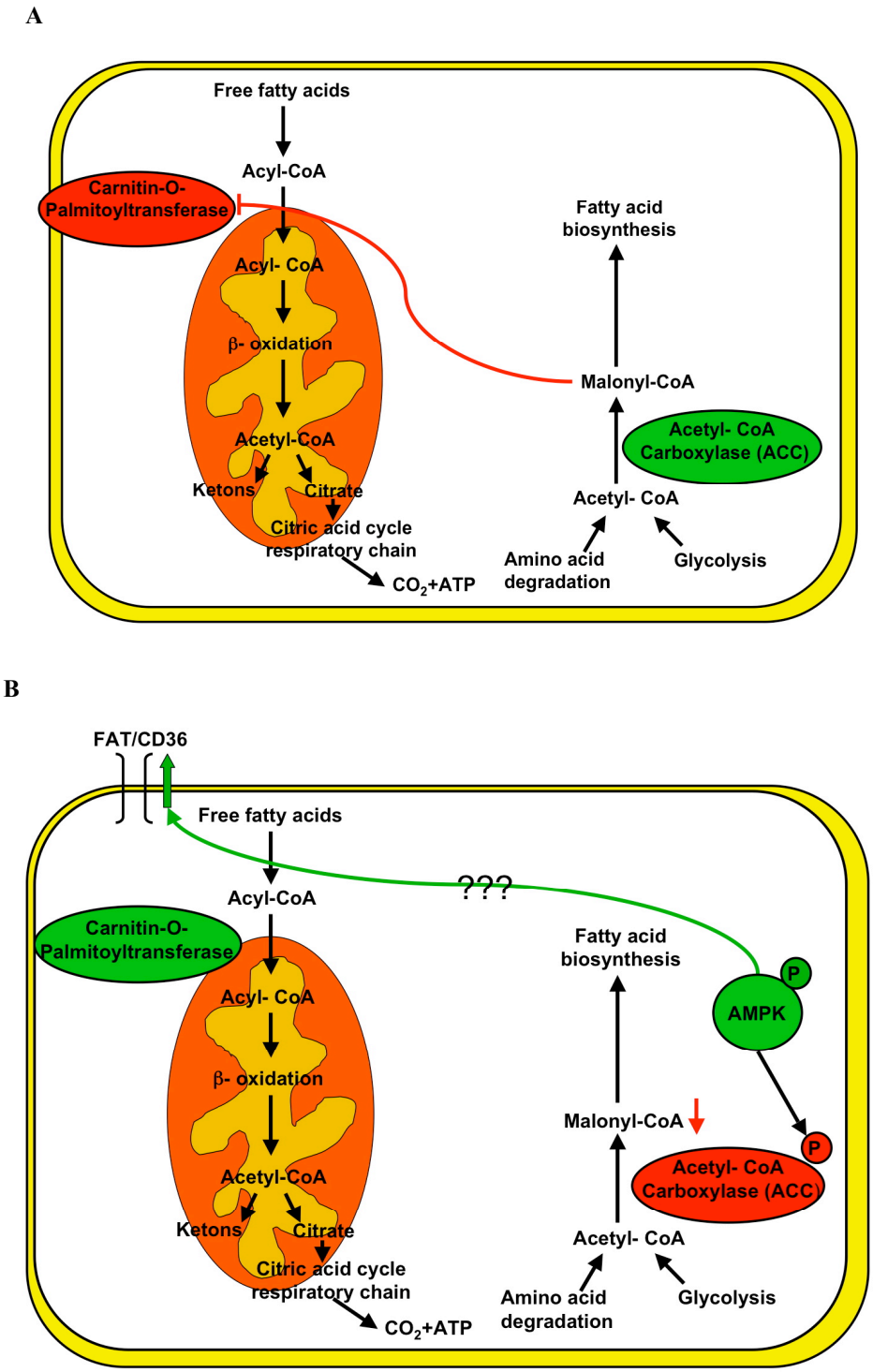

Figure 1–13: *(A) Inhibition of the carnitine palmitoyl transferase via malonyl-CoA. (B) Disinhibition, if ACC is phosphorylated and, therefore, concentration of malonyl-CoA decreases.*

1.6.2.3 AMPK in Cardiac Glucose Metabolism

Although the role of AMPK in glucose metabolism is incompletely understood, stimulation of glucose uptake is a broadly accepted mechanism (Luiken *et al.*, 2004). Different studies have shown an increased expression of GLUT 1 and GLUT4 transporters, whereby data about the involved targets are not uniform (Holmes *et al.*, 1999; Fryer *et al.*, 2002; Nishino *et al.*, 2004; Russell *et al.*, 2004; Li *et al.*, 2005; Yang & Holman, 2005).

However, an inactivation of AMPK via Akt as well as inhibition of the enzyme by insulin was reported. Surprisingly, there are data that suggest a potentialisation of insulin signalling downstream target B under pharmacological stimulation. This might be an approach to explain the properties of oral anti-diabetics of the biguanide type.

Further, glycolysis is stimulated by AMPK activating the key enzyme in the glycolytic pathway, phosphofructokinase (PFK1), indirectly by phosphorylation of PFK2, which converts fructose-6-phosphate to fructose-2,6-bisphosphate, an allosteric stimulator of PFK1 (Marsin *et al.*, 2000) (**Figure 1–14**). Due to this fact, AMPK seems to play an essential role in the response to cellular stresses like anaerobic exercise and hypoxia (Arad *et al.*, 2007).

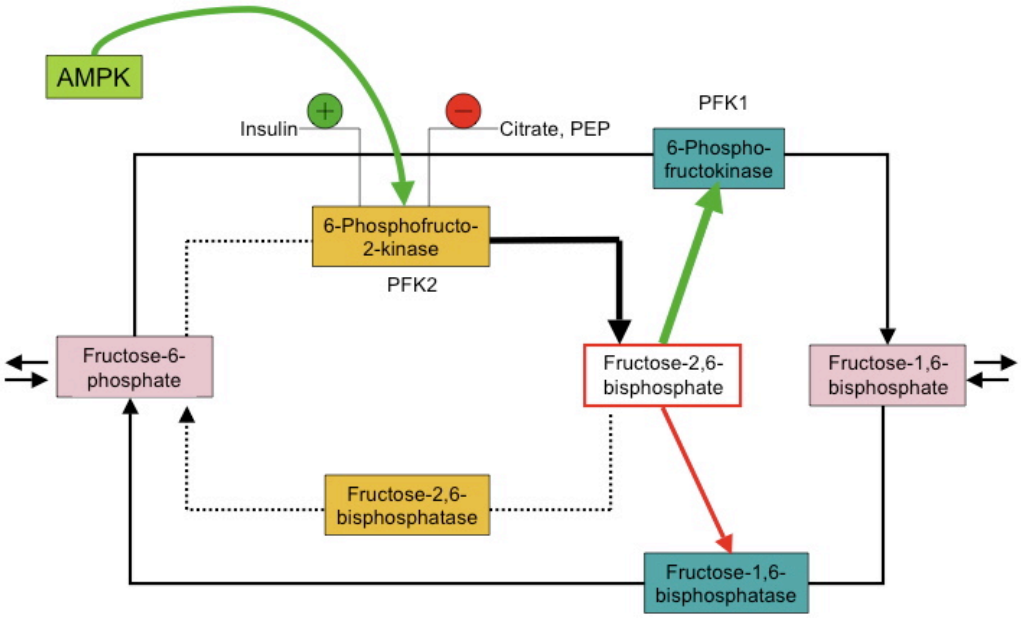

Figure 1–14: *Impact of AMPK in the glycolytic pathway*

1.6.2.4 AMPK in the Glycogen Metabolism

There is plenty of evidence that primary glycogen storage diseases (e.g., Pompe disease, McArdle disease) increase AMPK activity while decreasing glycogen synthase activity (GS) (Nielsen *et al.*, 2002). However, the Seidman group has clearly shown impairment of glycogen metabolism by AMPK mutations (Arad *et al.*, 2002a). It is far from being well defined, whether it is due to the altered phosphorylation status of glycogen metabolism (e.g. glycogen synthase, phosphorylase kinase) enzymes or caused by an increased glucose uptake (Carling & Hardie, 1989; Halse *et al.*, 2003; Arad *et al.*, 2007).

Further, the mediation of transcription of genes involved in lipid and glucose metabolism is worthwhile to mention (Jorgensen *et al.*, 2006).

To date the only known disease causing mutations in AMPK occur in the human *PRKAG2* gene encoding for the γ2 subunit, and in the porcine *PRKAG3* gene encoding for the γ3 subunit.

In 1995 the Seidman group reported an association between WPW pattern and left ventricular hypertrophy in a large family. It was described as an autosomal dominant inheritance being located on the long arm of chromosome 7 (MacRae *et al.*, 1995).

The molecular pathogenesis remained unclear until 2001 as 2 groups (Blair *et al.*, 2001; Gollob *et al.*, 2001a; Gollob *et al.*, 2001b) reported four mutations in the *PRKAG2* in five different families. Further, Arad *et al.*, 2002a published three mutations responsible for disease in six families, including the Asn488Ile mutation in the family in which this syndrome was originally defined (MacRae *et al.*, 1995).

The clinical features associated with *PRKAG2* missense mutations are summarized in the table below.

Mutation	***Fam. #***	***Pat. #***	***Age of Onset***	***LVH***	***LV*** *(Dysfunction/ Dilatation)*	***Pre-excitation***	***CSD /PPM***	***SCD***	***SVT***	***AFib***	***Reference***
Arg302Gln	*8*	*78*	*J-A*	*Y*	*Pos*	*Y*	*Y*	*Y*	*Y*	*Y*	*(Gollob et al., 2001a; Arad et al., 2002a)*
Leu351ins	*1*	*5*	*A*	*Y*	*Y*	*Y*	*Y*	*Com*	*-*	*Y*	*(Blair et al., 2001)*
His383Arg	*1*	*3*	*P*	*Y*	*Y*	*Y*	*-*	*-*	*Y*	*-*	*(Blair et al., 2001)*
Thr400Asn	*1*	*1*	*A*	*Y*	*-*	*Y*	*Y*	*-*	*-*	*-*	*(Arad et al., 2002a)*
Asn488Ile	*1*	*40*	*J-A*	*Y*	*Pos*	*Y*	*Y*	*Rare*	*Rare*	*-*	*(Arad et al., 2002a; Murphy et al., 2005)*
Tyr487His	*1*	*2*	*J*	*Y*	*-*	*Y*	*-*	*-*	*-*	*-*	*(Arad et al., 2005)*
Glu506Lys	*1*	*8*	*A*	*Massive +RVH*	*-*	*Y*	*-*	*-*	*-*	*Pos*	*(Bayrak et al., 2006)*
Arg531Gly	*1*	*4*	*P*	*N*	*N*	*Y*	*Y*	*Pos*	*Pos*	*--*	*(Gollob et al., 2001b)*
Arg531Gln	*3*	*3*	*Neo*	*Y*	*-*	*Y*	*-*	*-*	*-*		*(Burwinkel et al., 2005)*
Ser548Pro	*1*	*1*	*A*		*-*	*-*	*Y*	*-*	*-*		*(Laforet et al., 2006)*

Table 1-2*: Mutations in AMPK γ subunit; Clinical cardiac features associated with PRKAG2 missense mutations; J, juvenile; A, adult; P, paediatric; Neo, neonatal; Pos, possible; Com, common; LVH, left ventricular hypertrophy; LV, left ventricle; CSD/PPM, conduction system disease requiring pacemaker*

implantation, SCD, sudden cardiac death; AFib, atrial fibrillation; SVT, supraventricular tachycardia including atrioventricular reentry tachycardia; RVH; right ventricular hypertrophy; Y, yes; N, not reported; -, not reported but sample size and clinical data are sufficient to exclude; modified from Arad et al., 2007

Left ventricular hypertrophy represents the most common cardiac manifestation (in 80% of genetically affected patients). The principal electrophysiological abnormality in young individuals is ventricular preexcitation, found in approximately two thirds of patients harbouring a *PRKAG2* missense mutation. Conduction system disorders occur in approximately 50% of affected people, often necessitating pacemaker implantation (Arad *et al.*, 2007). Sudden cardiac death is not uncommon. Further, extra cardiac manifestations are usually less pronounced exceptional in neonatal disease (Burwinkel *et al.*, 2005) but may include seizures, skeletal myopathy (Murphy *et al.*, 2005; Laforet *et al.*, 2006) and hypertension (Gollob *et al.*, 2001b).

Currently two different theories about the mechanism by which *PRKAG2* mutations cause cardiac hypertrophy exist. The first one was mentioned in this chapter above suggesting a failure in enzyme activity leading to energy deficiency of the myocyte (Ashrafian & Watkins, 2007). Other researchers propose *PRKAG2* cardiomyopathy being a unique type of glycogen storage disease primarily involving the heart (Arad *et al.*, 2002a). The last one is supported by the known association between WPW and cardiomyopathy as seen in other glycogenoses (e.g. Danon disease, Pompe disease)

1.6.2.5 Effects of PRKAG2 Mutations on AMPK Activity

Several approaches have been taken to define the molecular mechanism of human mutations on AMPK function. These investigations are complicated by the fact that γ2 containing enzyme complexes account for the minority of AMPK in the heart and elsewhere (Cheung *et al.*, 2000; Li *et al.*, 2006). Different mutations were studied in yeasts and mammalian cell culture models (Jiang & Carlson, 1996; Hamilton *et al.*, 2001; Arad *et al.*, 2002a; Daniel & Carling, 2002; Hawley *et al.*, 2003; Barnes *et al.*, 2004; Scott *et al.*, 2004; Burwinkel *et al.*, 2005). These data raised the current consensus that in presence of adequate upstream kinases (LKB1, CaMKK), human mutations increase the basal activity of AMPK and reduce the sensitivity of the protein to AMP (Arad *et al.*, 2007)

1.7 Aims of the Study

Both the Redwood/Watkins laboratory and their collaborators, the Carling laboratory in London, have been performing yeast-two-hybrid screens to identify novel binding partners of AMPK. A screen of a human cardiac library using the unique N-terminal region of AMPK γ2 as bait identified cardiac troponin I as a putative interactor; biochemical experiments confirmed that this protein was a good *in vitro* AMPK substrate and furthermore it was shown that AMPK phosphorylation altered contractile regulation mediated by troponin I (Oliveira *et al.*, 2007). Another screen of the same library using the catalytic α1 subunit of AMPK revealed an interaction with the five C-terminal domains of cardiac MyBP-C. Prior to the start of my project, it was shown that AMPK was able to phosphorylate the C8- C10 fragment of cMyBP-C *in vitro*, and, based on the knowledge of AMPK phosphorylation sequences, the Carling laboratory suggested that the likely phosphorylation sites were residues Ser1024 and/ or Thr1026 in the C8 domain. The result of the α1 yeast two-hybrid screen and the subsequent preliminary phosphorylation studies formed the starting point for my studies described in this thesis.

It was decided to test the hypothesis that the suggested residues constituted an AMPK site by phosphorylating recombinant C8 domain fragment *in vitro* with AMPK, and to produce C8 with the putative phosphorylation sites mutated. Primers were designed to mutate serine 1024 and threonine 1026 simultaneously to two aspartic acid residues. These cannot be phosphorylated by AMPK and the aspartic acid residues also mimic phosphorylated serine and threonine, making that the domain appears constitutively phosphorylated, which may be useful for subsequent functional experiments (see (Gautel *et al.*, 1995).

All the experimental work was performed in the laboratory of Dr. Redwood and Prof. Watkins at Wellcome Trust Center for Human Genetics in Oxford UK, an institution of the University of Oxford, UK.

2 Chapter Material and Methods

2.1 Enzymes, Chemicals and Equipment

Chemicals were purchased from Sigma-Aldrich Inc., BDH Biochemicals or ICN Biomedicals Ltd. Restriction enzymes were obtained from New England Biolabs (UK) Ltd. DNA polymerases were purchased from Invitrogen Ltd. (*Pfu* DNA polymerase) or Bioline UK Ltd. (*Taq* DNA polymerase). Other DNA modifying enzymes were purchased from New England Biolabs and Promega (UK) Ltd.

Primers were synthesised by MWG Biotech AG and provided lyophilised. They were resuspended in sterile distilled water to 100 pmol/µl and stored at –20°C.

Polymerase chain reactions were carried out on a MJ Research PTC- 200 thermocycler. Centrifuges used were typically a bench top Biofuge (Heraeus® Instruments) for volumes up to 1.5 mls, a Jouan CR-4-22 (Jouan Inc.) for volumes 2-6 mls, and a Sorvall® RC-5B (Kendro Laboratory Products) for volumes greater than 6 mls. Chromatography columns were purchased from Amersham Pharmacia Biotech Ltd.

2.2 Cloning of cMyBP-C- Encoding DNA Sequences

2.2.1 Amplification of DNA Sequence using PCR

T7-promoter and T7- terminator primers flanking the sequence of interest were used. The templates used for amplification had been previously cloned in our laboratory and were either a λZapII human cardiac cDNA library (Clontech, USA), or the full length *MYBPC3* construct. The high fidelity, proofreading *Pfu* DNA Polymerase was used to help prevent the misincorporation of nucleotides into the final sequence. A typical PCR was set up as follows:

	µl
Template (100-700ng/µl)	0.5
Forward Primer (10 pmol/µl)	5
Reverse Primer (10 pmol/µl)	5
dNTP (2mM)	5
10× Cloned *Pfu* buffer	5
sterile, deionised H_2O	28.5
Cloned *Pfu* DNA Polymerase	1

The PCR mix was heated to 94°C for 10 minutes to allow full denaturation of the DNA, followed by thermal cycling for 30-35 cycles, where one cycle was typically as below:

94°C	40 seconds	(denaturation)
55°C	40 seconds	(annealing)
72°C	2 minutes per kb DNA	(extension)

A final extension time of 10 minutes at 72°C occurred before the PCR mix was cooled to 12°C.

2.2.2 Site-directed Mutagenesis

Plasmids containing the C0-C2, C8 and the C8-C10 fragments had previously been cloned in our laboratory. To introduce missense mutations into the wild type sequences, site-directed mutagenesis was used. Briefly, complementary primers incorporating the mutation were used in conjunction with the flanking vector primers to amplify two halves of the sequence by PCR. These can be used to self-prime and form the full-length sequence. Further PCR rounds with the flanking vector primers then amplified the product, which was digested with restriction enzyme sites for further cloning.

2.2.3 Agarose Gel Electrophoresis

Agarose gel electrophoresis was used to visualise PCR products alongside a marker (2-log DNA ladder, New England Biolabs® Inc.). Typically, a 1.5% agarose gel was made by boiling 0.75 g agarose in 50 ml 1× TBE (National Diagnostics (UK) Ltd), then allowing it to cool to ~60°C. Ethidium bromide was added to 0.2 µg/ml, and the gel poured and allowed to set for 30 minutes. Gels were run in 1× TBE at 70-100V.

Ethidium bromide intercalating into the DNA allows the product to be visualised under UV illumination. Slices of gel containing the desired DNA fragment were removed and the DNA extracted from the gel using the GeneClean II® Kit (Qbiogene UK), following the manufacturer's protocol.

2.2.4 Restriction Enzyme Digest

DNA fragments were digested simultaneously with *Nde* I and *Hind* III in buffer #2 (New England Biolabs® Inc.) for 2 hours at 37°C, then cooled to 4°C. The DNA was purified from the digest mix using the GeneClean II® kit. Vectors pET-28a (Novagen®) and pMW172(Way *et al.*, 1989) were similarly digested with *Nde* I and *Hind* III. In order to prevent religation of the vector, the 5' phosphate groups were removed by incubating with calf intestine alkaline phosphatase for 60 minutes at 37°C. Digested vector was purified using agarose gel electrophoresis and the gel slice containing the desired DNA removed and purified using the GeneClean II® kit. DNA insert and vector were ligated in a mix of volume 10 µl containing 1 µl T4 ligase (3 units/µl) at either 25°C for 4 hours, or 15°C for 16 hours.

2.2.5 Preperation of Competent Cells

DH10β *E.coli* cells were streaked onto an L-agar plate and colonies grown at 37°C overnight. One colony was used to inoculate 100 ml sterile Miller's LB medium (Sigma-Aldrich, Inc.) which was grown in a shaking incubator (220 rpm) at 37°C overnight. 800 µl of this starter culture was used to inoculate 400 ml LB, which was grown shaking at 37°C until the visible light absorbance at 600 nm (A_{600}) was 0.6-0.8. Cells were centrifuged at 750 ×g, 4°C for 5 minutes, and resuspended in 200 ml sterile 100 mM $CaCl_2$/ 20%glycerol. After incubation on ice for 20 minutes, the cells were centrifuged as before and resuspended in 8 mls 100 mM $CaCl_2$/ 20%glycerol. Aliquots (200 µl) in sterile eppendorfs were stored at –80°C. Other strains of *E.coli* used were made calcium competent using the same method.

2.2.6 Transformation

Ligation mix (10 µl), cooled to 4°C, was added to 100 µl competent DH10β *E.coli* cells and left on ice for 20 minutes. This mixture was heat shocked for 45 seconds at 42°C, and returned to ice for 1 minute. To allow the cells to recover, 700-800 µl blank LB medium was added to the cells and they were allowed to grow at 37°C for

1hour before being plated on L-agar plates containing antibiotics (kanamycin at 30 μg/ml or ampicillin at 100 μg/ml). Plates were incubated at 37°C overnight

2.2.7 Plasmid Purification

Colonies resulting from transformation were used to inoculate 5 mls LB medium containing appropriate antibiotics, which were grown at 37°C, shaking at 220 rpm for ~8 hours. Plasmid DNA was purified from this culture using the QIAprep Spin Miniprep Kit (Qiagen (UK) Ltd) following the manufacturer's protocol. To check that the insert had been properly cloned, 10 μl of each plasmid miniprep were restriction digested with *Nde* I and *Hind* III, and 1 μl was used as template in a small scale PCR. Agarose gel electrophoresis was used to check that digest and PCR products were of the correct size. Culture containing a correct clone was used to inoculate 400 ml LB medium with appropriate antibiotics, which was grown shaking overnight at 37°C. This culture was used to extract a large amount of plasmid DNA, using the QIAprep Maxi Prep Kit (Qiagen (UK) Ltd), following the manufacturer's protocol.

2.2.8 Sequence Verification

Samples of all clones were sent for sequencing to the DNA Sequencing Facility, Department of Biochemistry, University of Oxford. Results were compared to published sequence to ensure the clone sequence was accurate and in the correct reading frame with respect to the start codon and histidine tag. This was done using Megalign™ (DNASTAR Inc).

2.3 Protein Expression and Purification

2.3.1 Protein Expression

Two protein expression vectors were used during the course of this study. pMW172 was kindly donated by Dr. M. Way. pET-28a, purchased from Novagen®, was chosen because there was an N-terminal histidine tag and restriction enzyme sites that allowed easy subcloning from the pMW172 vector when necessary.

Constructs were transformed into BL21(DE3)pLysS cells (Novagen®) and colonies grown on L-agar plates inoculated with appropriate antibiotics (chloramphenicol at 25

μg/ml and ampicillin at 100 μg/ml or kanamycin at 30 μg/ml) at 37ºC overnight. Single colonies were used to inoculate 100 ml LB media, which was grown overnight at 37ºC on a shaking platform at 200-250 rpm. 15 ml of starter culture was used to inoculate typically six flasks of 800 ml of LB media which were then grown at 37ºC on the shaking platform until the cells reached the mid-log phase of growth where A_{600} = 0.6-0.8 (typically 2.5 hours). IPTG was then added to a concentration of 400 μM to induce protein expression, which continued under conditions most favourable for the production of soluble protein (typically 37ºC for 3 hours). At the end of protein expression, cells were harvested by centrifugation at 10,000 ×g, 4ºC for 6 minutes. The cell pellet was stored at –80ºC before protein was extracted and purified.

2.3.2 Extraction of Soluble protein

Cell pellets were thawed and resuspended in denaturing lysis buffer (10 ml buffer/pellet from 800 ml cell culture), plus TAME and TLCK. Once the cells had been resuspended, PMSF was added and the lysate kept on ice for at least 15 minutes. DNAse I, $MgCl_2$ and $MnCl_2$ were then added and the lysate kept on ice for a further 15 minutes, before being spun at 20,000 ×g for 20 minutes at 4°C. The supernatant was retained for purification of protein.

2.3.3 Extraction of Insoluble Protein

Cell pellets were thawed and resuspended in 10 ml native lysis buffer per pellet from 800 ml culture (see 2.6 for a list of all buffers), plus protease inhibitors: 10 μg/ml TAME, 5 μg/ml TLCK and 0.5 mM PMSF. Approximately 10 mg/pellet lysozyme was added to the lysate, which was then placed on ice for at least 15 minutes, followed by sonication with a microtip at 25-30% amplitude for 6 × 30 seconds. 2 mg DNAse I, 10 mM $MgCl_2$ and 2 mM $MnCl_2$ were added to the lysate, which was again left on ice for 15 minutes, before being spun at 20,000 ×g for 20 minutes at 4°C. The supernatant was retained for purification of soluble protein.

2.3.4 Purification of Soluble His-tagged Protein

4-6 ml Ni^{2+}-NTA resin (Qiagen (UK) Ltd.) was added to the soluble cell extract and left mixing at 4°C for 1 hour. The extract/Ni^{2+}-NTA mix was then passed through a filter column, whereby Ni^{2+}-NTA resin and bound protein was retained, and unbound

protein passed through the filter by gravity (retained for SDS-PAGE analysis). The Ni^{2+}-NTA resin was then washed with 3× 8 ml native wash solution (retained for SDS-PAGE analysis), and eluted with 7× 1 ml native elution buffer (with a high imidazole content: see 2.6). Samples were taken of each elution fraction for SDS-PAGE analysis, and those containing protein were either mixed with an equal volume of cyro-protecting glycerol and stored at -80°C (if purity was high), or retained for further purification.

2.3.5 Purification of Insoluble His-tagged Protein

An equal volume of His-Trap chelating buffer A was added to the cell extract, which was then loaded onto a superloop (150 ml), attached to an *ÄKTA*FPLC® (Amersham Pharmacia Biotech Ltd.). Two column volumes of water were passed through a 1ml or 5ml chelating column, followed by two column volumes of $NiSO_4$. Excess $NiSO_4$ was removed with further 2 column volumes of water, and the column was attached to the FPLC. The system was equilibrated with His-Trap chelating buffer A, and the cell extract passed over the column. Flow through was retained for SDS-PAGE analysis. Protein was then eluted from the column with an increasing gradient of His-Trap chelating buffer B (with a high imidazole content). Samples were taken of each elution fraction for SDS-PAGE analysis, and those containing protein were either stored at -80°C (if purity was high), or retained for further purification.

2.3.6 Ion Exchange Chromatography

Proteins could be further purified on the basis of a charge interaction. Positively charged proteins bind to cations in a Q column and negatively charged proteins bind to anions in an S column. Proteins were either dialyzed, buffer exchanged or diluted into the appropriate buffer A (low salt concentration: see 2.6) and passed over an appropriately sized column attached to the FPLC by injection from a 2 ml loop or the superloop. Flow through was retained for SDS-PAGE analysis, and the protein was eluted with an increasing gradient of buffer B (high salt). Samples were taken of each elution fraction for SDS-PAGE analysis, and those containing protein were either stored at -80°C (if purity was high), or retained for further purification.

2.3.7 Size Exclusion Chromatography

A size exclusion (gel filtration) column was attached to the FPLC and equilibrated in the appropriate buffer (e.g. that in which the protein is dissolved). Buffer was passed over the column at a speed of 0.3-0.5 ml/min. Proteins were loaded onto the 2 ml loop and injected onto the column, passing through it in order of decreasing size. Elution fractions were collected and analysed by SDS-PAGE. Those fractions containing pure protein were stored at -80°C, mixed with an equal volume of glycerol, if they were not denatured with urea-containing buffer.

2.3.8 SDS Polyacrylamide Gel Electrophoresis

Sodium dodecyl sulphate (SDS) is an anionic detergent that, when in the presence of a reducing agent and heat, binds to denatured protein stoichiometrically and in a non-sequence dependent manner. SDS-polypeptides can be separated on a gel as they migrate according to their molecular weight, thus when run alongside standard markers, the approximate molecular weight of a protein can be determined or confirmed. Gels are run in a reservoir buffer that differs in pH and ionic strength to the gel such that the negatively charged SDS-polypeptide migrates through a highly porous stacking gel, followed by a separating gel with higher acrylamide content to increase the resolution of the samples. In this study the Mini-PROTEAN II gel apparatus system (Bio-Rad Laboratories (UK) Ltd) was used, with ultra pure ProtoGel® (National Diagnostics (UK) Ltd) to pour gels.

Protein samples were typically 15 µl protein added to 5 µl 4 × SDS loading buffer. For cell samples, 90 µl cells were spun at 16,000 ×g for 1 minute then the pellet resuspended in 30 µl 4 × SDS loading buffer. Gel samples were boiled at 95°C for 5 minutes, and 5 µl (typically) loaded onto the gel which was run at 200 V for 50 minutes. The gel plates were separated and the gel stained with Coomassie stain for 5 minutes before being destained in a mix of 10% methanol and 10% acetic acid. When fully destained, gels were scanned using an Epson Perfection 1260 scanner.

2.3.9 Quantification of Protein

Protein quantification was accomplished by using BCA™ Protein Assay Kit (Pierce Biotechnology Inc.). This assay allows colorimetric detection and quantification of total protein by combining the well-known reduction of Cu^{2+} to Cu^{1+} caused by the

reaction of Cu^{2+} with peptide bonds in alkaline conditions (the biuret reaction) with the reaction of Cu^{1+} with bicinchoninic acid (BCA) in which two molecules of BCA chelate with one Cu^{1+} and form a complex that is purple in colour. Such complex is soluble in water and absorbs light at 562 nm in a nearly linear way with increasing protein concentrations. The following briefly describes the procedure undertaken to quantify a certain protein.

Typically, a series of bovine serum albumin (BSA) samples of known concentration (standards) were prepared in 1.5 mL microcentrifuge tubes. Protein samples to be quantified were prepared in triplicate by mixing 10 μl of protein with 40 μl of deionized water. BCA™ Working reagent was then prepared by mixing 10 ml of BCA™ Reagent A (which contains BCA in an alkaline environment) with 200 ml of BCA™ Reagent B (which contains cupricsulphate) (50:1 ratio of Reagent A to B). 1 ml of BCA™ Working Reagent was added to each tube and each reaction was mixed well. The reactions were then incubated at 37ºC, for 30 minutes and, after this, the absorbance of all the samples was measured at 562 nm. Finally, a BSA standard curve was prepared by plotting the absorbance measurements of the BSA standards against their respective concentrations and the concentration of the protein was determined out of this standard curve.

2.3.10 Western Blotting

Western Blotting is a technique that allows immunological detection of proteins following electrophoresis. It relies on the fact that most epitopes (sites recognized by antibodies, generally comprising several amino acids) are still recognizable following denaturing of the protein and binding to the surface of a membrane. Its high degree of sensitivity and specificity makes it, in general, an excellent tool for protein analysis even in situations of complex mixtures containing only traces of the desired protein. In this study, Western Blotting was carried out as described below.

In general, protein samples to be analyzed were prepared and separated by SDS-PAGE as described in section 2.3.8. Following this, and using the Mini Trans-Blot Electrophoretic Transfer Cell (Bio-Rad Laboratories Ltd.) system, the gel was sandwiched with an Immuno-Blot PVDF membrane (Bio-Rad Laboratories Ltd.) as shown in Figure 2.1 and the cassette was then placed in the transfer tank (inside the electrode module) filled with Western Blotting Transfer Buffer (see section 2.6 for composition). Electrophoretic transfer was performed at 200 mA, 4ºC, for ~4 hours, with stirring. The membrane (blot) was then blocked with Western Blotting Blocking Buffer (see section 2.6 for composition) for 1 hour, at room temperature, on a shaking

platform, in order to prevent unoccupied protein binding sites from non-specifically immobilizing antibodies in the following steps. After this, the blot was incubated with an appropriate primary antibody (diluted in Western Blotting Blocking Buffer) at 4ºC, overnight. After extensive washing in Western Blotting Washing Buffer (see section 2.6 for composition), the blot was incubated for 1 hour at room temperature with an appropriate horseradish peroxidase (HRP)-conjugated secondary antibody diluted in Western Blotting Blocking Buffer. Finally, after further extensive washing in Western Blotting Washing Buffer, the blot was developed using SuperSignal West Pico Chemiluminescent Substrate (Pierce Biotechnology Inc.) according to the manufacturer's instructions.

Figure 2–1: *Diagram of the preparation of the transfer "sandwich"*

2.4 Protein Modifications

2.4.1 Protein Concentration

If necessary, proteins were concentrated using the Vivaspin 6 or 20 ml ultrafiltration device (Vivascience (UK) Ltd.), with a 5000 Da molecular weight cut-off. Protein was placed in the concentrator and centrifuged in a swing-bucket centrifuge at a maximum of 3000 ×g until the desired volume of protein remained.

2.4.2 Refolding of Denatured Protein

Dialysis was used to change the buffer of protein in denaturing solutions into phosphorylation assay buffer without urea. The dialysis procedure took place with a narrow dialysis tube, knotted at one end and closed with a clamp under gentle pressure at the other end. The tube was put in 1000 ml beaker containing the desired buffer and stirred using a magnetic bar at 4°C for more than 3 hours.

2.4.3 Cleavage of His-tag

When removing of the histidine tag from the N-terminus of a protein was necessary, it was possible to cleave the tag using the Thrombin Cleavage Capture kit (Novagen®). Protein was dialyzed into thrombin cleavage buffer, and the concentration measured so the correct quantity of thrombin could be added (1 unit per mg protein). The thrombin/protein mix was left at 4°C overnight, then 32 µl streptavidin-agarose slurry was added per unit of thrombin. This was allowed to mix at 4°C for 1 hour for the streptavidin to capture the biotinylated thrombin, and was then passed through a gravity flow column. Cleaved protein (flow through) was retained and checked by SDS-PAGE against uncleaved protein. Cleaved tag was removed by size exclusion chromatography or incubation with Ni^{2+}-NTA resin (Qiagen (UK) Ltd.).

2.4.4 In vitro Phosphorylation Assay using 5'-AMP-Activated Kinase

The AMPKK (recombinant CaMKKb)-activated recombinant AMPK complexes used in this study [a1b1 2Long, a1b1 2short] were a kind gift from Dr. Joanna Davies and Professor David Carling (MRC Clinical Sciences Centre, Imperial College London).

In general, phosphorylation reactions of 30 µl or 20 µl were set up using a desired amount of substrate in phosphorylation assay buffer, 125 µM AMP, 1 µL activated AMPK and, finally, 5 µl of a solution of ATP/$MgCl_2$ (for example, a 50 µl solution would contain 1 µl ^{32}P-ATP, 0.5 µl 100 mM ATP, 1.25 µl 1 M $MgCl_2$ and 47.25 µl H_2O). Following this, reactions were incubated at 37ºC for ~1 hour. Samples were analyzed for substrate phosphorylation by SDS-PAGE, followed by autoradiography and/or phospho imaging.

2.4.5 2-Dimensional Phosphoamino Acid Analysis

After phosphorylation reaction as described earlier 2 µl 10 mg/ml BSA (carrier protein) and 250 µl 100% TCA were added to 25 µl phosphorylated protein. This mix was incubated on ice for 1 hour. Following centrifugation at 13,000 rpm for 10 minutes, supernatant was carefully removed because it contains unincorporated ^{32}P-ATP. The pellet was washed with 500 µl 100% ethanol and centrifuged at 13,000 rpm for 5 minutes. After removing as most as possible of ethanol, the pellet was air- dried and resuspended in 100 µl 5.7M HCl for chopping the protein fragment in single amino acids and incubated at 100°C for 30 minutes.

After removing HCl by drying in a Speedvac the pellet was resuspended in 5 µl pH 1.9 buffer with phosphoamino acid standards (Serine, Threonine, Tyrosine). This mix was applied to a cellulose plate. In the next step, the plate was wetted and electrophoresis in pH 1.9 buffer at 1500 V for 20 minutes was performed using the HTLE-7002, Hunter thin layer electrophoresis system (C.B.S Scientific company, INC.). After drying of the plate via hair dryer it was rewetted in pH 3.5 buffer. The following electrophoresis was performed in pH 3.5 buffer at 1300 V for 16 minutes in the HTLE-7002, Hunter thin layer electrophoresis system (C.B.S Scientific company, INC.) at the orthogonal direction of the first electrophoresis. After complete drying of the cellulose plate it was sprayed with ninhydrin for visualization of the amino acid standards. Following another drying step an autoradiography was performed and compared with amino acid standards on the cellulose plate.

2.5 Primers

T7 Promoter (pET-28a)
5’ -TAA TAC GAC TCA CTA TAG GG - 3’
T7 Terminator (pET-28a)
3’ -GCT AGT TAT TGC TCA GCG GT- 5’
T7 forward (pMW-172)
5’ -GAC TCA CTA TAG GGA GAC C- 3’
T7 reverse (pMW-172)
3’ -CGG GCT TTG TTA GCA GCC G- 5’
cMyBP-C WT C8- F
5’ -GCA GAA AAG CAT ATG CTG CCC AGG CAC CTG CGC CAG- 3’
cMyBP-C WT C8- R
3’ -GCA GAA AAG CTT CTA TGG CTT GTC AAC AAC CTG CAG- 5’
Mutant A C8- S1020A- F
5’-GCA GGC GAG GAG GTG GCC ATC CGC AAC AGC CCC- 3’
Mutant A C8- S1020A- R
3’ -CGT CCG CTC CTC CAC CGG TAG GCG TTG TCG GGG- 5’
Mutant B C8- S1040A- F
5’ -GCT CGC CGC GTG CAT GCA GGC ACT TAC CAG GTG- 3’
Mutant B C8- S1040A- R
3’ -CGA GCG GCG CAC GTA CGT CCG TGA ATG GTC CAC- 5’
Mutant C C8- S1020A; S1024A- F
5’ -GCA GGC GAG GAG GTG GCC ATC CGC AAC GCC CCC ACA GAC ACC ATC -3’
Mutant C C8- S1020A; S1024A- R
3’-CGT CCG CTC CTC CAC CGG TAG GCG TTG CGG GGG TGT CTG TGG TAG -5’
Mutant F C8- S1024D; T1026D- F
5’- AGC ATC CGC AAC GAC CCC GAT GAC ACC ATC CTG – 3’

Mutant F C8- S1024D; T1026D- R
3'- CAG GAT GGT GTC ATC GGG GTC GTT GCG GAT GCA- 5'
cMyBP- C WT C9 F
5'- ACT GCA GAA CAT ATG CCA AGT CCT CCC CAG GAT CTC- 3'
cMyBP- C WT C9 R
3'- GCA GAA AAG CTT CTA TGG GGC CTC GGA GAA GTC CAG- 5'
HexHis Forward
5'- TAT GCA TCA TCA TCA TCA TCA- 3'
HexHis Reverse
3'- TAT GAT GAT GAT GAT GAT GCA- 5'

2.6 List of buffers

DNA Loading Buffer	40% Glycerol 0.5mL EDTA pH8.0 a minute amount of Bromophenol Blue
Native lysis buffer	50mM sodium phosphate pH8.0 300mM sodium chloride 10mM imidazole
Native washing buffer	50mM sodium phosphate pH8.0 300mM sodium chloride 20mM imidazole
Native elution buffer	50mM sodium phosphate pH8.0 300mM sodium chloride 250mM imidazole
Denaturing lysis buffer	50mM sodium phosphate pH8.0 300mM sodium chloride 10mM imidazole 6M Urea
Denaturing washing buffer	50mM sodium phosphate pH8.0 300mM sodium chloride 20mM imidazole 6M Urea
Denaturing elution buffer	50mM sodium phosphate pH8.0 300mM sodium chloride 250mM imidazole 6M Urea
New improved lysis buffer	25mM Tris-HCl pH7.5 20% sucrose 1mM EDTA pH8.0 200mM NaCl 5M urea 0.1% Triton x100

MyBP- C reconstitution buffer 3M	50mM $NaPO_4$ 300mM NaCl 3M Urea
MyBP- C reconstitution buffer 1.5M	50mM $NaPO_4$ 300mM NaCl 1.5M Urea
Phosphorylation assay buffer	50mM Hepes pH 7.4 150mM KCl 5mM $MgCl_2$ 0.5mM DTT
SDS-PAGE stacking gel buffer	125mM tris hydrochloride pH6.8 0.2% SDS
SDS-PAGE separating gel buffer	375mM tris hydrochloride pH8.8 0.2% SDS
SDS-PAGE running buffer	25mM tris-base pH8.8 19.2mM glycine 1% SDS
SDS-PAGE stacking gel buffer for low Molecular weight	30% acrylamide/0.8% bisacrylamide 3M Tris-HC Glycerol Water 25% APS TEMED
SDS-PAGE resolving gel buffer for low Molecular weight	30% acrylamide/0.8% bisacrylamide 3M Tris-HC Glycerol Water 25% APS TEMED
SDS-PAGE protein loading buffer	50mM tris hydrochloride pH6.8 40% glycerol 2% SDS 10% β-mercaptoethanol spatula bromophenol blue
Western Blotting Blocking Buffer	0.05M Tris-HCl pH7.5 0.15M NaCl 0.05% Tween 20 2% (w/v) Low Fat Milk Powder

Western Blotting Transfer Buffer	0.05M Tris Base 0.4M Glycine 0.05% SDS 20% Methanol
Western Blotting Washing Buffer	0.05M Tris-HCl pH7.5 0.15M NaCl 0.05% Tween 20
Coomassie stain	0.5% coomassie blue 50% methanol 10% acetic acid
Destain	10% Methanol 10% Acetic Acid
Thrombin cleavage buffer	200mM tris hydrochloride pH8.4 1.5M sodium chloride 25mM calcium chloride
HIS-trap chelating buffer A	20mM tris hydrochloride pH8.0 500mM sodium chloride 6M urea 1mM β-mercaptoethanol
HIS- trap chelating buffer B	20mM tris hydrochloride pH8.0 500mM sodium chloride 1mM β-mercaptoethanol 500mM imidazole
Q buffer A	50mM tris hydrochloride pH8.0 1mM EDTA pH8.0 1mM β-mercaptoethanol 6M urea
Q buffer B	50mM tris hydrochloride pH8.0 1mM EDTA pH8.0 1mM β-mercaptoethanol 6M urea 2M sodium chloride
S buffer A	20mM MOPS pH6.5 1mM EDTA pH8.0 1mM β-mercaptoethanol 6M urea
S buffer B	20mM MOPS pH6.5 1mM EDTA pH8.0 1mM β-mercaptoethanol 6M urea 2M sodium chloride

3 Results

3.1 Introduction

Work carried out in this study required the expression and purification of a variety of single cMyBP-C domains or groups of domains. Just a few of them had previously been expressed and purified in our laboratory, hence procedures had to be established to obtain a sufficient yield for each protein needed. This chapter describes the processes whereby favourable conditions for expression and purification of soluble protein were determined. Expression of some of the domains did not yield high levels of soluble protein. However, the experiments performed for the detection of phosphorylatable residues do not require a huge amount of soluble protein. Optimisation of the methods and protein refolding is also described.

3.2 Expression and Purification of Recombinant cMyBP-C Domains

3.2.1 Choice of Expression Vector

The construct of C8 wildtype domain had previously been cloned in the (Novagen®) pET-28a vector in our laboratory.

Previous attempts at expression and purification of this domain in the pMW172 vector with and without a hexahistidine-tag inserted as a linker at the *NdeI* site were not successful. The pET series of vectors (Novagen®), based on the initial vectors described by Studier *et al.*, 1990, have a wide range of options regarding fusion tags and multiple cloning sites. In our laboratory, the pET-28a has been chosen, as it contains an intrinsic N-terminal histidine-tag that can specifically bind to a Ni^{2+}-resin, from which the expressed protein could be eluted by an imidazole gradient. There was also a thrombin cleavage site C-terminal of the His-tag allowing removal of the tag from the recombinant protein if necessary. Additionally, the restriction enzyme sites in the multiple cloning region allowed easy transfer of sequences from pMW172 using the *NdeI* and *HindIII* sites with which they were originally cloned. Although the protein expression levels were typically reduced using this vector in previous experiments carried out in our group, the protein purification was much facilitated.

Therefore, the majority of MyBP-C domains used in this study were expressed from this vector and purified initially using Ni^{2+}-histidine affinity techniques.

3.2.2 Choice of Protein Extraction

Once *E.coli* expressing the desired protein have been grown and harvested, they need to be lysed so that the protein can become solubilised for purification. There are two ways of doing this: Lysis under native or under denaturing conditions.

Resuspension under denaturing conditions (e.g. in the presence of urea) ensures that all protein in the cell is solubilised to give the highest possible yield. However, urea has to be removed by dialysis for correct refolding of the protein, as it is required in its native state for the further experiments.

Attempts to purify the C8 domains under native conditions failed and I decided to switch to the denaturing procedure in presence of 6 M urea.

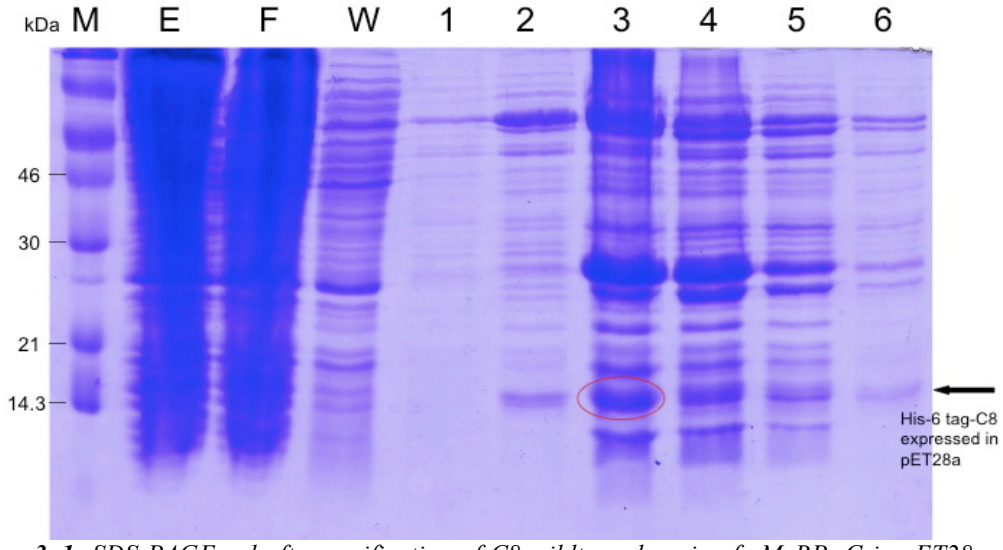

Figure 3–1: *SDS-PAGE gel after purification of C8 wildtype domain of cMyBP- C in pET28a under native conditions and after gravity Ni^{2+} column; many impurities; M, marker; E, eluate fraction; F, flowthrough fraction; W, washing fraction; 1,2,..., protein fractions eluted from the column by 250 mM imidazole*

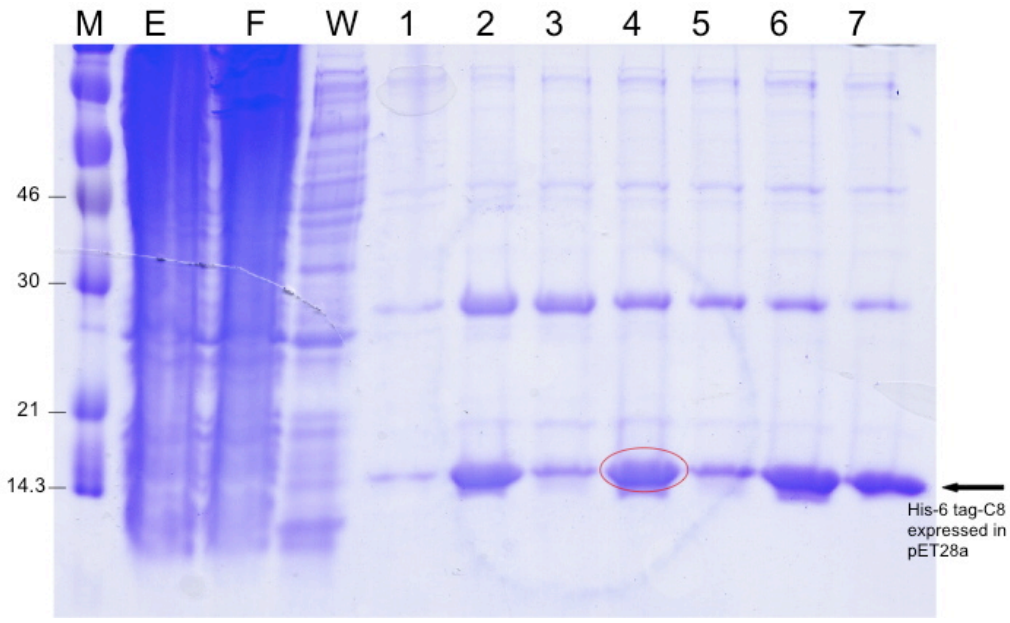

Figure 3–2: *SDS-PAGE gel after purification of C8 domain of cMyBP- C in pET28a under denaturing conditions, after gravity Ni^{2+} column; relatively pure*

The first step of purification of proteins expressed in the pET-28a vector was a Ni^{2+}-NTA resin column (Qiagen UK Ltd.) as described in chapter 2, followed by a gel filtration column on the FPLC machine.

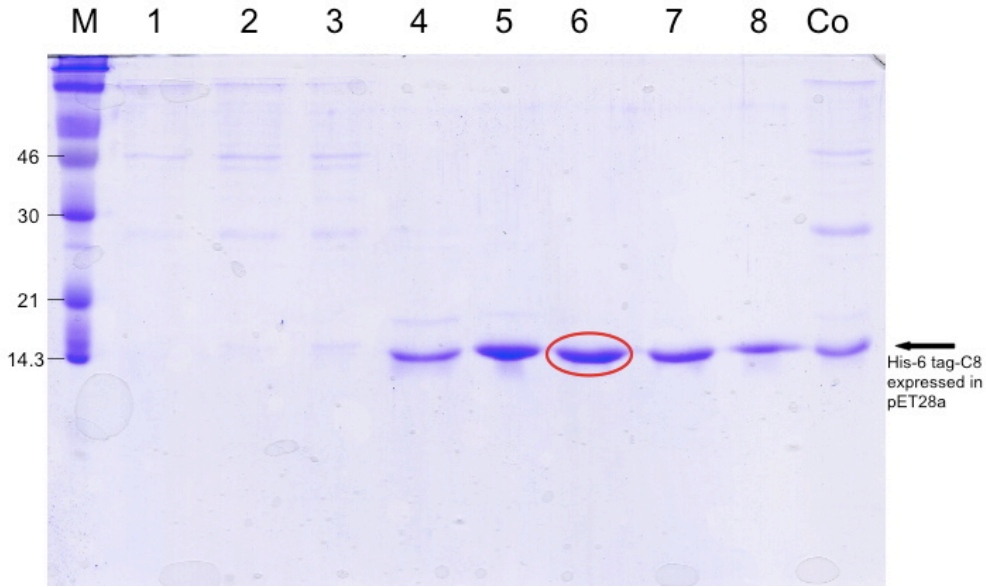

Figure 3–3: *SDS-PAGE gel after purification C8 domain of cMyBP- C in pET28a under denaturing conditions, after Gel filtration column; fractions 5-8 pure; Co, control*

After pooling the pure fractions (e.g. 5-8 in the figure above) and performing a protein assay for quantification of the yield, the protein was either stored at -80°C or kept at 4°C for further work. Since the protein was purified in presence of urea it was not necessary to add glycerol for storing at -80°C.

It is essential for the phosphorylation experiments to dialyse the protein into the appropriate buffer while ensuring correct refolding of the domain. The standard protocol for removing urea uses a gradient dialysis, three hours in MyBP-C reconstitution buffer containing 3 M urea, three hours in MyBP-C reconstitution buffer containing 1.5 M urea and eventually in the phosphorylation assay buffer, which contains no urea. This approach was unsuccessful, however, as a considerable amount of precipitation occurred during dialysis, indicating insoluble protein and of course reduces the amount of the protein desired.

After a couple of unsuccessful attempts to remove urea with gradient dialysis, I decided to dialyse immediately in phosphorylation assay buffer. For unknown reasons this protocol was sufficient to yield a proper amount of protein.

After assessing the quantity of protein and running a sample on a SDS-PAGE gel, a phosphorylation reaction was performed. It was carried out using γ ^{32}P-ATP and AMP-activated kinase (AMPK) set up as described in the previous chapter.

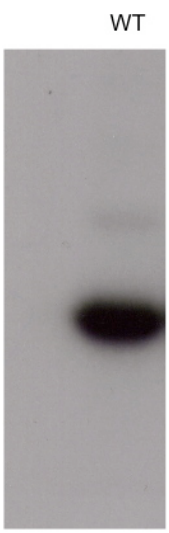

As shown in the figure above and as we had expected from the results obtained by Carling and co-workers, the C8 domain is a good *in vitro* substrate for AMPK. The amount of ^{32}P incorporated and the time course of incorporation was similar to troponin I, an established substrate (data not shown). Therefore, the first part of the hypothesis, that C8 was an AMPK substrate, was apparently proven and the C8 (Ser1024D;Thr1026D) mutant was then generated.

Figure 3–4: *Autoradiography of MyBP-C C8 domain after phosphorylation by AMPK*

3.2.3 Mutation of Phosphorylation Sites S1024 and T1026

After performing the first step of double mutagenesis PCR, the products I and II were run on an agarose gel and cut out. In the second step, a PCR reaction was set up containing the purified fragments. For obtaining a higher yield of the desired DNA fragment a third PCR step was done. This reaction was also run on a gel, cut out and Gene-cleaned. Following digestion of both the plasmid and the fragment, the plasmid was treated with calf intestine phosphatase to prevent a recircularization. The enzyme

removes the 3'-phosphate group so that the ligase is unable to connect both ends of the plasmid. In order to remove this enzyme from the subsequent ligation step, a Gene-clean procedure without the TBE-modifier was performed.

For successful ligation it is necessary to mix the cut plasmid and the cut fragment at approximately 1:3 ratio. Therefore, I ran an aliquot of the plasmid and the fragment on a 1.5% agarose gel to estimate the concentration of each. The ligation reaction (10 μl) was then set up for at least 4 hours at room temperature.

Then DH10β *E.coli* cells were transformed with the ligation mix and spread onto a L-agar plate containing kanamycin at 30 μg/ml. Plates were incubated at 37°C overnight.

Colonies resulting from the transformation were screened by PCR with T7- promoter and T7- terminator primers. Positive clones, detected by agarose gel electrophoresis, were used to inoculate 5 ml LB medium containing kanamycin at 30 μg/ml, which was grown at 37°C overnight with shaking. One ml was used to inoculate 400 ml LB medium containing kanamycin at 30 μg/ml, which were incubated overnight on a shaking platform at 37°C.

The harvested pellet was used to purify the desired plasmid with the QIAprep Spin Maxiprep Kit (Quiagen UK Ltd).

The sequence of the plasmid was compared using Megalign^{TM} (DNASTAR Inc.) to the published sequence to ensure both that the engineered mutations were present and that no errors have been incorporated during the PCR mutagenesis procedure.

The verified plasmid was used to transform BL21(DE3)pLysS cells and these were plated on L-agar plates containing appropriate antibiotics (chloramphenicol 25 μg/ml; kanamycin 30 μg/ml) and incubated overnight at 37°C.

One colony was used to inoculate 100 ml LB medium containing appropriate antibiotics, which were incubated at 37°C on a shaking platform overnight. From that culture 15 ml were used to inoculate 800 ml LB medium containing appropriate antibiotics. After adding IPTG to a concentration of 0.4mM the protein was expressed. Cells were harvested usually after 3 hours protein expression and the pellet stored at -80°C.

The C8 mutant was purified using the same protocol as for the wild type protein.

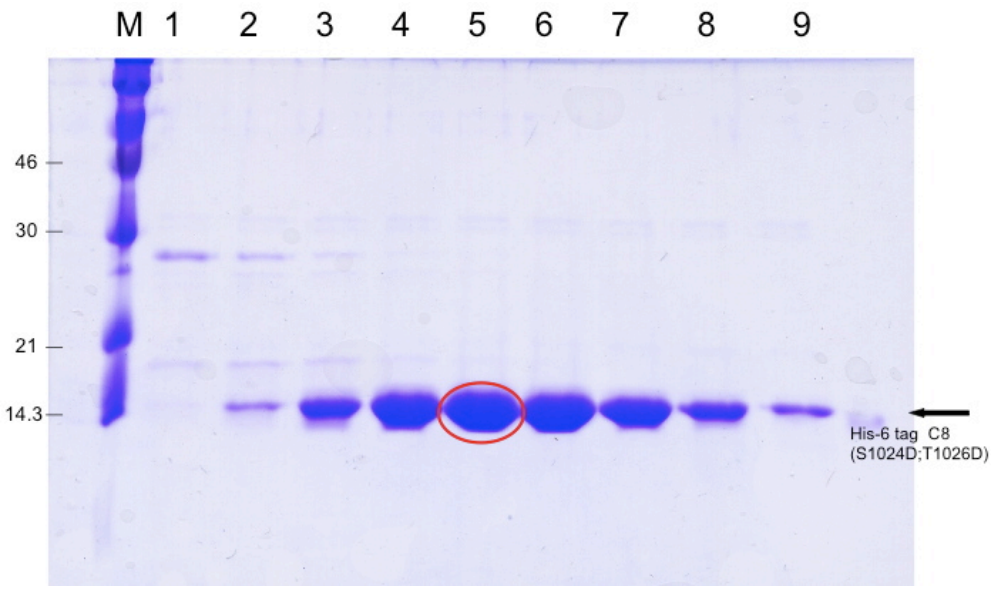

Figure 3–5: *purification mutant C8 (S1024D;T1026D) domain of cMyBP- C in pET28a under denaturing conditions, after Gel filtration column; fractions 4-9 pure*

Now the mutant domain was dialyzed overnight in phosphorylation assay buffer, which did not contain urea. After assessing the quantity of protein and running a sample on a SDS-PAGE gel, the phosphorylation reaction was performed. It was carried out using γ ^{32}P-ATP and AMP-activated kinase (AMPK). Based on the prediction of Carling and co-workers, we expected a significant reduction of phosphorylation of the mutated domain compared with wild type. However, as shown in **Figure 3–6** the mutant protein is still phosphorylated to a similar level as wild type. This experiment disproves the hypothesis that either S1024 or T1026 serves as a substrate for AMPK *in vitro*.

Figure 3–6: *Autoradiography of C8 WT and C8mt (S1024D;T1026D) still phosphorylated in a similar intensity as the WT domain; C8mt (S1024D;T1026D) is later labelled in this chapter mt F*

Relying on the data that I got from the phosphorylation experiment of the C8 WT, the most logical step to do at this stage was performing a phosphoamino acid analysis to show whether it was serine and/or threonine residues that were modified. The basic principle of this assay is the two dimensional separation of the amino acids of a ^{32}P-labelled protein after acid hydrolysis.

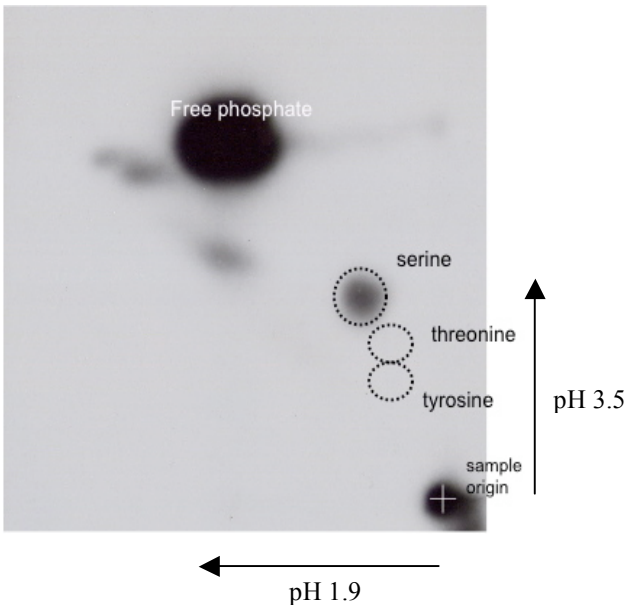

Figure 3–7: *Phosphoamino acid analysis C8 WT domain*

This experiment showed conclusively that the only phosphorylated amino acid in the labelled C8 domain was serine. The next consequent step had to be the identification of the other serines and the mutation of these to unphosphorylatable alanine residues. Two additional serines were identified: Ser1020 and Ser1040.

```
            L   P   R   H   L   R   Q   T   I   Q   K   K   V   G
975     CTG CCC AGG CAC CTG CGC CAG ACC ATT CAG AAG AAG GTC GGG
        GAC GGG TCC GTG GAC GCG GTC TGG TAA GTC TTC TTC CAG CCC

            E   P   V   N   L   L   I   F   Q   G   K   P   R   P
989     GAG CCT GTG AAC CTT CTC ATC CCT TTC CAG GGC AAG CCC CGG
        CTC GGA CAC TTG GAA GAG TAG GGA AAG GTC CCG TTC GGG GCC

            Q   V   T   W   T   K   E   G   Q   P   L   A   G   E
1003    CCT CAG GTG ACC TGG ACC AAA GAG GGG CAG CCC CTG GCA GGC
        GGA GTC CAC TGG ACC TGG TTT CTC CCC GTC GGG GAC CGT CCG

            E   V   P   S   I   R   N   S   P   T   D   T   I   L
1017    GAG GAG GTG AGC ATC CGC AAC AGC CCC ACA GAC ACC ATC CTG
        CTC CTC CAC TCG TAG GCG TTG TCG GGG TGT CTG TGG TAG GAC

            F   I   R   A   A   R   R   V   H   S   G   T   Y   Q
1031    TTC ATC CGG GCC GCT CGC CGC GTG CAT TCA GGC ACT TAC CAG
        AAG TAG GCC CGG CGA GCG GCG CAC GTA AGT CCG TGA ATG GTC

            V   T   V   R   I   E   N   M   E   D   K   A   T   L
1045    GTG ACG GTG CGC ATT GAG AAC ATG GAG GAC AAG GCC ACG CTG
        CAC TGC CAC GCG TAA CTC TTG TAC CTC CTG TTC CGG TGC GAC

            V   L   Q   V   V   D   K   P
1059    GTG CTG CAG GTT GTT GAC AAG CCA
        CAC GAC GTC CAA CAA CTG TTC GGT
```

Figure 3–8: *MyBP-C domain C8 sequence showing the serine residues highlighted in* red.

3.2.4 Cloning, Expression and Purification of other C8 Mutant Domains

A [S1020A]
B [S1040A]
C [S1020A;S1024A]
D [S1024D;T1026D;S1040A]
E [S1020A;S1024A;S1040A]
F [S1024D;T1026D]

Table 3-1 *shows the labelling of the created mutant domains*

Cloning, expression and purification of the mutant domains took place in the same manner as the Ser1024Asp;Thr1026Asp double mutant described above. Each was obtained at a similar yield and purity as wild type (**Figure 3–9** below).

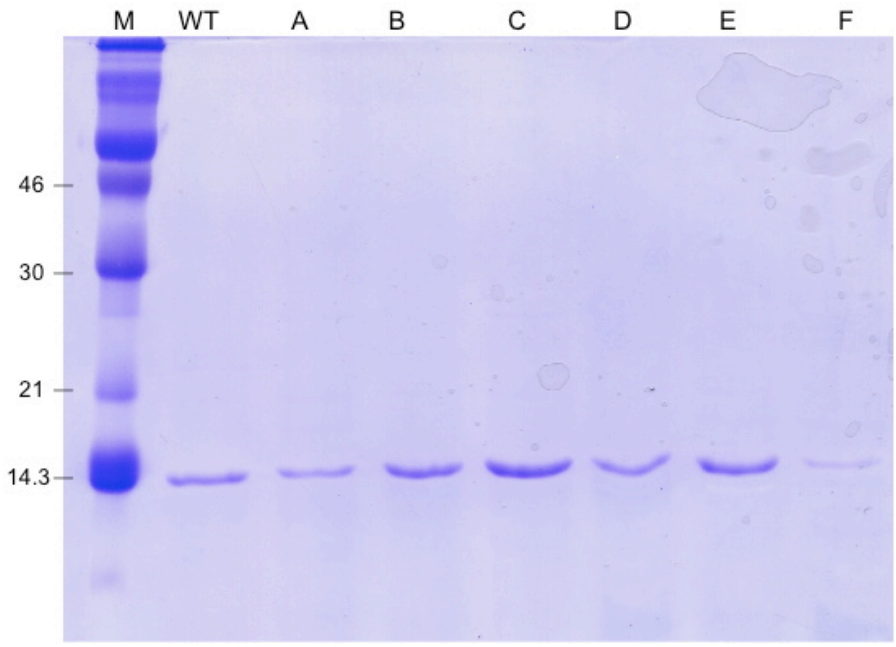

Figure 3–9: *SDS-PAGE gel of C8 WT and all generated mutants after dialysis*

At this stage a Western blot was performed to check for presence of the his-tag in all the expressed and purified mutant domains (**Figure 3–10** below).

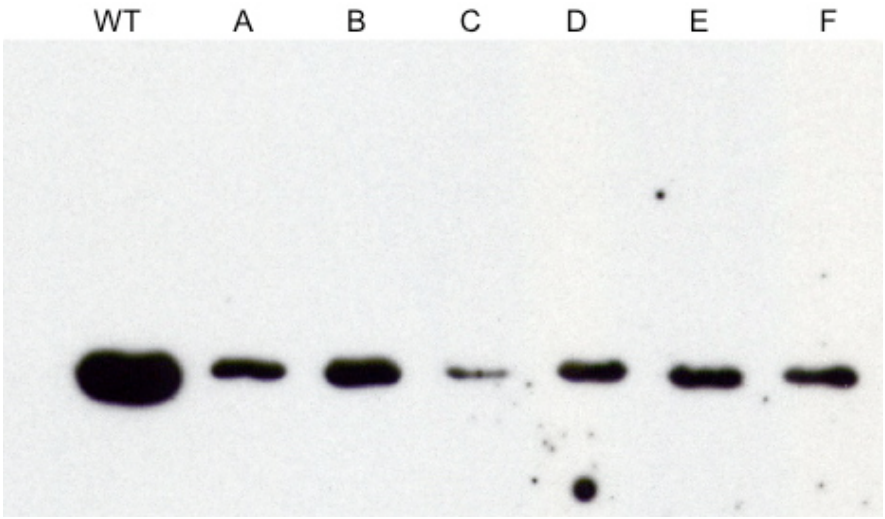

Figure 3–10: *Western-blot of all engineered C8 mutant domains using an antibody against the N-terminal Histidine-tag*

A phosphorylation assay was performed using all the created mutant domains. Surprisingly, this revealed that all the C8 mutants showed significant levels of ^{32}P

incorporation, even mutant E, in which every serine was mutated to unphosphorylatable alanine residues (**Figure 3–11** below).

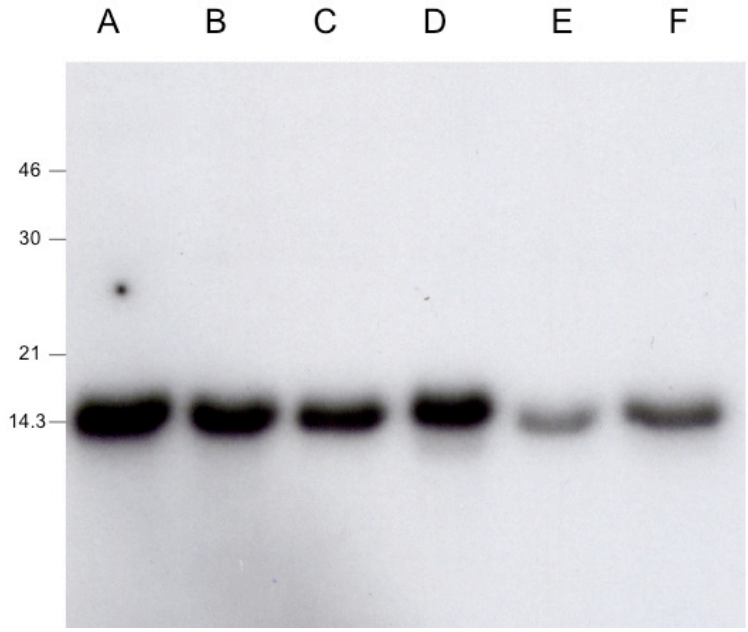

***Figure 3–11**: Autoradiography after phosphorylation assay of cMyBP-C C8 WT and created mutant C8 domains*

This absolutely unexpected result raised the possibility, previously considered unlikely, that a serine residue in the non-cMyBP-C leader sequence encoded by the plasmid was phosphorylated. As shown in **Figure 3–12** there are five serine residues present in this sequence, four of which can be cleaved off by thrombin treatment. In order to test the involvement of these extra serine residues, I decided to perform proteolytic digests with thrombin.

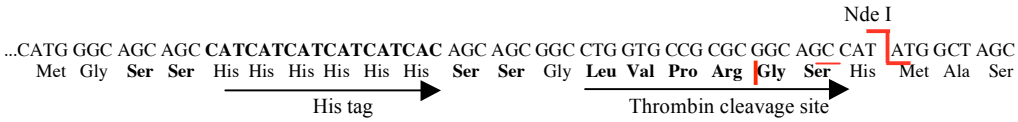

***Figure 3–12:** Section from pET 28a including His-tag, Thrombin cleavage site and NdeI cutting site (MW:1899Da)*

3.2.5 Cleavage of the Backbone

In order to optimise the conditions for the thrombin cleavage reaction I performed a thrombin time course and separated the products by SDS- PAGE (**Figure 3–13**).

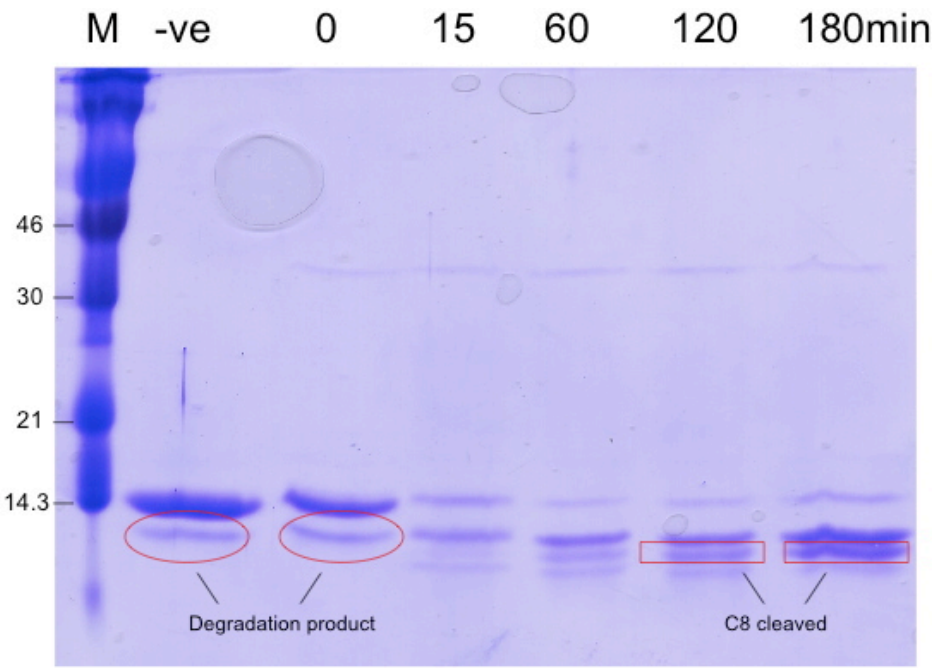

Figure 3–13: *SDS-PAGE gel of thrombin cleavage time course*

This experiment revealed a sufficient thrombin cleavage time of 120min. As mentioned above there is still one serine, which might be phosphorylated, even after the leading sequence is cleaved from the domain. My presumption was that the kinase is unable to recognize this residue as a phosphorylatable amino acid after thrombin cleavage due to it being the second amino acid from the N-terminus. Therefore I performed two experiments:

First: Phosphorylation of the C8 domain and afterwards a digest with thrombin (**Figure 3–14**).

Second: Treatment with thrombin and then a phosphorylation assay (**Figure 3–15**).

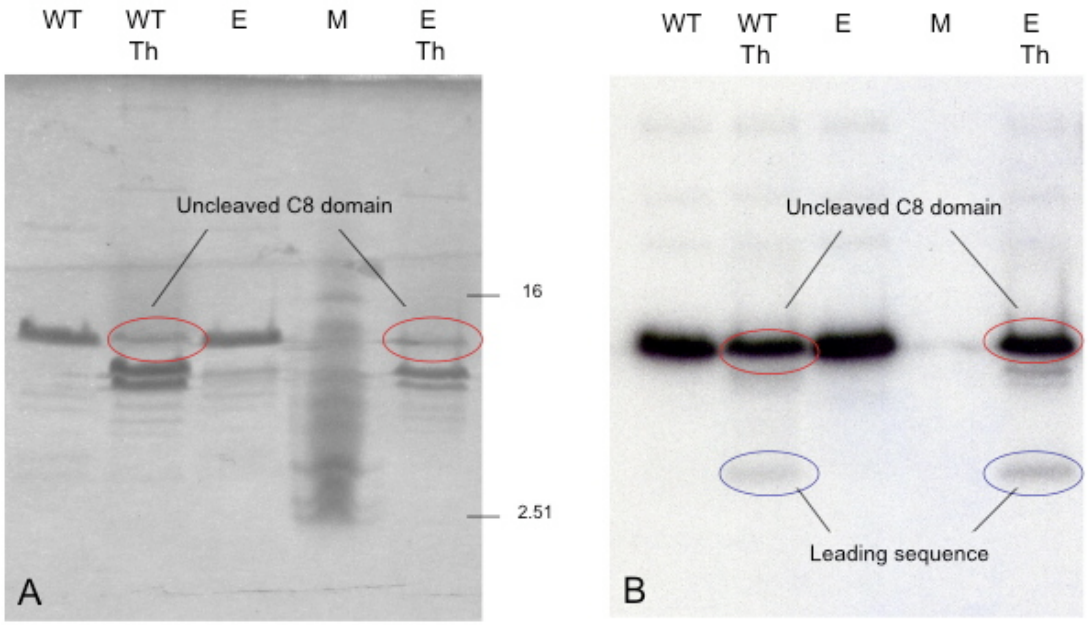

Figure 3–14: *First step phosphorylation reaction and second step thrombin cleavage(A) shows the stained SDS- PAGE gel after phospho reaction; (B) shows autoradiography. WT, C8 wildtype domain; E, C8 mutants as described in* ***Table 3-1****; Th, thrombin treated; M, marker*

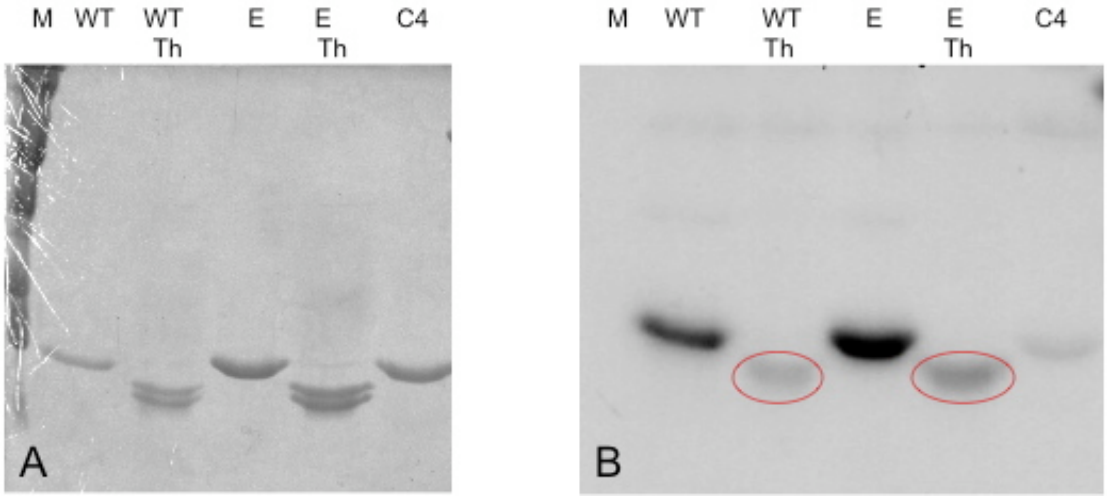

Figure 3–15: *First step thrombin cleavage and second step phosphorylation reaction; (A) shows the stained SDS- PAGE gel after phosphorylation reaction; (B) shows autoradiography, the encircled band shows the cleaved C8 domain containing the unphosphorylatable serine; WT, C8 wildtype domain; E and D, C8 mutants as described in* ***Table 3-1****; C4, cMyBP-C C4 domain; Th, thrombin treated; M, marker*

The stained SDS-PAGE gel in **Figure 3–14** shows that the protein with the N-terminal tag removed migrates approx. 2000 Da lower than the uncleaved peptide and that the thrombin digest of both wildtype domain and mutant E are >80% complete. The autoradiograph shows that the incorporated ^{32}P is not present in the digested C8 domain and taken together with the failure of this fragment to be phosphorylated after cleavage (**Figure 3–15**), this shows conclusively that the ^{32}P is incorporated into one

of the five non-cMyBP-C serine residues encoded by the plasmid. If it was one of the serines that was removed by thrombin digestion, then the short leader sequence (calculated MW: 1899 Da) would be expected to contain the bulk of the ^{32}P in **Figure 3–14**. However, only a very small proportion is found in this fragment, thus suggesting that the chief phosphorylation site is the serine present in the LVPR' G**S** thrombin recognition site. This residue is the second amino acid in the cleaved C8 fragment – so why is the ^{32}P incorporation in the cleaved band in **Figure 3–14**? This is because phosphorylation at this serine must inhibit thrombin cleavage; hence the cleaved C8 domain observed is unphosphorylated and the upper band contains phosphorylated undigested fusion protein. This serine is unable to be phosphorylated in the cleaved C8 as in this protein it is the second amino acid and some of the flanking residues necessary for kinase recognition are lost.

3.2.6 Phosphorylation of C8-C10

Upon completing the above experiments in which I had refuted the hypothesis that the C8 domain of cMyBP-C contains AMPK phosphorylation sites, I decided to repeat exactly the experiment that was done by Carling and co-workers in London.

C8-C10 has been cloned in the pMW172 vector containing the additional hexahistidine-tag in our laboratory previously. Unexpectedly, I had problems to purify the expressed protein.

It was not possible starting the purification procedure with the previously used "Denaturing lysis buffer" and a Ni^{2+}-NTA resin column as the first step, because the yield obtained was very low.

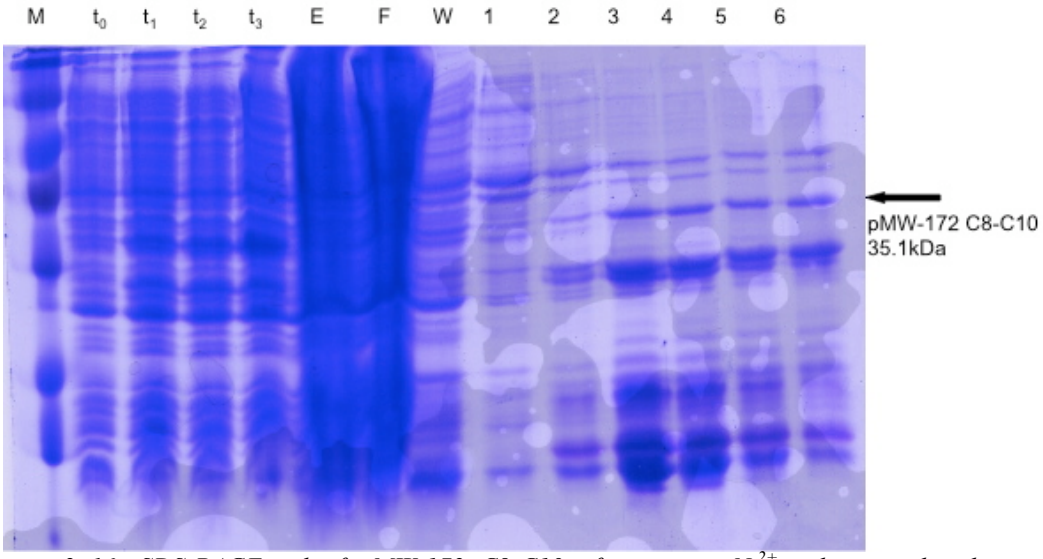

Figure 3–16: *SDS-PAGE gel of pMW-172 C8-C10 after gravity Ni^{2+} column under denaturing conditions; t_0-t_3, samples taken at point in time during protein expression after induction with IPTG (0, 1hour etc.) M, marker; E, eluate fraction; F, flowthrough fraction; W, washing fraction; 1,2,…, protein fractions eluted from the column by 250 mM imidazole*

After a couple of unsuccessful attempts purifying the fragment I tried a different lysis buffer (labelled "New improved lysis buffer") that contains 5 M urea and 1mM EDTA.

As C8-10 has a pI of 8.66 and hence predicted to be basic at neutral pH, I chose for the first step in the purification procedure a negatively charged S-cation exchange column. The protocol is the same as that one for the Ni^{2+}-NTA column except for adding some lysozyme before sonication. The lysate is diluted in a 1:1 ratio in buffer A (low salt concentration) and loaded into the Super-loop of the FPLC machine. Then the protein is eluted by a NaCl gradient (no picture). As the second purification step a FPLC His-column run by an imidazole gradient seems to be a possible alternative to do. For that reason it was necessary to remove EDTA from the collected sample by dialysis overnight in "Denaturing lysis buffer". Then the Super-loop was loaded with the sample and injected onto the His-column. The protein is eluted by running an imidazole gradient from lysis buffer (10 mM) to elution buffer that contains 250 mM imidazole (**Figure 3–17**).

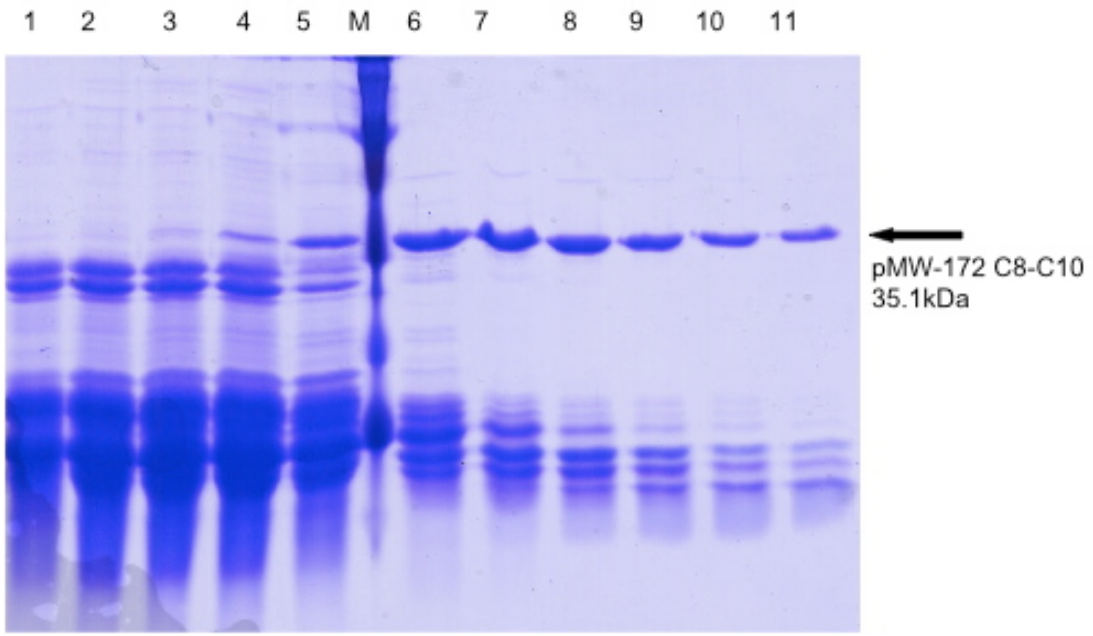

Figure 3–17: *SDS-PAGE gel of fragment C8-C10 after FPLC his-tag column eluted with imidazole gradient; 1,2,…, protein fractions eluted from the column; Fractions 6-11 were pooled for FPLC gel filtration column; M, marker*

As the last purification step of this fragment I performed a FPLC gel filtration column as previously described in this chapter.

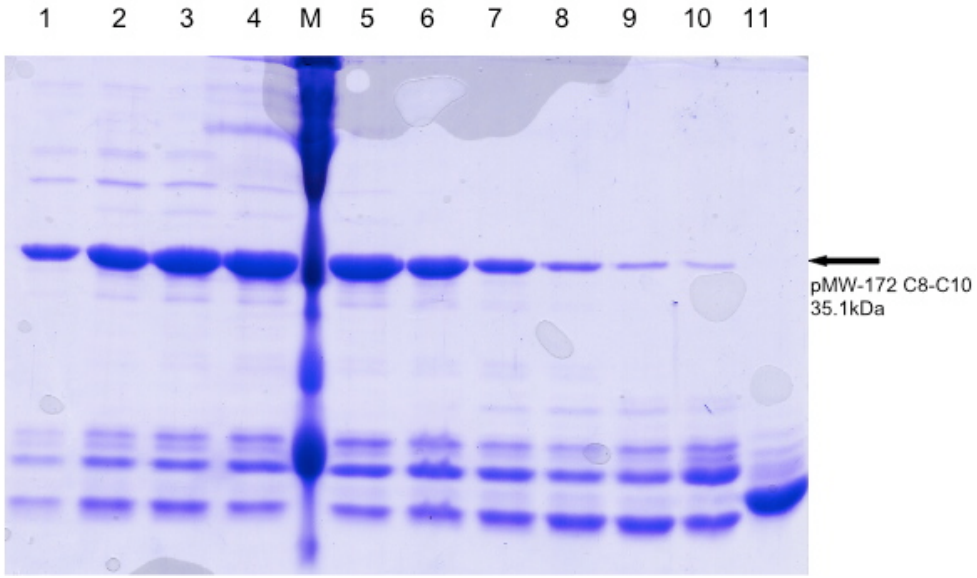

Figure 3–18: *SDS-PAGE gel of fragment C8-C10 after FPLC gel filtration column; 1,2,…, protein fractions eluted from the column; M, marker*

Despite the fact that the gel filtration column did not separate very nicely I worked further on, because for the phosphorylation experiments it has not to be absolutely pure.

As expected, autoradiography after phosphorylation of the C8-C10 with the AMP-activated protein kinase was positive. The sarcomeric protein troponin C is known not

be a target of the AMPK and was used as a negative control in this experiment. As positive control I applied the C8 mutant D. Loading different concentrations of the two proteins causes the difference between C8 intensity in comparison to C8-C10 in this picture.

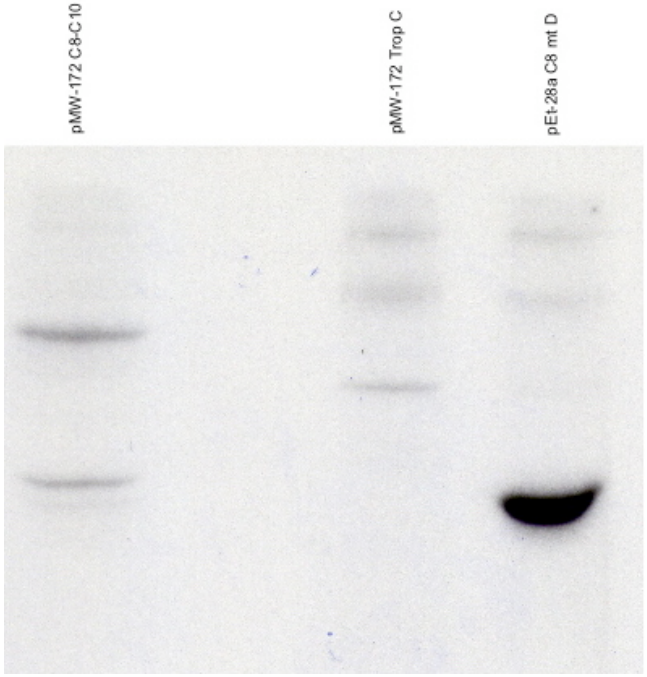

Figure 3–19: *Autoradiography of C8- C10 fragment after phosphorylation by AMPK; Troponin C is used as a negative control; C8 mt D is used as a positive control; difference between the phosphorylation intensity of the C8 mt D fragment in comparison to C8-C10 in this picture is caused by loading different concentrations of the two proteins.*

3.2.7 Expression of pMW 172 C9 WT and pMW C10 WT

The next consequent experiment was to screen the two remaining domains for phosphorylation by AMPK.

Firstly, I decided to engineer the C9 WT domain in pMW172 vector containing a hexahistidine-tag. This domain was never expressed before, and, therefore, I had to generate the C9 sequence by using pMW172 C8-C10 WT and suitable primers.

Next steps were performed as described in chapter 2. After transformation of DH10β *E.coli* and subsequent inoculation of 400 ml LB-medium containing proper antibiotics a Maxi-Prep was done. In the following step the hexahistidine-tag was inserted and a DH10β *E.coli* strain was transformed. As sequencing results of the plasmid received by Maxi-Prep were positive, BL21(DE3)pLysS *E.coli* cells were transformed for expressing the fragment.

After harvesting cells by centrifugation and resuspension in the 6 M urea containing "Denaturing buffer", I chose a Ni^{2+}- NTA resin column as the first purification step of this domain.

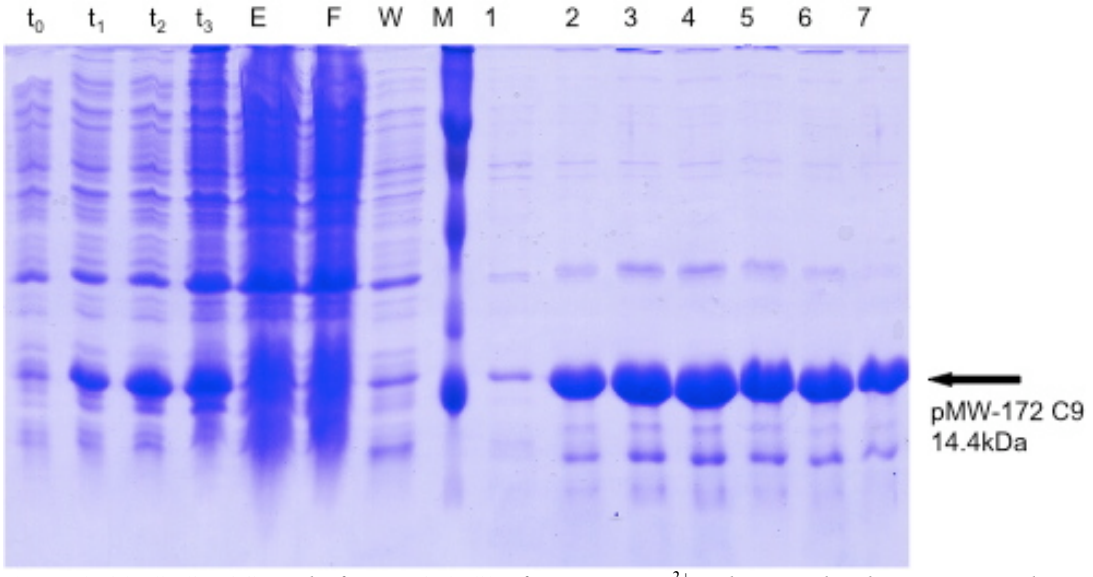

Figure 3–20: *SDS-PAGE gel of pMW-172 C9 after gravity Ni^{2+} column under denaturing conditions; t_0-t_3, samples taken at point in time during protein expression after induction with IPTG (0, 1hour etc.) M, marker; E, eluate fraction; F, flowthrough fraction; W, washing fraction; 1,2,…, protein fractions eluted from the column by 250 mM imidazole*

Running a size exclusion column on the FPLC machine was performed as the second purification step.

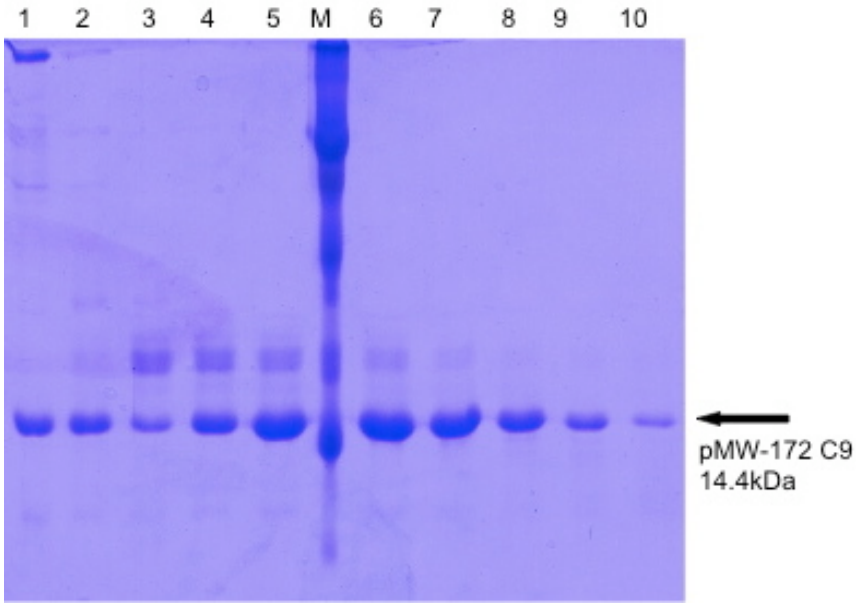

Figure 3–21: *SDS-PAGE gel of of pMW-172 C9 after FPLC gel filtration column; 1,2,…, protein fractions eluted from the column; M, marker*

Refolding of the denatured domain took place using urea gradient buffers. For three hours the sample stored in 6 M elution buffers was put in 3 M reconstitution buffer

followed by an overnight dialysis in 1.5 M reconstitution buffer. Dialysis in urea free phosphorylation assay buffer was done for further three hours. After measuring the protein concentration via a protein assay and double-checking by running a SDS-PAGE gel, the fragment was prepared for phosphorylation experiments.

The plasmid pMW172 containing C10 domain and hexahistidine-tag was generated in our laboratory previously. BL21(DE3)pLysS cells were transformed, cells harvested by centrifugation and resuspended under denaturing conditions. After performing a run on a Ni^{2+}- NTA resin column, I decided straight to dialyse in urea free phosphorylation assay buffer in the hope that the very high molecular impurities may be removed by precipitation.

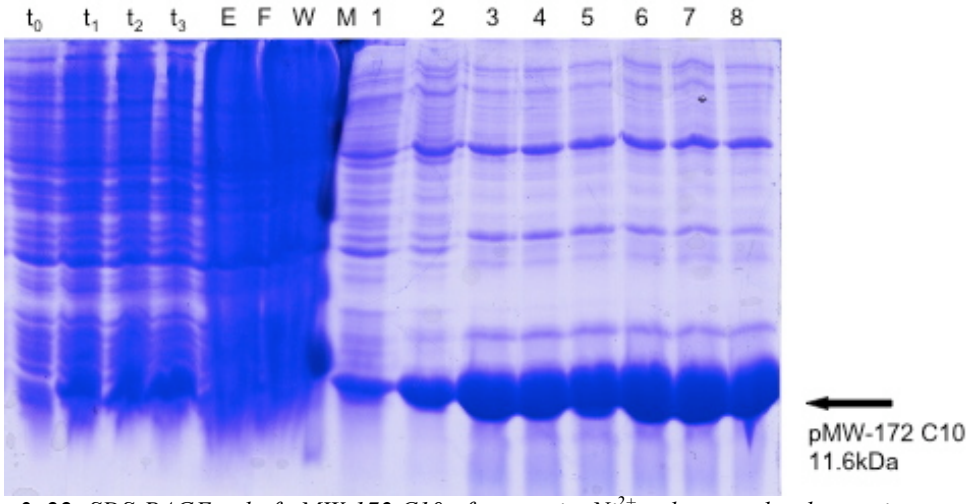

Figure 3–22: *SDS-PAGE gel of pMW-172 C10 after gravity Ni^{2+} column under denaturing conditions; t_0-t_3, samples taken at point in time during protein expression after induction with IPTG (0, 1hour etc.) M, marker; E, eluate fraction; F, flowthrough fraction; W, washing fraction; 1,2,..., protein fractions eluted from the column by 250 mM imidazole*

Removing the very high molecular impurities by precipitation is proved by **Figure 3–23** although the yield of C10 was reduced.

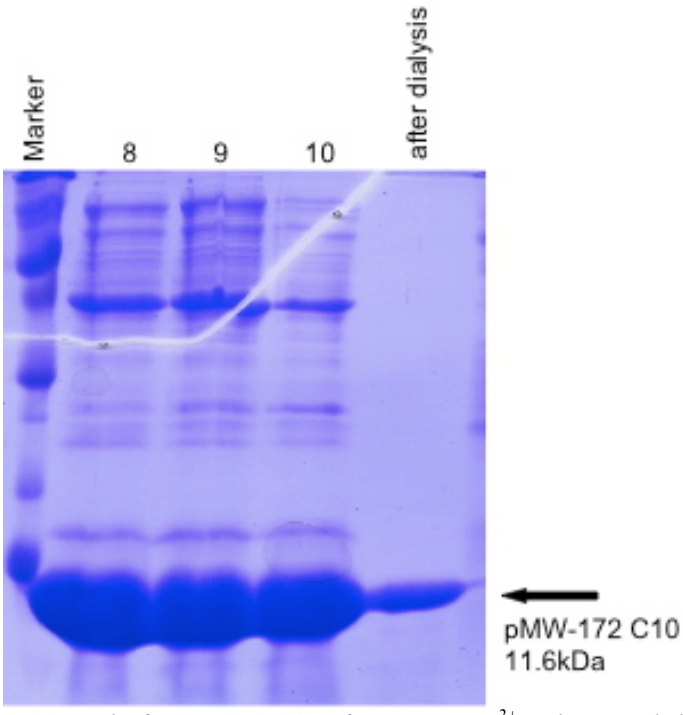

Figure 3–23: *SDS-PAGE gel of pMW-172 C10 after gravity Ni^{2+} column and the lane on the right shows a C10 fragment after dialysis*

3.2.8 Phosphorylation of pMW172 C9WT and pMW172 C10WT

The last section but one describes the phosphorylation results of the two C-terminal domains of cMyBP-C.

Due to the fact that the fragments under investigation are different in molecular weight, it is necessary to work with equimolar amounts rather than with same absolute amounts of protein. Therefore, 10 μmol of each sample were loaded in each lane. The sarcomeric protein Troponin T was chosen to act as a negative control as it is known to be not a substrate of the AMPK. In the next three lanes fragments (C8-C10, C10, C9) were run that are expressed in the pMW172 vector. As described earlier in this chapter this vector itself is known not to contain any phosphorylatable moiety. The last two cMyBP-C fragments investigated in this experiment are the N-terminal C0-C2WT fragment containing three known phosphorylatable residues at Ser273, Ser282 and Ser302. These serine moieties can be phosphorylated in response to β-adrenergic agonists via cAMP-dependent protein kinase (PKA)(Jeacocke & England, 1980; Hartzell & Titus, 1982; Lim & Walsh, 1986; Garvey *et al.*, 1988; Venema & Kuo, 1993). It has also been reported to be phosphorylated by an endogenous calcium/calmodulin-dependent kinase that is associated with cMyBP-C(Hartzell & Glass, 1984; Schlender & Bean, 1991). Protein kinase C has also been described to

phosphorylate MyBP-C *in vitro* (Lim *et al.*, 1985; Venema & Kuo, 1993). Regarding these known facts, I wanted to investigate, whether the N-terminal residues already reported are also a substrate of the AMPK. Fragment C0-C2WT was expressed in pET-28a previously in our laboratory. Additionally, I used fragment C8WT expressed also in pET-28a. This vector itself, as described earlier in this chapter, contains a serine residue that acts as a substrate of the AMPK. The only way to get rid of this moiety is to cleave the fragment with thrombin before performing the phosphorylation experiment. On the other hand, it is a helpful tool to use it uncleaved as a positive control.

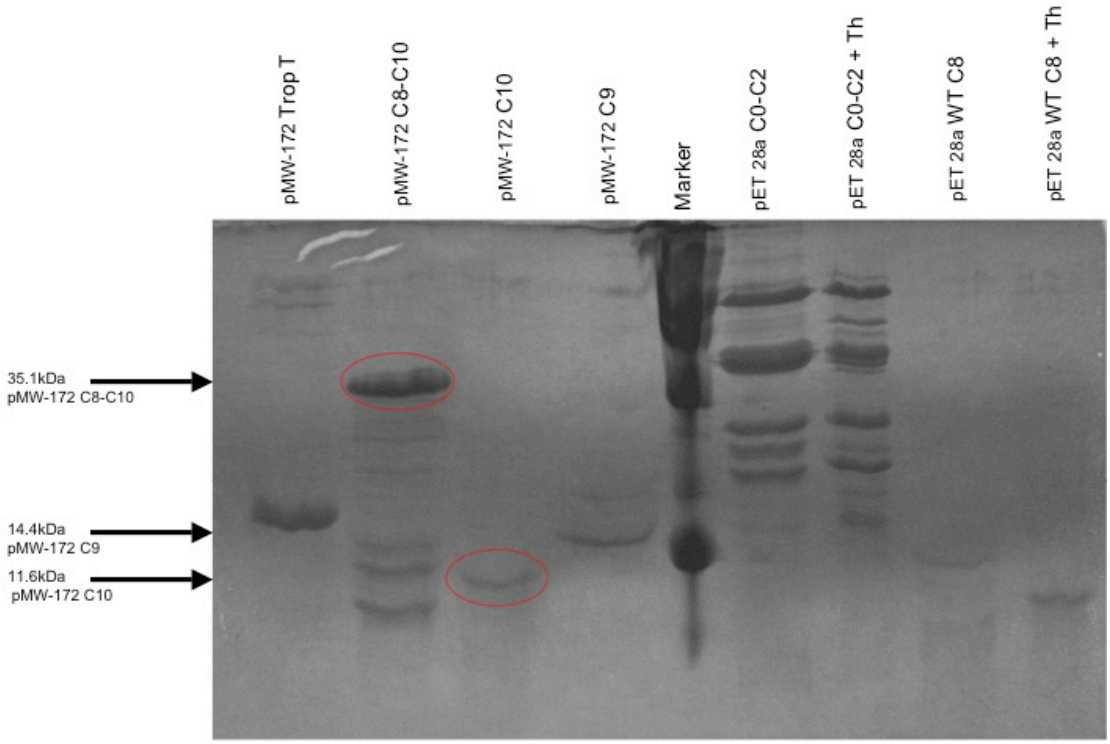

Figure 3–24: *SDS-PAGE gel after phosphorylation reaction; Troponin T is used as a negative control; cMyBP-C fragments C8-C10, C9 and C10 are expressed in the not phosphorylatable plasmid pMW172; cMyBP-C fragments C0-C2, C8 are expressed in the a phosphorylable serine residue containing pET-28a;*

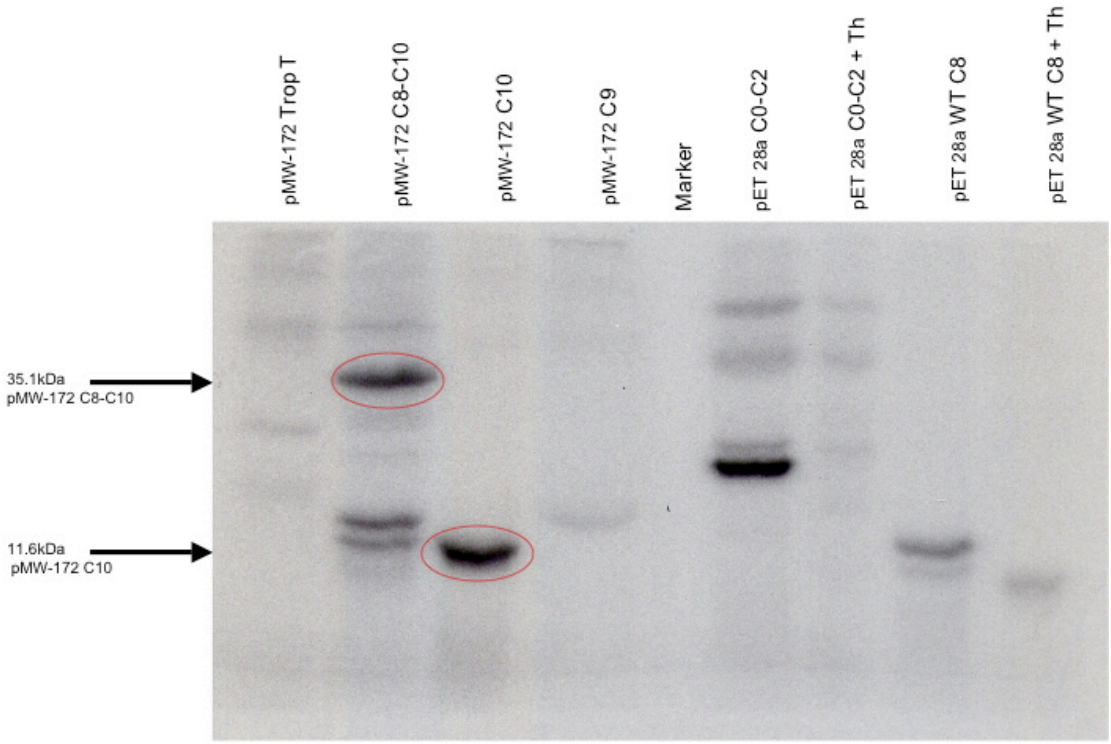

Figure 3–25: *Autoradiography; Troponin T is used as a negative control; cMyBP-C fragments C8-C10, C9 and C10 are expressed in the not phosphorylatable plasmid pMW172; cMyBP-C fragments C0-C2, C8 are expressed in the a phosphorylable serine residue containing pET-28a;*

As shown in the pictures above, the C10 fragment expressed in pMW172 is a substrate of AMPK. The intensity of phosphorylation matches with that of C8-C10 domains suggesting C10 is the solely C-terminal domain of cMyBP-C, which is a substrate of 5'-AMP-activated protein kinase.

Furthermore, the figure shows that the N-terminal serine residues cannot be phosphorylated by AMPK. The autoradiography film clearly indicates that a thrombin treatment before phosphorylation experiment abolishes the backbone of the plasmid containing a phosphorylatable serine. After thrombin cleavage no phosphorylation is detectable neither in C0-C2WT fragment nor in C8WT domain.

3.2.9 Phospho amino acid analysis pMW172 C10WT

In the last experiment of this study I tried to figure out if a serine, threonine or tyrosine amino acid acts as substrate of AMPK.

The most suitable method for this purpose is phospho amino acid analysis as described in chapter 2 and already used earlier in this study.

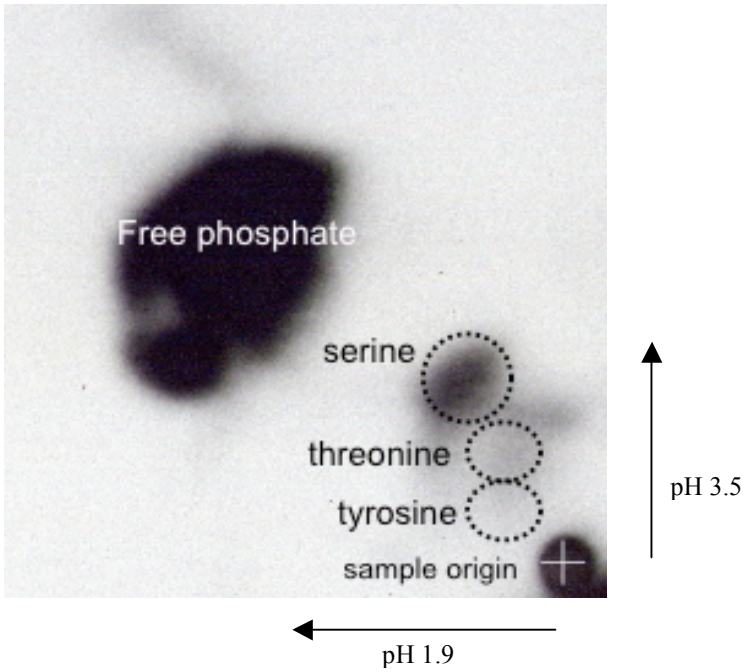

Figure 3–26: *Autoradiography after phospho amino acid analysis of C10*

As shown in autoradiography film it seems to be a serine moiety that serves as a substrate of the AMP-activated protein kinase.

There are 5 serine residues in the C10 domain (Ser 1182, Ser1191, Ser1207, Ser1213, Ser 1213) (Gautel *et al.*, 1995).

4 Chapter Discussion

4.1 Summary of Results

The existence of MyBP-C in striated muscle has been known for over 35 years and about 150 mutations in the gene encoding cMyBP-C have been found to be a common cause of hypertrophic cardiomyopathy. Despite this, the structure and function of MyBP-C remains less well understood than most other sarcomeric proteins, with roles in both regulation of contraction and thick filament formation/stability being proposed. In addition to the well known interactions of MyBP-C with other proteins of the sarcomeric apparatus (LMM, titin, actin) and with PKA, CaMKK and PKC at the N-terminal end of the protein, the aim of this study was to investigate interactions of MyBP-C's C-terminus with the 5'-AMP-activated protein kinase. This enzyme came in the focus of research during the last decade as it appears to function in a plethora of cell processes. Further, it has been elucidated that mutations in *PRKAG2*, encoding for the γ2 subunit of AMPK, causes left ventricular hypertrophy associated with conduction system diseases (e.g. Wolf-Parkinson-White syndrome). Important questions that have to be answered for a better understanding of this issue are, beside others, the identification of the full repertoire of cardiac protein targets.

My project aimed at identifying the site or sites of AMPK phosphorylation within the C-terminal three domains of cMyBP-C as suggested by earlier yeast-two-hybrid-screen data and biochemical work. The latter hinted that the C8 domain was most likely the target, and it is this fragment that my work began with. Having optimised the expression and purification of recombinant wild type MyBP-C C8 domain and a number of mutated C8 domains as discussed in Chapter 3, it was possible to disprove the hypothesis of phosphorylatable residues being in this domain. In contrast, it was revealed that a phosphorylatable serine moiety was present in the N-terminal leader of the recombinant protein, encoded by the vector pET-28a. This serine lies in the thrombin recognition sequence itself and its phosphorylation inhibits cleavage. However, it was shown *in vitro* that a phosphorylatable serine residue is located in the C10 domain of the protein and this further confirms the association of the C8-C10 fragment of MyBP-C with AMPK, first observed in the yeast two-hybrid assay. The hypotheses that arise from these results will be discussed in this chapter. Additionally,

I showed that the N-terminal domains of cMyBP-C (C0-C2), which contain the well characterized PKA and CaMII sites, are not a good substrate for AMPK *in vitro*.

4.2 Possible Targeted Residues of C10 for the AMP-Activated Kinase

As mentioned in the previous chapter, five serine residues could serve as phosphorylatable residues for AMPK.

After comparing positions of serine residues with the published recognition motif of AMPK (Dale *et al.*, 1995) Hyd-(X,Bas)-x-x-Ser/Thr-x-x-x-Hyd it is most likely that Ser1213 is at least one of the phosphorylatable residues, because it is the only one that fits with the recognition motif. However, it is important to note that this motif has a very broad range of recognition.

For a residue of C10 to be easily phosphorylated, it would have to lie on an exposed position in the structure. Although the exact structure of C10 has yet to be solved, the domain is a member of the IgI protein family, which shows a high degree of structural conservation. A number of structures of IgI- like domains have been elucidated, all of which display characteristic β-sheet sandwich. The Redwood/Watkins laboratory with collaborators at Imperial College, London have solved the structure of the C1 domain of cMyBP-C (Govada *et al.*, 2008) (**Figure 4–1**). Alignment of the two domain sequences shows that Ser1213 in C10 is equivalent to Ser217 in C1; this latter residue lies on a β-sheet turn and hence fulfils the criteria for accessibility.

Figure 4–1: *The structure of the C1 domain showing the position of Ser217 in red, equivalent to Ser1213 in the C10 domain.*

Regarding these facts my presumption has to be proven by further mutagenesis studies in our laboratory.

4.3 How could Phosphorylation of C10 Affect the Arrangement of the Collar?

As mentioned in chapter 1, our favoured model of the arrangement of MyBP-C around the thick filament involves multimerisation of the protein to form a trimeric collar (McClellan *et al.*, 2001; Flashman *et al.*, 2004). In this model, three cMyBP-C molecules consecutively dimerize, in a staggered and parallel fashion, with the C5-C10 regions, incorporating C5:C8 and C7:C10 binding, forming a collar- like structure around the thick filament, while the N-terminus extends into the interfilament space, allowing for its interaction with the S2 region of myosin. This is again illustrated in the figure below.

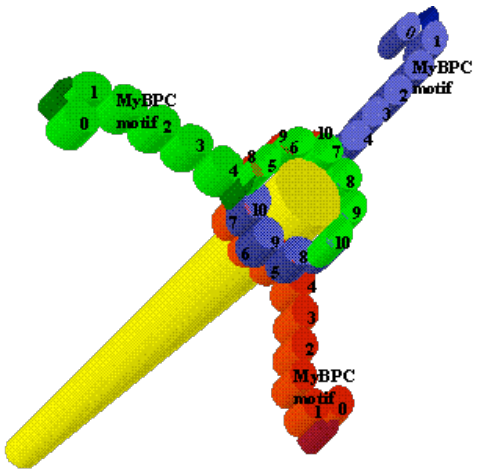

Figure 4–2: *The proposed trimeric collar arrangement of cMyBP-C around the thick filament. cMyBP-C molecules are arranged in a staggered parallel fashion, with domains C5-C10 encircling myosin, and domains C0-C4 extending into the interfilament space. (Flashman* et al.*, 2004)*

This trimeric collar model of arrangement of the cMyBP-C got more support very recently by using yeast two-hybrid and *in vitro* protein binding assays (Flashman *et al.*, 2008).

4.3.1 Regarding C7:C10 Interaction

The fact that two HCM-causing mutations, Arg654His and Asn755Lys, when introduced into the C5 domain could decrease the affinity of its interaction with C8, was one of the most important arguments for the trimeric collar model (Moolman-Smook *et al.*, 2002). Thereby, a pathophysiological explanation for the left ventricular hypertrophy is proposed in which ultrastructural alterations in the arrangement of MyBP-C leads ultimately to hypertrophy. Interestingly, the extent to which binding of the C5:C8 domains was modified, correlated with the severity of the described phenotype associated with the mutation. Further, there is evidence for another interaction between C7:10, detected in yeast two-hybrid assay. It was postulated that these interactions might be dynamically formed and released, thereby functioning as a modulator of cross-bridge formation (Moolman-Smook *et al.*, 2002).

Assuming that the arrangement of the trimeric collar is indeed dynamically formed and released, it seems possible that phosphorylation of C10 acts like a switcher of the C7:C10 interaction. Whether phosphorylation allows or abolishes interactions remains an open question, but both possibilities are feasible. If phosphorylation along with the

situation at the N-terminus of MyBP-C allows/enhances interaction, it would maintain a tight sarcomeric structure, thereby ensuring an optimal transmission of power at the crossbridges.

An interruption of the C7:C10 interaction caused by phosphorylation of C10 might lead to looser formation of the collar. This would reposition the shorter arm of the V-shape structure in a way disable to interact with the S2 subunit of the myosin rod.

As described in chapter 1, AMPK is stimulated by an increased AMP/ATP ratio caused by cellular stresses. Assuming, interaction C7:C10 is diminished subsequently to phosphorylation, the abolished interaction of C0-C2:S2 would result in an increased actomyosin ATPase activity.

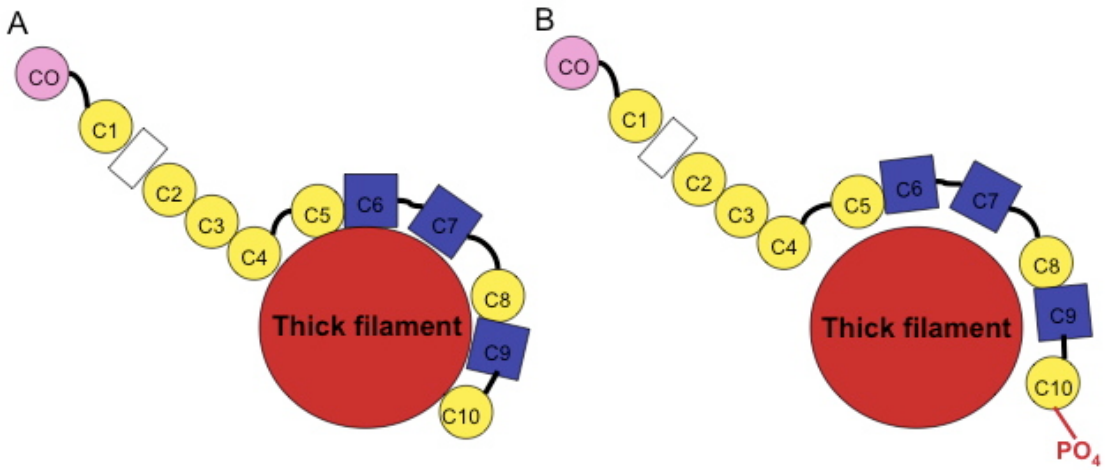

Figure 4–3: *(A) Proposed arrangement of cMyBP-C around the myosin filament. (B) Hypothesized reposition subsequent to phosphorylation of C10*

4.3.2 Regarding C10:LMM Interaction

C10 interacts with LMM region of β-myosin heavy chain between residues 1554 and 1581 (Flashman *et al.*, 2007). It is feasible that C10 phosphorylation may regulate this interaction, and hence affect the arrangement of collar as discussed above for C7:C10 binding.

In summary I propose that the detected phosphorylatable residue in chapter 3.2.8 in C10 acts for the C7:C10 and/ or the C10:LMM interaction like the three phosphorylation sites Ser273, Ser282 and Ser302 (A-C) in the N-terminus of the cMyBP-C for its interaction with the S2 region of the myosin filament. The N-terminal phosphorylation sites function as an “on and off-swichter” of cMyBP-C interaction with the S2 region of the thick filament and therefore as a regulator of contraction.

My hypothesis has to be proven by further *in vitro* protein- protein interaction studies, of course, but as known for a long time it is very common that the status of phosphorylation of a protein operates as a possibility to allow or abolish protein interactions.

4.4 Medical implications

4.4.1 How would PRKAG2 Mutations Affect the Proposed Modulation?

As mentioned in chapter 1 it appears to be the current consensus that *PRKAG2* mutations in the presence of adequate upstream kinases increase the basal activity of AMPK, albeit they reduce the sensitivity of the enzyme to AMP (Arad *et al.*, 2007). Increased basal activity would probably cause phosphorylation of C10 during resting conditions. In case phosphorylation functions as an "off-switcher" of the C7:C10 interaction, it would result ultimately in an increased activity of the actomyosin ATPase. This is consistent with the "energy deficiency" theory saying that the final pathway of diseases caused by genes involved in energetic metabolism and leading to left ventricular hypertrophy is a lack of high energy phosphates (Ashrafian *et al.*, 2003; Ashrafian & Watkins, 2007).

Assuming phosphorylation of C10 would cause enhancement of the C7:C10 interaction, the tightly packed collar could not be regulated in any way. Therefore these interactions could not act as a modulator of cross-bridge formation, due to the fact that they are not dynamically formed and released.

Similar effects would be expected for the C10:LMM interaction, meaning, if the interaction is abolished subsequently to phosphorylation, a disordered structure of the sarcomeric apparatus would result.

A constitutive interaction C10:LMM that can not be altered, would be the consequence of an increased AMPK activity in case the phosphorylation promote this protein-protein interaction.

4.4.2 Mutations in MYBP3

Until today no single amino acid mutation of one of the potential phosphorylation sites in C10 (Ser1182; Ser1191; Ser1207; Ser1213; Ser1231) is reported. But it is not

impossible that a mutation will be found within the next years. A study from 2003 proposed mutations in the *MYBPC3* gene in fact, due to its association with an often benign phenotype, as the most common cause for HCM. Therefore, the prevalence might be underestimated (Richard *et al.*, 2003) and mutation being still undiscovered.

4.4.3 Cardioprotection During Low Flow Ischemia

As mentioned in chapter 1, Yuan *et al.*, 2006 identified five phosphorylation sites of canine cMyBP-C in a study by extensive phosphorylation mapping, including three novel sites in the regulatory C1-C2 linker region. Further, this group and others have shown an altered phosphorylation status in pathological hearts particularly during/after periods of hypoxia (Sadayappan *et al.*, 2005; Sadayappan *et al.*, 2006). These groups proposed a cardioprotective role of cMyBP-C for the heart during low-flow ischemia, albeit the mechanism is not understood. Taken together this newly detected phosphorylation site in the C10 domain might contribute to the property of cardioprotection.

A feasible explanation could be for the case as phosphorylation allows interaction between C7 and C10. Then, during phosphorylation (AMPK being activated in response to cellular stresses) cMyBP-C would take the position capable to interact with the myosin S2 subunit and therefore reduces the actomyosin ATPase activity as discussed above. Reduced ATPase activity would act to decrease energy demand of the cell and thereby preventing it from further cellular stresses.

4.5 Future Prospects

Due to my performed experiments, it was possible to disprove the hypothesis of a substrate of AMPK being in the domain of a protein of the sarcomeric apparatus and at the same time to identify an undescribed substrate of AMPK in the same protein but in a different domain *in vitro.* However, there are a couple of questions, which I was not able to answer in this study.

The most crucial one concerns the detected phosphorylatable serine residue in the C10 domain of the cMyBP-C. In further site-directed-mutagenesis studies and subsequent phosphorylation assays, as I described for the C8 domain in chapter 2.2.2 and chapter 2.4.4, has to be elucidated which of the five described serine residues in C10 (Ser1182; Ser1191; Ser1207; Ser1213; Ser1231) is the targeted amino acid of AMPK.

As discussed earlier in this chapter, the most likely one being Ser1213 due its fitting in the reported AMPK recognition sequence.

In protein binding studies the question should be addressed, whether phosphorylation of a serine residue in C10 influences either the C7:C10 interaction or the C10:LMM or both. These experiments might be carried out with BIAcore X biosensor (Biacore AB) as it has already been described in the literature for the C5:C8-C10 interaction (Moolman-Smook *et al.*, 2002). Furthermore, this tool would allow investigating if the phosphorylation status enhances or abolish interaction of these proteins.

For a better understanding of the pathophysiology how AMPK-mutations cause left ventricular hypertrophy and, whether phosphorylation of the C10 domain of cMyBP-C may be involved or not, accomplishment of phosphorylation experiments with different, recombinant produced, AMPK-mutations are inevitable to prove the hypothesis that AMPK- mutations change the phosphorylation status of C10.

As described in chapter 1.6.2.5 mutations of the *PRKAG2* gene encoding for the γ2 subunit of AMPK increase the basal activity of this enzyme. According to my hypothesis explained earlier in this chapter, an increased basal activity of AMPK would cause the phosphorylation of a larger fraction of C10 and therefore a looser formation of the collar of cMyBP-C around the thick filament. This might be result in an abolishment of the S2:C1-C2 interaction and cause an increase of actomyosin ATPase activity as described by Yang *et al.*, 2001. Ultimately, this fact would contribute to the energy deficiency hypothesis, a well accepted theory of the role how AMPK mutations lead to HCM as discussed in chapter 1.4.1.

References

Alyonycheva TN, Mikawa T, Reinach FC & Fischman DA. (1997). Isoform-specific interaction of the myosin-binding proteins (MyBPs) with skeletal and cardiac myosin is a property of the C-terminal immunoglobulin domain. J Biol Chem 272, 20866-20872.

Arad M, Benson DW, Perez-Atayde AR, McKenna WJ, Sparks EA, Kanter RJ, McGarry K, Seidman JG & Seidman CE. (2002a). Constitutively active AMP kinase mutations cause glycogen storage disease mimicking hypertrophic cardiomyopathy. J Clin Invest 109, 357-362.

Arad M, Maron BJ, Gorham JM, Johnson WH, Jr., Saul JP, Perez-Atayde AR, Spirito P, Wright GB, Kanter RJ, Seidman CE & Seidman JG. (2005). Glycogen storage diseases presenting as hypertrophic cardiomyopathy. N Engl J Med 352, 362-372.

Arad M, Seidman CE & Seidman JG. (2007). AMP-activated protein kinase in the heart: role during health and disease. Circ Res 100, 474-488.

Arad M, Seidman JG & Seidman CE. (2002b). Phenotypic diversity in hypertrophic cardiomyopathy. Hum Mol Genet 11, 2499-2506.

Ashrafian H, Redwood C, Blair E & Watkins H. (2003). Hypertrophic cardiomyopathy:a paradigm for myocardial energy depletion. Trends Genet 19, 263-268.

Ashrafian H & Watkins H. (2007). Reviews of translational medicine and genomics in cardiovascular disease: new disease taxonomy and therapeutic implications cardiomyopathies: therapeutics based on molecular phenotype. J Am Coll Cardiol 49, 1251-1264.

Bahler M, Moser H, Eppenberger HM & Wallimann T. (1985). Heart C-protein is transiently expressed during skeletal muscle development in the embryo, but persists in cultured myogenic cells. Dev Biol 112, 345-352.

Barnes BR, Marklund S, Steiler TL, Walter M, Hjalm G, Amarger V, Mahlapuu M, Leng Y, Johansson C, Galuska D, Lindgren K, Abrink M, Stapleton D, Zierath JR & Andersson L. (2004). The 5'-AMP-activated protein kinase gamma3 isoform has a key role in carbohydrate and lipid metabolism in glycolytic skeletal muscle. J Biol Chem 279, 38441-38447.

Bateman A. (1997). The structure of a domain common to archaebacteria and the homocystinuria disease protein. Trends Biochem Sci 22, 12-13.

Bayrak F, Komurcu-Bayrak E, Mutlu B, Kahveci G, Basaran Y & Erginel-Unaltuna N. (2006). Ventricular pre-excitation and cardiac hypertrophy mimicking hypertrophic cardiomyopathy in a Turkish family with a novel PRKAG2 mutation. Eur J Heart Fail 8, 712-715.

Bennett P, Craig R, Starr R & Offer G. (1986). The ultrastructural location of C-protein, X-protein and H-protein in rabbit muscle. J Muscle Res Cell Motil 7, 550-567.

Blair E, Redwood C, Ashrafian H, Oliveira M, Broxholme J, Kerr B, Salmon A, Ostman-Smith I & Watkins H. (2001). Mutations in the gamma(2) subunit of AMP-activated protein kinase cause familial hypertrophic cardiomyopathy: evidence for the central role of energy compromise in disease pathogenesis. Hum Mol Genet 10, 1215-1220.

Burwinkel B, Scott JW, Buhrer C, van Landeghem FK, Cox GF, Wilson CJ, Grahame Hardie D & Kilimann MW. (2005). Fatal congenital heart glycogenosis caused by a recurrent activating R531Q mutation in the gamma 2-subunit of AMP-activated protein kinase (PRKAG2), not by phosphorylase kinase deficiency. Am J Hum Genet 76, 1034-1049.

Carling D & Hardie DG. (1989). The substrate and sequence specificity of the AMP-activated protein kinase. Phosphorylation of glycogen synthase and phosphorylase kinase. Biochim Biophys Acta 1012, 81-86.

Carrier L, Bonne G, Bahrend E, Yu B, Richard P, Niel F, Hainque B, Cruaud C, Gary F, Labeit S, Bouhour JB, Dubourg O, Desnos M, Hagege AA, Trent RJ, Komajda M, Fiszman M & Schwartz K. (1997). Organization and sequence of human cardiac myosin binding protein C gene (MYBPC3) and identification of mutations predicted to produce truncated proteins in familial hypertrophic cardiomyopathy. Circ Res 80, 427-434.

Carrier L, Knoll R, Vignier N, Keller DI, Bausero P, Prudhon B, Isnard R, Ambroisine ML, Fiszman M, Ross J, Jr., Schwartz K & Chien KR. (2004). Asymmetric septal hypertrophy in heterozygous cMyBP-C null mice. Cardiovasc Res 63, 293-304.

Chabowski A, Momken I, Coort SL, Calles-Escandon J, Tandon NN, Glatz JF, Luiken JJ & Bonen A. (2006). Prolonged AMPK activation increases the expression of fatty acid transporters in cardiac myocytes and perfused hearts. Mol Cell Biochem 288, 201-212.

Cheung PC, Salt IP, Davies SP, Hardie DG & Carling D. (2000). Characterization of AMP-activated protein kinase gamma-subunit isoforms and their role in AMP binding. Biochem J 346 Pt 3, 659-669.

Craig R & Offer G. (1976). The location of C-protein in rabbit skeletal muscle. Proc R Soc Lond B Biol Sci 192, 451-461.

da Silva CG, Jarzyna R, Specht A & Kaczmarek E. (2006). Extracellular nucleotides and adenosine independently activate AMP-activated protein kinase in endothelial cells: involvement of P2 receptors and adenosine transporters. Circ Res 98, e39-47.

Dale S, Wilson WA, Edelman AM & Hardie DG. (1995). Similar substrate recognition motifs for mammalian AMP-activated protein kinase, higher plant HMG-CoA reductase kinase-A, yeast SNF1, and mammalian calmodulin-dependent protein kinase I. FEBS Lett 361, 191-195.

Daniel T & Carling D. (2002). Functional analysis of mutations in the gamma 2 subunit of AMP-activated protein kinase associated with cardiac hypertrophy and Wolff-Parkinson-White syndrome. J Biol Chem 277, 51017-51024.

Decker RS, Decker ML, Kulikovskaya I, Nakamura S, Lee DC, Harris K, Klocke FJ & Winegrad S. (2005). Myosin-binding protein C phosphorylation, myofibril structure, and contractile function during low-flow ischemia. Circulation 111, 906-912.

Dhoot GK, Hales MC, Grail BM & Perry SV. (1985). The isoforms of C protein and their distribution in mammalian skeletal muscle. J Muscle Res Cell Motil 6, 487-505.

Dyck JR & Lopaschuk GD. (2006). AMPK alterations in cardiac physiology and pathology: enemy or ally? J Physiol 574, 95-112.

Eakins F, HA AL-K, Kensler RW, Morris EP & Squire JM. (2002). 3D Structure of fish muscle myosin filaments. J Struct Biol 137, 154-163.

Flashman E, Korkie L, Watkins H, Redwood C & Moolman-Smook JC. (2008). Support for a trimeric collar of myosin binding protein C in cardiac and fast skeletal muscle, but not in slow skeletal muscle. FEBS Lett 582, 434-438.

Flashman E, Redwood C, Moolman-Smook J & Watkins H. (2004). Cardiac myosin binding protein C: its role in physiology and disease. Circ Res 94, 1279-1289.

Flashman E, Watkins H & Redwood C. (2007). Localization of the binding site of the C-terminal domain of cardiac myosin-binding protein-C on the myosin rod. Biochem J 401, 97-102.

Frederich M & Balschi JA. (2002). The relationship between AMP-activated protein kinase activity and AMP concentration in the isolated perfused rat heart. J Biol Chem 277, 1928-1932.

Freiburg A & Gautel M. (1996). A molecular map of the interactions between titin and myosin-binding protein C. Implications for sarcomeric assembly in familial hypertrophic cardiomyopathy. Eur J Biochem 235, 317-323.

Fryer LG, Foufelle F, Barnes K, Baldwin SA, Woods A & Carling D. (2002). Characterization of the role of the AMP-activated protein kinase in the stimulation of glucose transport in skeletal muscle cells. Biochem J 363, 167-174.

Furst DO, Vinkemeier U & Weber K. (1992). Mammalian skeletal muscle C-protein: purification from bovine muscle, binding to titin and the characterization of a full-length human cDNA. J Cell Sci 102 (Pt 4), 769-778.

Garvey JL, Kranias EG & Solaro RJ. (1988). Phosphorylation of C-protein, troponin I and phospholamban in isolated rabbit hearts. Biochem J 249, 709-714.

Gautel M, Furst DO, Cocco A & Schiaffino S. (1998). Isoform transitions of the myosin binding protein C family in developing human and mouse muscles: lack of isoform transcomplementation in cardiac muscle. Circ Res 82, 124-129.

Gautel M, Zuffardi O, Freiburg A & Labeit S. (1995). Phosphorylation switches specific for the cardiac isoform of myosin binding protein-C: a modulator of cardiac contraction? Embo J 14, 1952-1960.

Geier C, Perrot A, Ozcelik C, Binner P, Counsell D, Hoffmann K, Pilz B, Martiniak Y, Gehmlich K, van der Ven PF, Furst DO, Vornwald A, von Hodenberg E, Nurnberg P, Scheffold T, Dietz R & Osterziel KJ. (2003). Mutations in the human muscle LIM protein gene in families with hypertrophic cardiomyopathy. Circulation 107, 1390-1395.

Gollob MH, Green MS, Tang AS, Gollob T, Karibe A, Ali Hassan AS, Ahmad F, Lozado R, Shah G, Fananapazir L, Bachinski LL & Roberts R. (2001a). Identification of a gene responsible for familial Wolff-Parkinson-White syndrome. N Engl J Med 344, 1823-1831.

Gollob MH, Seger JJ, Gollob TN, Tapscott T, Gonzales O, Bachinski L & Roberts R. (2001b). Novel PRKAG2 mutation responsible for the genetic syndrome of ventricular preexcitation and conduction system disease with childhood onset and absence of cardiac hypertrophy. Circulation 104, 3030-3033.

Govada L, Carpenter L, da Fonseca PC, Helliwell JR, Rizkallah P, Flashman E, Chayen NE, Redwood C & Squire JM. (2008). Crystal structure of the C1 domain of cardiac myosin binding protein-C: implications for hypertrophic cardiomyopathy. J Mol Biol 378, 387-397.

Gruen M & Gautel M. (1999). Mutations in beta-myosin S2 that cause familial hypertrophic cardiomyopathy (FHC) abolish the interaction with the regulatory domain of myosin-binding protein-C. J Mol Biol 286, 933-949.

Gruen M, Prinz H & Gautel M. (1999). cAPK-phosphorylation controls the interaction of the regulatory domain of cardiac myosin binding protein C with myosin-S2 in an on-off fashion. FEBS Lett 453, 254-259.

Halse R, Fryer LG, McCormack JG, Carling D & Yeaman SJ. (2003). Regulation of glycogen synthase by glucose and glycogen: a possible role for AMP-activated protein kinase. Diabetes 52, 9-15.

Hamilton SR, Stapleton D, O'Donnell JB, Jr., Kung JT, Dalal SR, Kemp BE & Witters LA. (2001). An activating mutation in the gamma1 subunit of the AMP-activated protein kinase. FEBS Lett 500, 163-168.

Hardie DG. (2003). Minireview: the AMP-activated protein kinase cascade: the key sensor of cellular energy status. Endocrinology 144, 5179-5183.

Hardie DG & Carling D. (1997). The AMP-activated protein kinase--fuel gauge of the mammalian cell? Eur J Biochem 246, 259-273.

Hardie DG & Hawley SA. (2001). AMP-activated protein kinase: the energy charge hypothesis revisited. Bioessays 23, 1112-1119.

Hardie DG, Hawley SA & Scott JW. (2006). AMP-activated protein kinase--development of the energy sensor concept. J Physiol 574, 7-15.

Harris SP, Bartley CR, Hacker TA, McDonald KS, Douglas PS, Greaser ML, Powers PA & Moss RL. (2002). Hypertrophic cardiomyopathy in cardiac myosin binding protein-C knockout mice. Circ Res 90, 594-601.

Hartzell HC & Glass DB. (1984). Phosphorylation of purified cardiac muscle C-protein by purified cAMP-dependent and endogenous Ca2+-calmodulin-dependent protein kinases. J Biol Chem 259, 15587-15596.

Hartzell HC & Sale WS. (1985). Structure of C protein purified from cardiac muscle. J Cell Biol 100, 208-215.

Hartzell HC & Titus L. (1982). Effects of cholinergic and adrenergic agonists on phosphorylation of a 165,000-dalton myofibrillar protein in intact cardiac muscle. J Biol Chem 257, 2111-2120.

Hawley SA, Boudeau J, Reid JL, Mustard KJ, Udd L, Makela TP, Alessi DR & Hardie DG. (2003). Complexes between the LKB1 tumor suppressor, STRAD alpha/beta and MO25 alpha/beta are upstream kinases in the AMP-activated protein kinase cascade. J Biol 2, 28.

Hawley SA, Pan DA, Mustard KJ, Ross L, Bain J, Edelman AM, Frenguelli BG & Hardie DG. (2005). Calmodulin-dependent protein kinase kinase-beta is an alternative upstream kinase for AMP-activated protein kinase. Cell Metab 2, 9-19.

Herold G. (2005). Innere Medizin. 171.

Herron TJ, Rostkova E, Kunst G, Chaturvedi R, Gautel M & Kentish JC. (2006). Activation of myocardial contraction by the N-terminal domains of myosin binding protein-C. Circ Res 98, 1290-1298.

Holmes BF, Kurth-Kraczek EJ & Winder WW. (1999). Chronic activation of 5'-AMP-activated protein kinase increases GLUT-4, hexokinase, and glycogen in muscle. J Appl Physiol 87, 1990-1995.

Hudson ER, Pan DA, James J, Lucocq JM, Hawley SA, Green KA, Baba O, Terashima T & Hardie DG. (2003). A novel domain in AMP-activated protein kinase causes glycogen storage bodies similar to those seen in hereditary cardiac arrhythmias. Curr Biol 13, 861-866.

Huxley HE & Brown W. (1967). The low-angle x-ray diagram of vertebrate striated muscle and its behaviour during contraction and rigor. J Mol Biol 30, 383-434.

Jeacocke SA & England PJ. (1980). Phosphorylation of a myofibrillar protein of Mr 150 000 in perfused rat heart, and the tentative indentification of this as C-protein. FEBS Lett 122, 129-132.

Jiang R & Carlson M. (1996). Glucose regulates protein interactions within the yeast SNF1 protein kinase complex. Genes Dev 10, 3105-3115.

Jorgensen SB, Richter EA & Wojtaszewski JF. (2006). Role of AMPK in skeletal muscle metabolic regulation and adaptation in relation to exercise. J Physiol 574, 17-31.

Kahn BB, Alquier T, Carling D & Hardie DG. (2005). AMP-activated protein kinase: ancient energy gauge provides clues to modern understanding of metabolism. Cell Metab 1, 15-25.

Kawashima M, Kitani S, Tanaka T & Obinata T. (1986). The earliest form of C-protein expressed during striated muscle development is immunologically the same as cardiac-type C-protein. J Biochem (Tokyo) 99, 1037-1047.

Kemp BE. (2004). Bateman domains and adenosine derivatives form a binding contract. J Clin Invest 113, 182-184.

Koretz JF, Irving TC & Wang K. (1993). Filamentous aggregates of native titin and binding of C-protein and AMP-deaminase. Arch Biochem Biophys 304, 305-309.

Kulikovskaya I, McClellan G, Flavigny J, Carrier L & Winegrad S. (2003). Effect of MyBP-C binding to actin on contractility in heart muscle. J Gen Physiol 122, 761-774.

Kurasawa M, Sato N, Matsuda A, Koshida S, Totsuka T & Obinata T. (1999). Differential expression of C-protein isoforms in developing and degenerating mouse striated muscles. Muscle Nerve 22, 196-207.

Labeit S, Gautel M, Lakey A & Trinick J. (1992). Towards a molecular understanding of titin. Embo J 11, 1711-1716.

Laforet P, Richard P, Said MA, Romero NB, Lacene E, Leroy JP, Baussan C, Hogrel JY, Lavergne T, Wahbi K, Hainque B & Duboc D. (2006). A new mutation in PRKAG2 gene causing hypertrophic cardiomyopathy with conduction system disease and muscular glycogenosis. Neuromuscul Disord 16, 178-182.

Lang T, Yu L, Tu Q, Jiang J, Chen Z, Xin Y, Liu G & Zhao S. (2000). Molecular cloning, genomic organization, and mapping of PRKAG2, a heart abundant gamma2 subunit of 5'-AMP-activated protein kinase, to human chromosome 7q36. Genomics 70, 258-263.

Lankford EB, Epstein ND, Fananapazir L & Sweeney HL. (1995). Abnormal contractile properties of muscle fibers expressing beta-myosin heavy chain gene mutations in patients with hypertrophic cardiomyopathy. J Clin Invest 95, 1409-1414.

Levine R, Weisberg A, Kulikovskaya I, McClellan G & Winegrad S. (2001). Multiple structures of thick filaments in resting cardiac muscle and their influence on cross-bridge interactions. Biophys J 81, 1070-1082.

Li J, Coven DL, Miller EJ, Hu X, Young ME, Carling D, Sinusas AJ & Young LH. (2006). Activation of AMPK alpha- and gamma-isoform complexes in the intact ischemic rat heart. Am J Physiol Heart Circ Physiol 291, H1927-1934.

Li J, Miller EJ, Ninomiya-Tsuji J, Russell RR, 3rd & Young LH. (2005). AMP-activated protein kinase activates p38 mitogen-activated protein kinase by increasing recruitment of p38 MAPK to TAB1 in the ischemic heart. Circ Res 97, 872-879.

Lim MS, Sutherland C & Walsh MP. (1985). Phosphorylation of bovine cardiac C-protein by protein kinase C. Biochem Biophys Res Commun 132, 1187-1195.

Lim MS & Walsh MP. (1986). Phosphorylation of skeletal and cardiac muscle C-proteins by the catalytic subunit of cAMP-dependent protein kinase. Biochem Cell Biol 64, 622-630.

Liversage AD, Holmes D, Knight PJ, Tskhovrebova L & Trinick J. (2001). Titin and the sarcomere symmetry paradox. J Mol Biol 305, 401-409.

Luiken JJ, Coort SL, Koonen DP, van der Horst DJ, Bonen A, Zorzano A & Glatz JF. (2004). Regulation of cardiac long-chain fatty acid and glucose uptake by translocation of substrate transporters. Pflugers Arch 448, 1-15.

MacRae CA, Ghaisas N, Kass S, Donnelly S, Basson CT, Watkins HC, Anan R, Thierfelder LH, McGarry K, Rowland E & et al. (1995). Familial Hypertrophic cardiomyopathy with Wolff-Parkinson-White syndrome maps to a locus on chromosome 7q3. J Clin Invest 96, 1216-1220.

Marian AJ. (2000). Pathogenesis of diverse clinical and pathological phenotypes in hypertrophic cardiomyopathy. Lancet 355, 58-60.

Maron BJ, Gardin JM, Flack JM, Gidding SS, Kurosaki TT & Bild DE. (1995). Prevalence of hypertrophic cardiomyopathy in a general population of young adults. Echocardiographic analysis of 4111 subjects in the CARDIA Study. Coronary Artery Risk Development in (Young) Adults. Circulation 92, 785-789.

Marsin AS, Bertrand L, Rider MH, Deprez J, Beauloye C, Vincent MF, Van den Berghe G, Carling D & Hue L. (2000). Phosphorylation and activation of heart PFK-2 by AMPK has a role in the stimulation of glycolysis during ischaemia. Curr Biol 10, 1247-1255.

McClellan G, Kulikovskaya I & Winegrad S. (2001). Changes in cardiac contractility related to calcium-mediated changes in phosphorylation of myosin-binding protein C. Biophys J 81, 1083-1092.

Mohamed AS, Dignam JD & Schlender KK. (1998). Cardiac myosin-binding protein C (MyBP-C): identification of protein kinase A and protein kinase C phosphorylation sites. Arch Biochem Biophys 358, 313-319.

Moolman-Smook J, Flashman E, de Lange W, Li Z, Corfield V, Redwood C & Watkins H. (2002). Identification of novel interactions between domains of Myosin binding protein-C that are modulated by hypertrophic cardiomyopathy missense mutations. Circ Res 91, 704-711.

Moos C, Offer G, Starr R & Bennett P. (1975). Interaction of C-protein with myosin, myosin rod and light meromyosin. J Mol Biol 97, 1-9.

Murphy RT, Mogensen J, McGarry K, Bahl A, Evans A, Osman E, Syrris P, Gorman G, Farrell M, Holton JL, Hanna MG, Hughes S, Elliott PM, Macrae CA & McKenna WJ. (2005). Adenosine monophosphate-activated protein kinase disease mimicks hypertrophic cardiomyopathy and Wolff-Parkinson-White syndrome: natural history. J Am Coll Cardiol 45, 922-930.

Nielsen JN, Wojtaszewski JF, Haller RG, Hardie DG, Kemp BE, Richter EA & Vissing J. (2002). Role of 5'AMP-activated protein kinase in glycogen synthase activity and glucose utilization: insights from patients with McArdle's disease. J Physiol 541, 979-989.

Nishino Y, Miura T, Miki T, Sakamoto J, Nakamura Y, Ikeda Y, Kobayashi H & Shimamoto K. (2004). Ischemic preconditioning activates AMPK in a PKC-dependent manner and induces GLUT4 up-regulation in the late phase of cardioprotection. Cardiovasc Res 61, 610-619.

Oakley CE, Chamoun J, Brown LJ & Hambly BD. (2007). Myosin binding protein-C: Enigmatic regulator of cardiac contraction. Int J Biochem Cell Biol.

Offer G, Moos C & Starr R. (1973). A new protein of the thick filaments of vertebrate skeletal myofibrils. Extractions, purification and characterization. J Mol Biol 74, 653-676.

Okagaki T, Weber FE, Fischman DA, Vaughan KT, Mikawa T & Reinach FC. (1993). The major myosin-binding domain of skeletal muscle MyBP-C (C protein) resides in the COOH-terminal, immunoglobulin C2 motif. J Cell Biol 123, 619-626.

Oliveira SM, Davies J, Carling D, Watkins H & Redwood C. (2007). Cardiac Troponin I is a Potential Novel Substrate for AMP-Activated Protein Kinase Biophysical Journal, 180a.

Pepe FA & Drucker B. (1975). The myosin filament. III. C-protein. J Mol Biol 99, 609-617.

Polekhina G, Gupta A, Michell BJ, van Denderen B, Murthy S, Feil SC, Jennings IG, Campbell DJ, Witters LA, Parker MW, Kemp BE & Stapleton D. (2003). AMPK beta subunit targets metabolic stress sensing to glycogen. Curr Biol 13, 867-871.

Redwood CS, Moolman-Smook JC & Watkins H. (1999). Properties of mutant contractile proteins that cause hypertrophic cardiomyopathy. Cardiovasc Res 44, 20-36.

Reinach FC, Masaki T & Fischman DA. (1983). Characterization of the C-protein from posterior latissimus dorsi muscle of the adult chicken: heterogeneity within a single sarcomere. J Cell Biol 96, 297-300.

Richard P, Charron P, Carrier L, Ledeuil C, Cheav T, Pichereau C, Benaiche A, Isnard R, Dubourg O, Burban M, Gueffet JP, Millaire A, Desnos M, Schwartz K, Hainque B & Komajda M. (2003). Hypertrophic cardiomyopathy: distribution of disease genes, spectrum of mutations, and implications for a molecular diagnosis strategy. Circulation 107, 2227-2232.

Richard P, Villard, E., Charron, P., Isnard, R. (2006). The genetic bases of cardiomyopathies. J Am Coll Cardiol 48, A79-A89.

Richardson P, McKenna W, Bristow M, Maisch B, Mautner B, O'Connell J, Olsen E, Thiene G, Goodwin J, Gyarfas I, Martin I & Nordet P. (1996). Report of the 1995 World Health Organization/International Society and Federation of Cardiology Task Force on the Definition and Classification of cardiomyopathies. Circulation 93, 841-842.

Robbins S & Cotran. (2006). Pathologic basis of disease. 560.

Rome E, Offer G & Pepe FA. (1973). X-ray diffraction of muscle labelled with antibody to C-protein. Nat New Biol 244, 152-154.

Russell RR, 3rd, Li J, Coven DL, Pypaert M, Zechner C, Palmeri M, Giordano FJ, Mu J, Birnbaum MJ & Young LH. (2004). AMP-activated protein kinase mediates ischemic glucose uptake and prevents postischemic cardiac dysfunction, apoptosis, and injury. J Clin Invest 114, 495-503.

Sadayappan S, Gulick J, Osinska H, Martin LA, Hahn HS, Dorn GW, 2nd, Klevitsky R, Seidman CE, Seidman JG & Robbins J. (2005). Cardiac myosin-binding protein-C phosphorylation and cardiac function. Circ Res 97, 1156-1163.

Sadayappan S, Osinska H, Klevitsky R, Lorenz JN, Sargent M, Molkentin JD, Seidman CE, Seidman JG & Robbins J. (2006). Cardiac myosin binding protein C phosphorylation is cardioprotective. Proc Natl Acad Sci U S A 103, 16918-16923.

Schlender KK & Bean LJ. (1991). Phosphorylation of chicken cardiac C-protein by calcium/calmodulin-dependent protein kinase II. J Biol Chem 266, 2811-2817.

Schlender KK, Hegazy MG & Thysseril TJ. (1987). Dephosphorylation of cardiac myofibril C-protein by protein phosphatase 1 and protein phosphatase 2A. Biochim Biophys Acta 928, 312-319.

Scott JW, Hawley SA, Green KA, Anis M, Stewart G, Scullion GA, Norman DG & Hardie DG. (2004). CBS domains form energy-sensing modules whose binding of adenosine ligands is disrupted by disease mutations. J Clin Invest 113, 274-284.

Seidman JG & Seidman C. (2001). The genetic basis for cardiomyopathy: from mutation identification to mechanistic paradigms. Cell 104, 557-567.

Soteriou A GM, Trinick J. (1993). A survey of interactions made by the giant protein titin J Cell Sci 104, 119-123.

Spirito P, Seidman CE, McKenna WJ & Maron BJ. (1997). The management of hypertrophic cardiomyopathy. N Engl J Med 336, 775-785.

Squire J, Cantino M, Chew M, Denny R, Harford J, Hudson L & Luther P. (1998). Myosin rod-packing schemes in vertebrate muscle thick filaments. J Struct Biol 122, 128-138.

Squire JM, Harford JJ, Edman AC & Sjostrom M. (1982). Fine structure of the A-band in cryo-sections. III. Crossbridge distribution and the axial structure of the human C-zone. J Mol Biol 155, 467-494.

Squire JM, Knupp C, Roessle M, Al-Khayat HA, Irving TC, Eakins F, Mok NS, Harford JJ & Reedy MK. (2005). X-ray diffraction studies of striated muscles. Adv Exp Med Biol 565, 45-60; discussion 359-369.

Squire JM, Luther PK & Knupp C. (2003). Structural evidence for the interaction of C-protein (MyBP-C) with actin and sequence identification of a possible actin-binding domain. J Mol Biol 331, 713-724.

Starr R, Almond R & Offer G. (1985). Location of C-protein, H-protein and X-protein in rabbit skeletal muscle fibre types. J Muscle Res Cell Motil 6, 227-256.

Starr R & Offer G. (1971). Polypeptide chains of intermediate molecular weight in myosin preparations. FEBS Lett 15, 40-44.

Studier FW, Rosenberg AH, Dunn JJ & Dubendorff JW. (1990). Use of T7 RNA polymerase to direct expression of cloned genes. Methods Enzymol 185, 60-89.

Swan RC & Fischman DA. (1986). Electron microscopy of C-protein molecules from chicken skeletal muscle. J Muscle Res Cell Motil 7, 160-166.

Sweeney HL, Feng HS, Yang Z & Watkins H. (1998). Functional analyses of troponin T mutations that cause hypertrophic cardiomyopathy: insights into disease pathogenesis and troponin function. Proc Natl Acad Sci U S A 95, 14406-14410.

Teare D. (1958). Asymmetrical hypertrophy of the heart in young adults. Br Heart J 20, 1-8.

Towler MC & Hardie DG. (2007). AMP-activated protein kinase in metabolic control and insulin signaling. Circ Res 100, 328-341.

Vaughan KT, Weber FE, Einheber S & Fischman DA. (1993a). Molecular cloning of chicken myosin-binding protein (MyBP) H (86-kDa protein) reveals extensive homology with MyBP-C (C-protein) with conserved immunoglobulin C2 and fibronectin type III motifs. J Biol Chem 268, 3670-3676.

Vaughan KT, Weber FE, Ried T, Ward DC, Reinach FC & Fischman DA. (1993b). Human myosin-binding protein H (MyBP-H): complete primary sequence, genomic organization, and chromosomal localization. Genomics 16, 34-40.

Venema RC & Kuo JF. (1993). Protein kinase C-mediated phosphorylation of troponin I and C-protein in isolated myocardial cells is associated with inhibition of myofibrillar actomyosin MgATPase. J Biol Chem 268, 2705-2711.

Ward SM, Dube DK, Fransen ME & Lemanski LF. (1996). Differential expression of C-protein isoforms in the developing heart of normal and cardiac lethal mutant axolotls (Ambystoma mexicanum). Dev Dyn 205, 93-103.

Warden SM, Richardson C, O'Donnell J, Jr., Stapleton D, Kemp BE & Witters LA. (2001). Post-translational modifications of the beta-1 subunit of AMP-activated protein kinase affect enzyme activity and cellular localization. Biochem J 354, 275-283.

Watkins H, Conner D, Thierfelder L, Jarcho JA, MacRae C, McKenna WJ, Maron BJ, Seidman JG & Seidman CE. (1995). Mutations in the cardiac myosin binding protein-C gene on chromosome 11 cause familial hypertrophic cardiomyopathy. Nat Genet 11, 434-437.

Watkins H, Seidman CE, Seidman JG, Feng HS & Sweeney HL. (1996). Expression and functional assessment of a truncated cardiac troponin T that causes hypertrophic cardiomyopathy. Evidence for a dominant negative action. J Clin Invest 98, 2456-2461.

Way M, Gooch J, Pope B & Weeds AG. (1989). Expression of human plasma gelsolin in Escherichia coli and dissection of actin binding sites by segmental deletion mutagenesis. J Cell Biol 109, 593-605.

Weber FE, Vaughan KT, Reinach FC & Fischman DA. (1993). Complete sequence of human fast-type and slow-type muscle myosin-binding-protein C (MyBP-C). Differential expression, conserved domain structure and chromosome assignment. Eur J Biochem 216, 661-669.

Weisberg A & Winegrad S. (1996). Alteration of myosin cross bridges by phosphorylation of myosin-binding protein C in cardiac muscle. Proc Natl Acad Sci U S A 93, 8999-9003.

Weisberg A & Winegrad S. (1998). Relation between crossbridge structure and actomyosin ATPase activity in rat heart. Circ Res 83, 60-72.

Winegrad S. (1999). Cardiac myosin binding protein C. Circ Res 84, 1117-1126.

Wolff MR, McDonald KS & Moss RL. (1995). Rate of tension development in cardiac muscle varies with level of activator calcium. Circ Res 76, 154-160.

Yamamoto K & Moos C. (1983). The C-proteins of rabbit red, white, and cardiac muscles. J Biol Chem 258, 8395-8401.

Yang J & Holman GD. (2005). Insulin and contraction stimulate exocytosis, but increased AMP-activated protein kinase activity resulting from oxidative metabolism stress slows endocytosis of GLUT4 in cardiomyocytes. J Biol Chem 280, 4070-4078.

Yang Q, Hewett TE, Klevitsky R, Sanbe A, Wang X & Robbins J. (2001). PKA-dependent phosphorylation of cardiac myosin binding protein C in transgenic mice. Cardiovasc Res 51, 80-88.

Yuan C, Guo Y, Ravi R, Przyklenk K, Shilkofski N, Diez R, Cole RN & Murphy AM. (2006). Myosin binding protein C is differentially phosphorylated upon myocardial stunning in canine and rat hearts-- evidence for novel phosphorylation sites. Proteomics 6, 4176-4186.

Verzeichnis der akademischen Lehrer

Meine akademischen Lehrer waren folgene Damen und Herren in Marburg:

Alter, Aumüller, Barth, Basler, Bauer, Baum, Becker,Berger, Bien, Cetin, Czubayko, Daut, Dietrich, Eilers,Feuser, Gerdes, Görg, Gress, Grimm, Grzeschik, Hertel, Herzum, Hoffmann, Hoyer, Jaques, Klose, König, Koolmann, Köster, Lill, Löffler, Löffler, Maisch, Mandrek, Meyer, Moll, Moosdorf, Mueller, Müller, Mutters, Neubauer, Oertel, Olbert, Rausch, Remschmidt, Renz, Richter, Röhm, Rothmund, Schäfer, Steiniger, Suske,Vogelmeier, Vogt, Wagner, Weihe, Wennemuth, Werner, Westermann, Wilhelm,Wulf

Oxford:

Farza, Oliveira, Pinter, Redwood, Watkins

New Orelans:

Beck, Hicks, Margolin, Whitlow, Bolton, Bowen, Tonnessen, Townsend, Richardson, Timmcke

Kapstadt

Botha, du Toit, Krüger, Slabbert, van der Merwe

Bern:

Bürgi, Egermann, Schiemann

Danksagung

Mein besonderer Dank gilt Herrn Prof. Dr. med. Gerhard Aumüller, ehemaliger Direktor des Institutes für Anatomie und Zellbiologie der Philipps-Universität Marburg. Durch seine intensive Föderung während meines studentischen Werdegangs war es mir möglich im Rahmen der vorliegenden Dissertation einen Forschungsaufenthalt an der University of Oxford zu realisieren. Er stand mir zu jeder Zeit mit seinem hochgeschätzten Rat zur Seite und hat mir jede nur denkliche Unterstützung zu Teil werden lassen.

Ebenso gilt mein besonderer Dank den Herren Dr. Charles Redwood und Prof. Hugh Watkins, die mir die Möglichkeit gegeben haben in ihrer Arbeitsgruppe die Exprimente für diese Arbeit durchzuführen. Insbesondere Dr. Redwood, möchte ich für sein persönliches Engagement und seine zu jederzeit zu Verfüngung gestellte Unterstützung danken. Desweitern möchte ich mich bei Dr. Pieles, Herrn Townsend, Dr. Oliveira, Dr. Farza, Dr. King, Dr. Robinson, Dr. Ashrafian und Dr. Pinter bedanken durch deren Hilfe Oxford eine entscheidende Station meines Lebens wurde. Insbesondere mit Dr. Pieles und Dr. Redwood verbindet mich eine wertvolle Freundschaft.

Danken möchte ich auch den Mitarbeitern der AG Aumüller für ihren wissenschaftlichten und freunschaftlichen Rat. Insbesondere Fr. Dr. Wilhelm, Fr. Keppler, Fr. Henkeler, Fr. Gutschank, Fr. Völk-Badouin, Fr. Dammshäuser, Fr. Hoffbauer, Fr. Stauch, Hr. Dreher, Dr. Gupta und meinem Freund Timo Brandenburger, mit dem ich auch weiterhin wissenschaftlich zusammenarbeiten werde.

Aufrichtig danken möchte ich auch meinem Freund, Mentor und Onkel, Herrn Prof. Dr. med. Thorolf Hager. Er war und wird mir stets Vorbild in meiner Tätigkeit als Arzt sein und stand mir jederzeit beratend und unterstützend zur Seite.

Von ganzem Herzen danken möchte ich meinen Eltern und Grosseltern, die durch ihre intensive Unterstützung und Liebe mir meine sehr kostenintensive Ausbildung ermöglicht haben.
Explizit danken möchte ich meiner Grossmutter. Ihre offene und warmherzige Art hat die Entwicklung meiner Persönlichkeit massgeblich beeinflusst.